

**POLITECNICO DI MILANO**  
School of Industrial and Information Engineering  
Master of Science in Biomedical Engineering –  
Biomechanics and Biomaterials - Cells and Tissues



**Analysis of platelet-derived Microparticles and their  
role in platelet activation and stimulation under  
static and dynamic conditions**

**Advisor:**

Prof. Alberto Redaelli

**Co-advisors:**

Prof. Marvin J. Slepian

Silvia Bozzi, PhD

**Autors:**

Marta Bonora, ID: 896977

Tomaso Gianiorio, ID: 895320

Academic year 2019 – 2020

# Acknowledgement

We would like to acknowledge our supervisors Professor, Alberto Redaelli, for giving us the possibility to work on this project and Professor Marvin J. Slepian for welcoming us as part of the team.

We also would like to thank Silvia Bozzi, PhD, for the support and technical advices she gave us during the work.

We would also like to acknowledge the Sarver Heart Centre team, Daniel, Sparky, Allegra, Kaitlyn, Adriana, Yana and Sam for their help and their friendship.

A special acknowledgment goes to our families for the opportunity they gave us to follow our dreams and for supporting us during this experience.

A kindly thought goes to all our friends, for the lovely time we've spent together and all their support.

Finally, we would like to thank each other for supporting, affection, patience and understanding.



# Contents

<i>List of figures</i> .....	<i>IV</i>
<i>List of tables</i> .....	<i>VII</i>
<i>Abbreviations</i> .....	<i>IX</i>
<i>Abstract</i> .....	<i>XI</i>
<i>Sommario</i> .....	<i>XXV</i>
<i>1. Introduction</i> .....	<i>1</i>
<i>2. Clinical background</i> .....	<i>3</i>
2.1 <i>Blood</i> .....	<i>3</i>
2.2 <i>Platelets</i> .....	<i>4</i>
2.3 <i>Coagulation process</i> .....	<i>7</i>
2.4 <i>Platelet-derived microparticles (PMPs)</i> .....	<i>14</i>
2.5 <i>Origin of PMPs</i> .....	<i>15</i>
2.6 <i>Structure of PMPs</i> .....	<i>16</i>
2.7 <i>Functions of PMPs</i> .....	<i>18</i>
2.8 <i>Clinical disorder related to PMPs</i> .....	<i>19</i>
<i>3. State of the art</i> .....	<i>21</i>
3.1 <i>PMP detection</i> .....	<i>21</i>
3.1.1 <i>Flow cytometry</i> .....	<i>21</i>
3.1.2 <i>Scanning Electron Microscopy (SEM)</i> .....	<i>24</i>
3.1.3 <i>Atomic Force Microscopy (AFM)</i> .....	<i>25</i>
3.1.4 <i>Enzyme-Linked Immunosorbent Assay (ELISA)</i> .....	<i>27</i>
3.2 <i>Isolation of PMPs</i> .....	<i>28</i>
3.2.1 <i>Centrifugation</i> .....	<i>28</i>

3.2.2	<i>Microfiltration</i> .....	29
3.3	<i>New techniques for PMPs detection</i> .....	29
3.3.1	<i>Proteomic Analysis</i> .....	29
3.3.2	<i>Impedance Based Flow cytometry</i> .....	30
3.4	<i>New techniques for counting PMPs and study PMPs size distribution</i> .	31
3.5	<i>PMPs pro-coagulant activities</i> .....	32
3.6	<i>Microparticles released as consequence of applied high shear</i> .....	35
3.7	<i>Platelets activity state (PAS)</i> .....	35
4.	<i>Materials and Methods</i> .....	39
4.1	<i>Blood collection</i> .....	39
4.2	<i>Platelets-Rich Plasma (PRP) preparation</i> .....	39
4.3	<i>Gel-Filtrated Platelets (GFP) collection</i> .....	39
4.4	<i>Platelet Count</i> .....	41
4.5	<i>Scanning Electron Microscope (SEM)</i> .....	42
4.6	<i>Atomic Force Microscopy (AFM)</i> .....	45
4.7	<i>Flow cytometry</i> .....	46
4.8	<i>PMP Production, Isolation and Storage</i> .....	49
4.8.1	<i>PMP production</i> .....	49
4.8.1.1	<i>Cold-Induced PMP Production</i> .....	49
4.8.1.2	<i>Agonist-Induced PMP production</i> .....	50
4.8.2	<i>PMPs isolation</i> .....	51
4.8.2.1	<i>Microcentrifugation</i> .....	51
4.8.2.2	<i>Microfiltration</i> .....	52
4.8.3	<i>PMP storage</i> .....	53
4.9	<i>Platelet Activity State (PAS) assay</i> .....	53
4.10	<i>Hemodynamic Shearing Device (HSD)</i> .....	55

4.11	<i>Experiments</i> .....	57
4.11.1	<i>Static Experiments</i> .....	57
4.11.1.1	<i>PMP effects on platelet activation</i> .....	57
4.11.1.2	<i>PMP effects on platelet activation compared with ADP</i> .....	58
4.11.2	<i>Dynamic experiments</i> .....	60
4.12	<i>Statistical analysis</i> .....	62
5	<i>Results</i> .....	63
5.1	<i>PMP Production, Isolation, and Storage</i> .....	63
5.1.1	<i>PMP Production</i> .....	63
5.1.1.1	<i>Cold-Induced PMP Production</i> .....	63
5.1.1.2	<i>Agonist-Induced PMP production</i> .....	65
5.1.2	<i>PMPs isolation</i> .....	67
5.1.2.1	<i>Microcentrifugation</i> .....	67
5.1.2.2	<i>Microfiltration</i> .....	69
5.1.3	<i>PMP Storage</i> .....	70
5.2	<i>Static experiments</i> .....	70
5.2.1	<i>PMP effects on platelet activation</i> .....	70
5.2.2	<i>PMP effects on platelet activation compared with ADP</i> .....	79
5.3	<i>Dynamic experiments</i> .....	84
6.	<i>Discussion</i> .....	91
7.	<i>Conclusion</i> .....	94
8.	<i>References</i> .....	96

## List of figures

Fig. I: HSD schematic view (left) and assembled HSD (right).	XIV
Fig. II: PMP production with different stimuli: sonication (left). calcium ionophore (right) The elements circled in red are PMPs. Magnification is 20000x	XVI
Fig. III: AFM acquisition of PMP produced by sonication: raw image (left), background	XVI
Fig. IV: PAS assay mean outputs (N=7, n=14). Data, shown as mean $\pm$ SD, were analyzed	XVII
Fig. V: Thrombin production plotted as a function of the time (N=7, n=14). Data are shown as mean $\pm$ SD	XVIII
Fig. VI: Comparison between PMP / PLT equal to 1 / 1000 and 1 / 5000 (N=7, n=14).	XVIII
Fig. VII: PAS assay mean outputs (N=5, n=10). Data, shown as mean $\pm$ SD,	XIX
Fig. VIII: PAS assay mean outputs plotted as a function of shear applied (N=4, n=8).	XX
Figure 1: Blood three layers after the centrifuge process	3
Figure 2: Platelet conformational change occurring during the activation. The figure shows:	9
Figure 3: Schematic representation of the three coagulation pathways	10
Figure 4: Schematic representation of the common pathway	14
Figure 5: During platelet activation or apoptosis the cell membrane	15
Figure 6: PMPs and exosomes. A resting platelet (left) contains $\alpha$ granules in which exosomes are stored.	18
Figure 7: Schematic diagram of a flow cytometer, from sheath focusing to data acquisition	21
Figure 8: Comparison of low and high sample pressure in flow cytometer	23
Figure 9: SEM image of a cantilever and a tip	26
Figure 10: Schematization of AFM working model	27
Figure 11: Thrombin generation by microparticles from healthy individuals	33
Figure 12: Schematization of the effects Ac-FIIa, used in the PAS assay execution, on	37
Figure 13: Chromatography processes inside glass columns	41
Figure 14: Refractometer	41
Figure 15: Hummer 8.0 Sputter System used to form gold coating on the samples	43
Figure 16: Gold coating process of the samples	44

Figure 17: Gating method to detect platelets. Forward scatter on the x-axis and side scatter on the y-axis.....	47
Figure 18: Flow cytometry acquisition of PMPs sample after isolation. According to the vertical threshold, the microparticles have been detected and classify as PMPs by gating those positive to antigen CD41.....	48
Figure 19: Flow cytometry acquisition. Background noise detected without the addition of markers .....	49
Figure 20: Sonicator. The microprobe is inserted in the tube to produce cavitation.....	50
Figure 21: Microcentrifuge Eppendorf 5414.....	52
Figure 22: Microfilter with siringe inlet.....	53
Figure 23: The HSD combines the geometry of a cone and plate viscometer and a cylindrical .....	55
Figure 24: Percentage of PMPs produced by cold storage as a function of storage time, .....	63
Figure 25: SSC on y-axis and FSC on x-axis. Q4 and Q3 contain particles smaller and.....	64
Figure 26:Percentage of PMPs over the total number of particles (N=8, n=16).....	65
Figure 27: PMP production with different stimuli: no stimulus (a), calcium ionophore (b) and sonication (c). The elements circled in red are PMPs. Magnification is 20000x .....	66
Figure 28: AFM acquisition of PMP produced by sonicated: raw image (left), background noise.....	66
Figure 29: Percentages of platelets (left) and PMPs (right) as a function of the centrifugation.....	67
Figure 30: PMPs (Q4) and platelets (Q3) plotted as function of SSC (y-axis) and FSC (x-axis) .....	68
Figure 31: Platelet and PMP percentages over the total number of particles (N=4, n=8).....	69
Figure 32: PMP percentages as a function of storage time (N=10, n=5). .....	70
Figure 33: Static experiments with PMP/platelet concentration ratio equal to 1 / 100 (N=6, n=12).....	72
Figure 34: Static experiments with PMP / PLT concentration ratio equal to 1 / 1000 (N=7, n=14).....	74
Figure 35: Static experiments with PMP/platelet concentration ratio equal to 1 / 5000 (N=7, n=14).....	76



Figure 36: PMPs-only and GFP + PMPs plotted as a function of time.(N=7, n=14).....	77
Figure 37: Thrombin production plotted as a function of the time (N=7, n=14). Data are shown as mean $\pm$ SD.....	78
Figure 38: Static experiments comparison between PMP / PLT equal to 1 / 1000 and 1 / 5000 .....	79
Figure 39: Comparison of thrombin production between PMP (1 / 1000 PMP / PLT) and ADP [10 and 20 $\mu$ M].....	81
Figure 40: Comparison of thrombin production between PMP (1 / 5000 PMP / PLT) and.....	83
Figure 41: Thrombin production plotted as a function of the time (N=5, n=10). Data are shown as mean $\pm$ SD.....	84
Figure 42: GFP + PMPs samples, plotted as a function of shear applied (N=4, n=8). .....	86
Figure 43: GFP + PMPs samples plotted as a function of shear applied (N=4, n=8). .....	88
Figure 44: GFP + PMPs samples plotted as a function of time (N=4, n=8). Data, shown as mean $\pm$ SD .....	89
Figure 45: Thrombin production plotted as a function of time (N=4, n=8). Data are shown as mean $\pm$ SD. ....	90

## List of tables

Table 1: The table represents the coagulation factor family classification .....	11
Table 2: Static experiments. Pro-coagulant activity of PMPs and comparison of PMPs activity with ADP .....	60
Table 3: Dynamic experiments. Pro-coagulant activity of PMPs under shear stress .....	62
Table 4: Normalized PAS values with respect to sonicated GFP after 60 minutes assay incubation for the static experiments with PMP / PLT concentration ratio equal to 1 / 100. N=6, n=12.....	71
Table 5: Normalized PAS values with respect to sonicated GFP after 60 minutes assay incubation for the.....	73
Table 6: Normalized PAS values with respect to sonicated GFP after 60 minutes assay incubation for the.....	75
Table 7: Normalized PAS values with respect to sonicated GFP after 60 minutes assay incubation for the static experiments with concentration ratio equal to 1 / 1000 PMP / PLT (N=5, n=10) .....	80
Table 8: Normalized PAS values with respect to sonicated GFP after 60 minutes assay incubation for the.....	82
Table 9: Normalized PAS values with respect to sonicated GFP after 60 minutes assay incubation of samples processed at 30 dyne/cm <sup>2</sup> . PMP / PLT concentration ratio equal to 1 / 1000. N=4, n=8.....	85
Table 10: Normalized PAS values with respect to sonicated GFP after 60 minutes assay incubation of samples processed at 70 dyne/cm <sup>2</sup> . PMP / PLT concentration ratio equal to 1 / 1000. N=4, n=8.....	86
Table 11: Normalized PAS values with respect to sonicated GFP after 60 minutes assay incubation of samples processed at 30 dyne/cm <sup>2</sup> . PMP / PLT concentration ratio equal to 1 / 5000. N=4, n=8.....	87
Table 12: Normalized PAS values with respect to sonicated GFP after 60 minutes assay incubation of samples processed at 70 dyne/cm <sup>2</sup> . PMP / PLT concentration ratio equal to 1 / 5000. N=4, n=8.....	88



# Abbreviations

AC-FII: Acetylated Factor II	GA: Glutaraldehyde
ACD-A: Anticoagulant Citrate Dextrose Solution A	GAG: Glycosaminoglycan
ADC: Analog-to-Digital Converter	GFP: Gel-Filtrated Plasma
ADP: Adenosine Diphosphate	GP: Glycoprotein
AFM: Atomic Force Microscopy	HBS:BSA: Hepes-buffered saline containing 0.5% bovine serum albumin
ANOVA: Analysis of Variance	HC: High Concentration
APC: Activated Protein C	HDMS: Bis(trimethylsilyl)amine
APC: Allophycocyanin	HIT: Heparin-Induced Thrombocytopenia
AT: Antithrombin	HSD: Hemodynamic Shearing Device
ATP: Adenosine Triphosphate	IDE: Integrated Development Environment
BSE: Backscattered Electrons	IgG: Immunoglobulin G
CaCl <sub>2</sub> : Calcium Chloride	ITP: Immune Thrombocytopenic
CCD: Charge Coupled Device	LC: Low Concentration
CD: Cluster of Differentiation	MCS: Mechanical Circulatory Support
CH-TH: Chromazym-TH	MK: Megakaryocyte
CL: Cathodoluminescence	MP: Microparticle
DLS: Dynamic Light Scattering	MS: Mass spectrometry
DMS: Demarcation Membrane System	NaOH: Sodium Hydroxide
DNA: Deoxyribonucleic Acid	NKC: Natural Killer Cell
EDTA: Ethylenediamine tetraacetic acid	NTA: Nanoparticle Tracking Analysis
ELISA: Enzyme-Linked Immunosorbent Assay	PAS: Platelet Activity State
EPCR: Endothelial Protein C Receptor	PB: Platelet Buffer
EV: Extracellular Vesicle	PBS: Phosphate Buffered Saline
FDA: Food & Drug Administration	PC: Protein C
FITC: Fluorescein isothiocyanate	PE: Phosphatidylethanolamine
FSC: Forward-Scattered Light	PEG: Poly(ethylene glycol)
	PFA: Paraformaldehyde

PFP: Platelets-Free-Platelets	SFCA: Surfactant-Free Cellulose Acetate
PK: Prekallikrein	SSC: Side-Scattered Light
PKC: Protein Kinase C	STM: Scanning Tunneling Microscope
PLT: platelets	TF: Tissue Factors
PMP: Platelet-derived Microparticle	TLR: Toll-like receptors
PNH: Paroxysmal Nocturnal Hemoglobinuria	TM: Thrombomodulin
PPP: Platelet-Poor Plasma	TriHCl:
PRP: Platelet-Rich-Platelets	Tris(hydroxymethyl)aminomethane hydrochloride
PS: Phosphatidylserine	TXA <sub>2</sub> : Thromboxane
PSPD: Position Sensitive Photo Diode	UHMWPE: Ultra High Molecular Weight Polyethylene
PVDF: Poly Vinylidene Difluoride	UV: Ultraviolet
RBC: Red Blood Cell	VK: Vitamin K
RCF: Relative Centrifugation Force	vWF: Von Willebrand Factor
RI: Refractive Index	WAS: Wiskott-Aldrich Syndrome
SA: Sodium Azide	WBC: White Blood Cell
SD: Standard Deviation	
SEM: Scanning Electron Microscopy	

# Abstract

In the last decade, increasing interest has been focused on platelet-derived microparticles (PMPs) to prevent and treat cardiovascular disorders. The aim of this work is to investigate the effect of PMPs on platelets activation and assess their pro-coagulant activity with respect to other agonists in static and dynamic conditions.

## Introduction

Platelets play a central role in normal hemostasis, thrombosis, hemorrhage and many cardiovascular diseases [1]. It was found that even microparticles shed from the membrane of the platelets have pro-coagulant potential. The level of PMPs increases in several prothrombotic and inflammatory disorders. The number of PMPs circulating in the human blood system are in a ratio of 1/300 – 1/3000 PMP/platelet (PMP / PLT). Indeed, it is believed that PMPs have effects also in healthy subjects. The role of PMPs in thrombosis has been investigated as a possible marker for identifying patients at risk of vascular disorders [2]. For this reason, medical and biomedical researchers have been focused on PMPs in the last decade [6] [5] [4] [7]. However, their clinical use has not been fully established yet, because standardized methodologies for PMP analysis are lacking.

## State of the art

Several works showed that PMPs formed during platelet activation have procoagulant activity [3] [4]. Berckmans et al. [4] demonstrated that by adding high concentrations of PMPs to plasma PMPs-free, the production of thrombin increases. Indeed, Kireev et al. [5], demonstrated that PMPs procoagulant activity is approximately 50- to 100-fold higher than that of activated platelets. In a clinical study, Nieuwland et al. investigated the procoagulant properties of PMPs generated *in vivo* showing that PMPs support thrombin generation [7]. In fact, PMPs play also an important role in atherosclerosis through inducing adherence of platelets in endothelial lesion site and by promoting the lesion plaque clotting in the arterial wall [6]. It was found that PMPs enhance platelet and fibrin deposition on the atherosclerotic vessel wall [8].

PMPs participate to clot formation in *in vivo* condition. In particular, PMPs bind to adhered platelets under high shear rate conditions stimulating further platelet deposition and so, thrombus growth [9]. Finally, Suades et al., found that PMPs number is correlated positively with thrombus weight. These results suggest that a high level of PMPs in blood promotes platelet coagulation and support PMPs involvement in clot formation [10]. By analyzing the effects of hydrodynamic forces on platelet activation and apoptosis, Leytin et al., found that pathologic shear stresses ( $>117$  dyne/cm<sup>2</sup>) induced platelet activation and then PMPs formation. Instead, physiologic shear stresses (10–44 dyne/cm<sup>2</sup>) did not affect the platelet responses [11]. Similarly, in a study conducted by Nomura et al., it was documented that the exposure of washed platelets to high shear stress ( $>108$  dyne/cm<sup>2</sup>) caused the release of PMPs. In contrast, exposure of washed platelet to low shear stress (12 dyne/cm<sup>2</sup>) did not cause either platelet aggregation or the formation of PMPs. They also reported that both platelet aggregation level and the number of microparticles released showed no significant differences between whole blood and washed platelet [12]. Sheriff et al. demonstrated that the threshold of shear for platelets activation and the PMPs release is around 60-70 dyne/cm<sup>2</sup>. According to this study it was also clear that a substantial proportion of the total prothrombinase activity recorded during stimulation experiments was due to the formation of PMPs, both immediately after a high-shear exposure and after an extended low-shear exposure [13].

### **Aim of the work**

The aim of this thesis is to evaluate the effect of PMPs on platelets activation *in vitro*. To this purpose specific protocols for the production and isolation of PMPs were designed. Once the PMPs samples were isolated, the interactions of PMPs with platelets were tested in static conditions. The PMPs activity was compared with quiescent platelets and then, to adenosine diphosphate (ADP). Finally, platelets and PMPs were exposed to mechanical stimulation in order to simulate dynamic conditions.

### **Materials and methods**

**Platelet preparation:** 30ml of adult volunteer blood was withdrawn via venipuncture. The blood was centrifuged (Beckman GS-6R Centrifuge) at 267 RCF for 15 minutes and platelets

rich-plasma (PRP) was collected. Gel-filtrated platelets (GFP) were obtained by gel-filtration chromatography.

**PMPs preparation:** Sonication and Calcium Ionophore were used to promote PMPs vesiculation from platelets. A Brandson Model 4C15 sonicator was used for 10 seconds at 10 Watt on 350  $\mu$ l of GFP while calcium ionophore A23187 [5 mM] was added in solution with 350  $\mu$ l of GFP. A scanning electron microscope (SEM) and an atomic force microscope (AFM) were used to ensure the PMPs presence. PMPs were isolated using microcentrifuge Eppendorf 5415 C; 1 ml of sonicated GFP [100 000 platelets/ $\mu$ l] was centrifuged with two different speeds sequentially: 4000 rpm (1310 RFC) for 20 minutes and 6000 rpm (2940 RFC) for 20 minutes. Flowcytometry (BD FACS Canto™) was used before the isolation to ensure the PMPs presence and after isolation to count the PMPs. The detection protocol was optimized by fluorescent beads and by marking the sample with Annexin V and antigen CD41+.

**Platelet Activity State (PAS) Assay:** The PAS assay measures the real-time rate of formation of thrombin. The test was performed with GFP, and the assay uses of acetylated prothrombin (Ac-FIIa) as the thrombin substrate. The modification of the prothrombinase method allowed the attainment of a linear correlation between the applied stimulus and thrombin generation, which is the index of induced activation of platelets [14] [15]. To perform PAS assay two different reagents are required: a tube solution which contains Ac-FIIa, HBS:BSA, Calcium Chloride and a well solution which contains HBS:BSA EDTA, Chromozym-TH. The sample (25  $\mu$ l) is incubated with tube solution (70  $\mu$ l) and Factor X (5  $\mu$ l) and then, added to well solution (150 $\mu$ l) to be read by spectrophotometer.



**Hemodynamic Shearing Device (HSD):** HSD is an instrument used to generate a known, constant shear on platelets; it is geometrically designed to generate uniform levels of shear stress on each particle. HSD combines the geometry of a cone and plate viscometer (plate) and a cylindrical coaxial Couette viscometer (ring), as shown in **Figure I**. HSD was used to generate shear stresses values up to 70 dyne/cm<sup>2</sup> such that flow remains laminar, inertial effects in the dynamic regime are minimal and secondary flow effects are not present [16] [17].

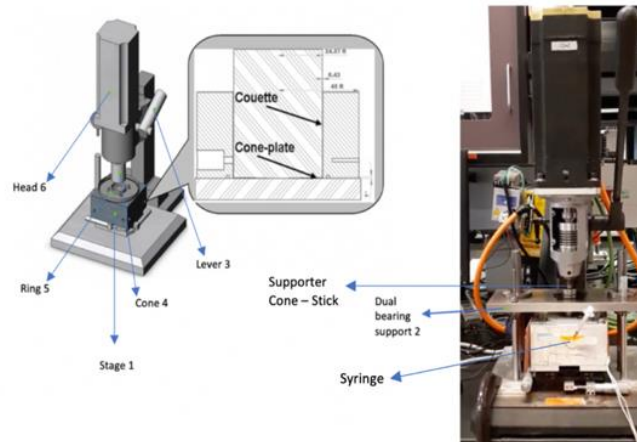


**Fig. I: HSD schematic view (left) and assembled HSD (right).  
Cone, Ring and Plate are made of UHMWPE**

## Static Experiments

### PMP effects on platelet activation

PMPs were added to GFP (quiescent platelets) in two different physiological concentration ratios, PMP / PLT, equal to 1 / 1000 (higher) and 1 / 5000 (lower). Commonly, the number of PMPs circulating in the human blood system are in a ratio of 1/300 – 1/3000 PMP/platelet (PMP / PLT). PMP alone (PMPs-only) were diluted with platelet buffer (PB) in same concentration in absence of GFP. The samples were incubated for 0, 10, 30 and 60 minutes at 37°C. Finally, PAS assay was used to estimate the activation of platelets. Pure GFP (GFP-only) was used as negative control while sonicated GFP as positive control. Samples were normalized with respect to the maximum activation (sonicated GFP).

### **PMP effects on platelet activation compared with ADP**

ADP as physiological coagulation agonist was used as further control of PMPs activities. ADP was purchased from Sigma Alderich (USA), aliquoted at 1 mM and stored at -20 °C. GFP + PMPs, GFP + ADP, GFP + ADP + PMPs were compared to estimate the role of PMPs in platelet activation with respect to ADP. PMPs were added to GFP-only (20'000 PLT/ $\mu$ l) in two different concentration ratios, PMP / PLT, equal to 1 / 1000 (higher) and 1 / 5000 (lower). PMPs alone (PMPs-only) were diluted with PB in same concentration in absence of GFP. ADP was added to the GFP (20'000 PLT/ $\mu$ l) in two different concentration: 10  $\mu$ M and 20  $\mu$ M. The samples were incubated for 0, 10, 30 and 60 minutes at 37°C. Finally, PAS assay was used to estimate the activation of platelets. Pure GFP (GFP-only) was used as negative control while sonicated GFP as positive control. Samples were normalized with respect to the maximum activation (sonicated GFP).

### **Dynamic experiments**

PMPs were added to GFP-only (20'000 PLT/ $\mu$ l) in two different concentration ratios, PMP / PLT, equal to 1 / 1000 (higher) and 1 / 5000 (lower). GFP + PMPs were exposed, by using HSD, to two different constant magnitude:

- Experiment 1: 30 dyne/cm<sup>2</sup> for 120 seconds
- Experiment 2: 70 dyne/ cm<sup>2</sup> for 120 seconds

The control samples were sonicated GFP, GFP-only and GFP + PMPs non-stimulated. Samples were normalized with respect to the maximum activation (sonicated GFP). Also in this case the samples were incubated for 0, 10, 30 and 60 minutes at 37°C. PAS assay was used to estimate the activation of platelets.

### **Statistical analysis**

Statistical analysis of the results was performed with GraphPad Prism 8 (GraphPad Software, Inc., CA, USA). Normal distribution of data was tested with the Shapiro-Wilk normality test. The One-way Analysis of Variance (ANOVA) test was used when normality hypothesis was satisfied for all the groups being tested. Conversely, non-parametric Brown-Forsythe and Welch one-way ANOVA tests were performed. Statistical significance was assumed for p-values at least lower than 0.05.

## Results

**Platelet activation:** SEM acquisitions of platelets treated with sonication and Calcium Ionophore are shown in **Figure II**. The acquisitions obtained by AFM before and after isolation are shown in **Figure III**.

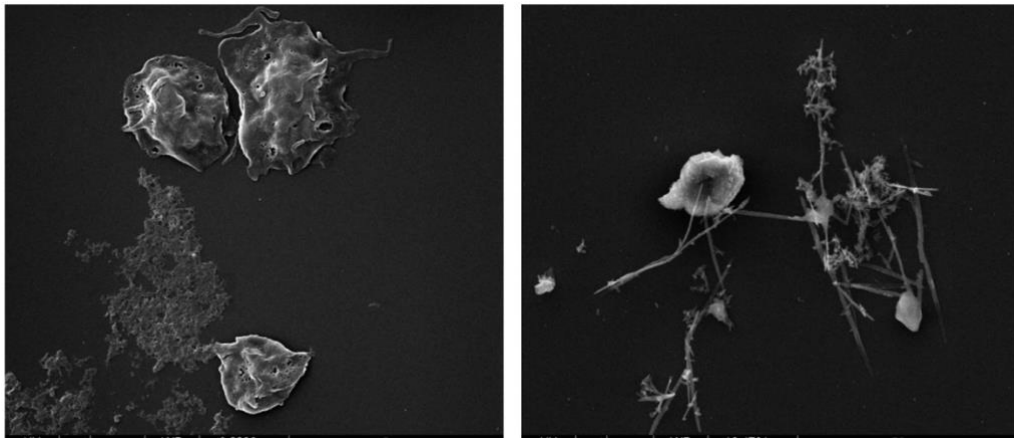


**Fig. II: PMP production with different stimuli: sonication (left), calcium ionophore (right) elements circled in red are PMPs. Magnification is 20000x**

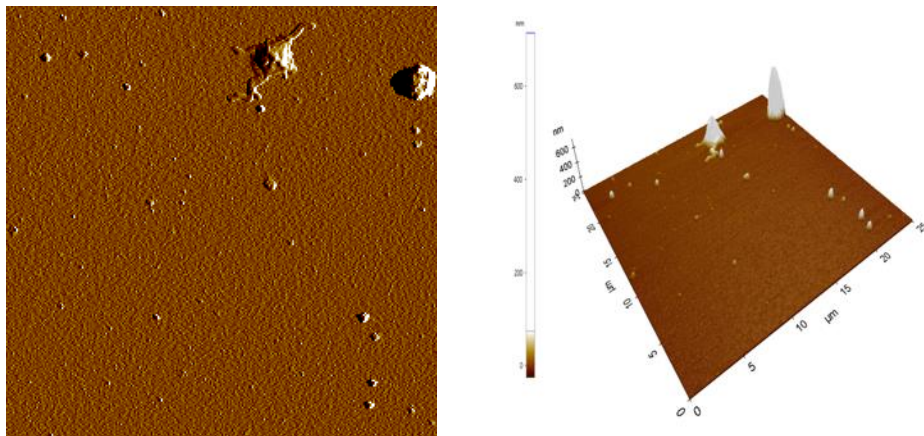


**Fig. III: AFM acquisition of PMP produced by sonication: raw image (left), background noise corrected 3D image (right). Scan dimension area :25x25x0.6µm**

Sonication was proved to be the best method for platelets activation. Indeed, calcium ionophore, would remain in solution even after the PMP isolation, affecting the platelets activation in further experiments.

### Static experiments

#### PMP effects on platelet activation

*1 / 1000 and 1 / 5000 PMP / PLT concentration ratio:* Statistical analysis was performed between GFP + PMPs or PMP-only and the negative control (GPF-only) and shown in **Figure IV**.

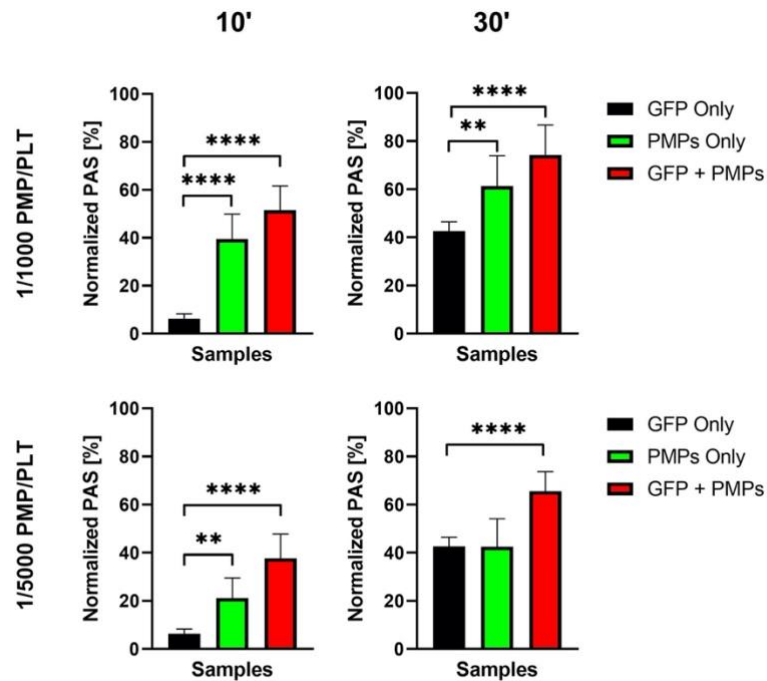


**Fig. IV: PAS assay mean outputs (N=7, n=14). Data, shown as mean  $\pm$  SD, were analyzed using Brown-Forsythe and Welch ANOVA test. \* $p < 0.05$ , \*\*  $p < 0.01$ , \*\*\*  $p < 0.0001$**

After 10 and 30 minutes of incubation, GFP-only and GFP + PMPs showed significant differences for both the used concentration ratios.

PMP-only showed a significant difference with GFP-only after 10 minutes for both the concentration ratios while after 30 minutes only for the higher concentration of PMP-only, a significant difference was found with respect to GFP-only.

*Dynamics of thrombin production over time:* In **Figure V** the thrombin generation trends are shown over time.

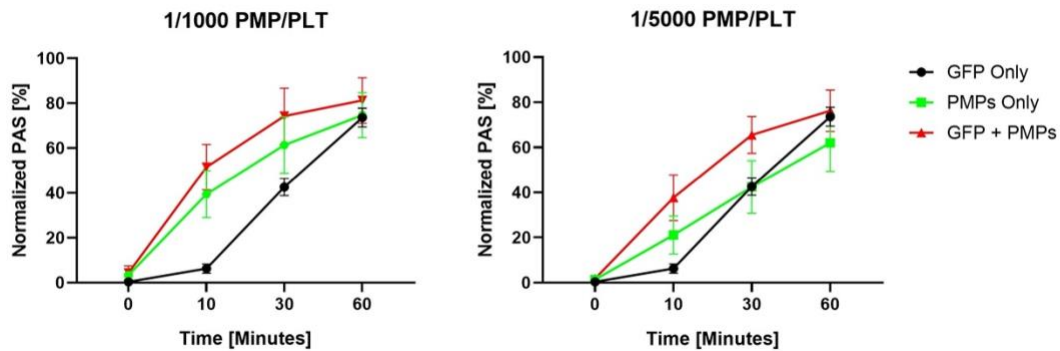


**Fig. V:** Thrombin production plotted as a function of the time (N=7, n=14). Data are shown as mean  $\pm$  SD

At 60 minutes of incubation the thrombin production tended to produce the same value for all the samples here analyzed, due to the exhaustion of reagents. However, the presence of PMPs alone and in solution with platelets promoted a faster achievement of maximum thrombin production.

*Comparison between 1 / 1000 and 1 / 5000:* A statistical analysis was performed between concentration ratios equal to 1 / 1000 and 1 / 5000 PMP / PLT (**Figure VI**).

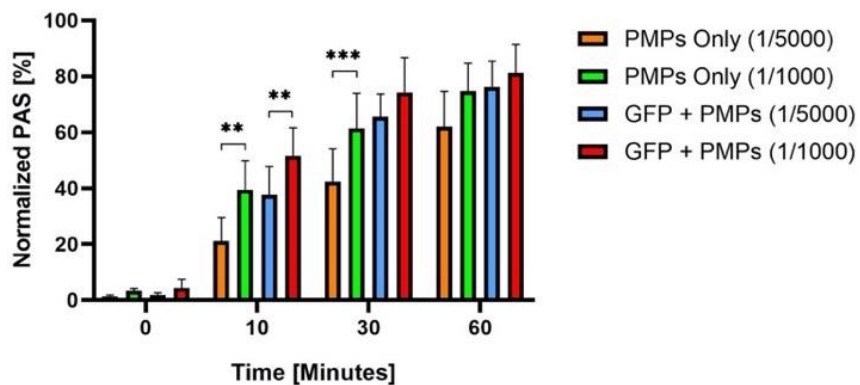


**Fig. VI:** Comparison between PMP / PLT equal to 1 / 1000 and 1 / 5000 (N=7, n=14).

Data, shown as mean  $\pm$  SD, were analyzed using Brown-Forsythe and Welch ANOVA test.

\*\* p<0.01, \*\*\* p<0.001

A significant difference was found between PMPs-only in higher and lower concentration ratios at 10 minutes and at 30 minutes. GFP + PMPs showed a significant difference between 1 / 1000

and 1 / 5000 only at 10 minutes. Thrombin production by PMPs was shown to be concentration dependent such that a higher concentration ratio (1/1000 PMP/PLT) caused a higher production of thrombin.

### PMP effects on platelet activation compared with ADP

*1 / 1000 and 1 / 5000 PMP / PLT concentration ratio:* as PMPs were determined to be pro-coagulant, their impact on platelet activation was measured in comparison to and in tandem with ADP. A statistical analysis was provided between GFP + PMPs, GFP + ADP and GFP + PMPs + ADP. The results are shown in **Figure VII**.

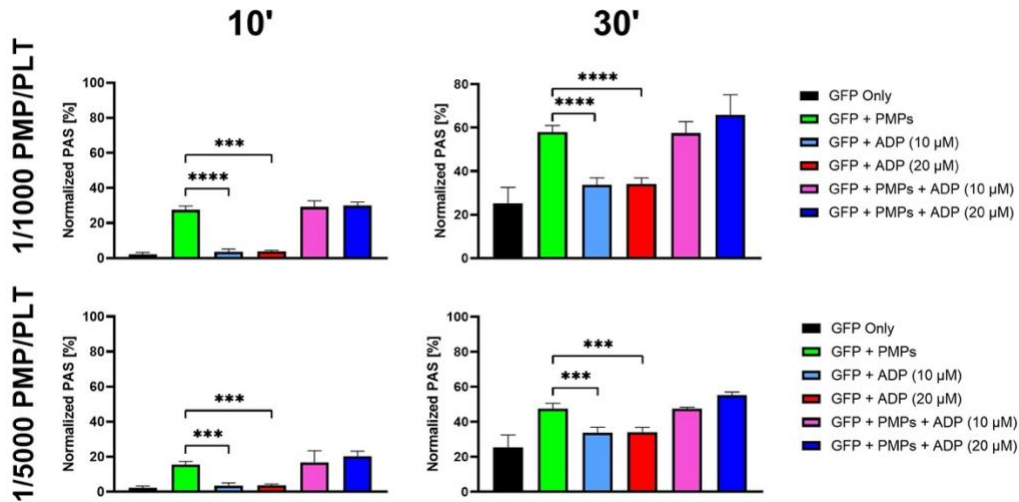


**Fig. VII: PAS assay mean outputs (N=5, n=10). Data, shown as mean ± SD, were analyzed using Brown-Forsythe and Welch ANOVA test.**

\* p < 0.05, \*\*\* p < 0.001, \*\*\*\* p < 0.0001

At 10 and 30 minutes a significant difference was found between the samples: GFP + PMPs (1 / 1000 and 1 / 5000) and GFP + ADP [10 and 20 μM]. GFP + PMPs induced higher PAS values rather than GFP + ADP ones hence, a greater thrombin production.

## Dynamic experiments

*Pro-thrombotic behavior of PMPs under shear-stress conditions:* GFP + PMPs, in concentration ratios equal to 1 / 1000 and 1 / 5000 PMP / PLT, was subjected to two different shear stresses in order to simulate physiological and pathological dynamic conditions. A statistical analysis was performed between stimulated and non-stimulated samples and between samples stimulated with different shear. The results are reported in **Figure VIII**.

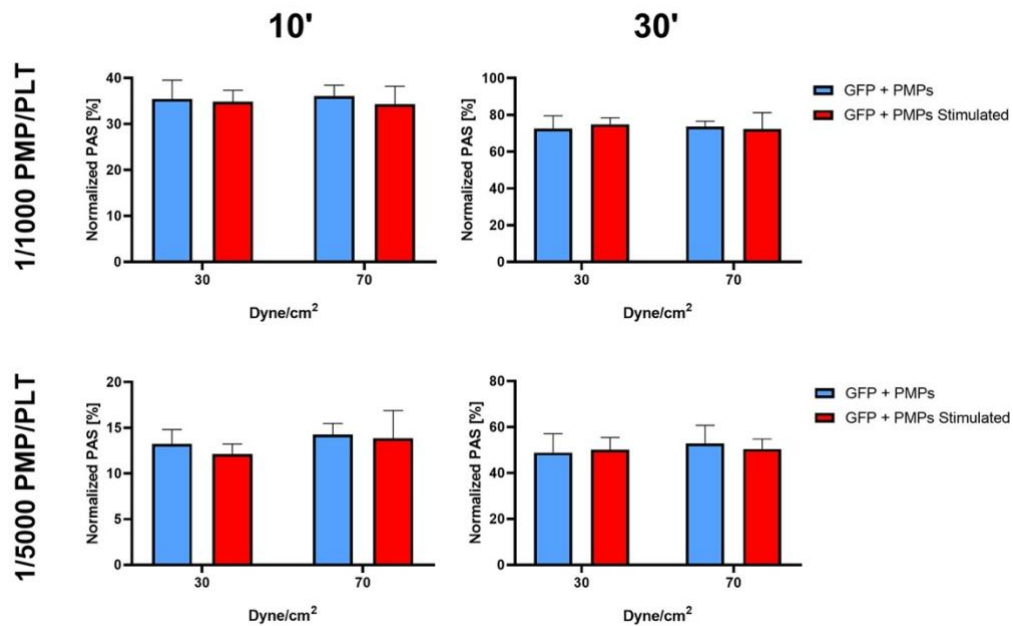


**Fig. VIII:** PAS assay mean outputs plotted as a function of shear applied (N=4, n=8).

Data, shown as mean  $\pm$  SD, were analyzed using Brown-Forsythe and Welch ANOVA test. \*  $p < 0.05$

It was found that there are no significant differences between GFP + PMPs stimulated and non-stimulated for both the concentration ratios used. In addition, it was also found that there are no significant differences between GFP + PMPs exposed to 30 dyne/cm<sup>2</sup> and GFP + PMPs exposed to 70 dyne/cm<sup>2</sup> for both the concentrations of PMPs used.

## Discussion

*Thrombogenicity tested in static conditions:* PMPs, in solution with platelets, were able to generate much higher thrombin quantities than those generated by the quiescent platelets.

Thrombin production by microparticles was found to be dependent on both the concentration and the incubation period. Literature supports our findings that PMPs are procoagulant [4] [6] [7]. Another interesting result was the fact that thrombin production was PMP concentration-dependent. The same result was achieved by Kireev et al. [5]. Indeed, they noticed that the maximal thrombin production rapidly increased with the increase of the concentration of PMPs added.

*PMP thrombogenicity compared with physiological agonist:* The thrombogenic activity of PMPs was shown to be significantly superior with respect to the action promoted by ADP on platelets activation. According to P.J Sims et al., ADP is considered a weak agonist of the coagulation [18]. This leads us to suppose that PMPs are thus strong activators able to surmount ADP pro-coagulant action, under these conditions.

*PMP thrombogenicity tested under shear-stress conditions:* constant shear levels were applied to simulate a dynamic condition. 30 dyne/cm<sup>2</sup> simulates a physiological shear stress while 70 dyne/cm<sup>2</sup> simulates a shear stress beyond physiological range (1-50 dyne/cm<sup>2</sup> venous and arteriosus range) [19]. Platelets treated with PMPs, stimulated and not stimulated, did not show significant differences over time for both shear levels applied. According to Leytin et al., physiologic shear stresses (30 dyne/cm<sup>2</sup>) did not affect the platelet responses [12].

In the non-physiological case, 70 dyne/cm<sup>2</sup>, it was assumed that the effect induced by the applied shear was too low to be distinguishable from the effect induced by PMPs already present. Indeed, Sheriff et al., documented that the high-shear threshold for which platelet activation occurs is around 70 dyne/cm<sup>2</sup> and that the number of activated platelets is shear magnitude-dependent [12].

Therefore, the PMPs created by the effect of high-shear on platelets did not make a significant contribution to the action of PMPs added to platelets before exposure.

In conclusion, from the first experiments we determined that PMPs effectively are pro-coagulant.

Successively, it was demonstrated that the PMPs have a higher procoagulant activity than ADP-activated platelets. In dynamic conditions, it has been established that the platelet activation, in presence of additional concentration of PMPs, this is not affected by the shear constant stimulation up to 70 dyne/cm<sup>2</sup>.



## **Conclusion**

In the last decades, the role of PMPs, in thrombogenicity and cardiovascular disorders, has changed from secondary to fundamental. In addition, new functions related to PMPs are continuously discovered. In this project PMPs pro-coagulant activity has been investigated. Our study has shown that:

- (1) PMPs act as a pro-coagulant factor
- (2) The thrombogenic potential related to PMPs is higher than that of ADP
- (3) The presence of high PMP concentration makes the shear stress effect negligible

The main limitation of the work is that our approach *in vitro*, by using GFP, does not replicate completely the physiological conditions. Moreover, the PAS assay did not allow to test higher concentration (non-physiological) of PMPs because of the quick saturation reached.

Among future experiments we planned to include a comparison between the pro-coagulant action of the platelets subjected to mechanical shear and the action of the platelets influenced by the presence of PMPs only. In addition, since in pathologies such as severe stenoses and in presence of exogenous devices such as MCS systems, stresses reach peaks of 1000 and 2000 dyne/cm<sup>2</sup>, we planned to simulate such stimuli to re-create similar pathological conditions. These two set of experiments, briefly shown, were temporarily postponed due to the inevitable situation generated by COVID-19.

## **References:**

- [1] A. D. Michelson, "Platelet Function Testing in Cardiovascular Diseases," *Circulation*, vol. 110, no. 19, pp. 489–93, 2004
- [2] Perrotta PL, Parsons J, Rinder HM, Snyder EL, "Platelet Transfusion Medicine" In *Platelets*, Elsevier, pp 1275-1303, 2013
- [3] Nieuwland R, Berckmans R J, Rotteveel-Eijkman R C, et al., "Cell-derived microparticles generated in patients during cardiopulmonary bypass is highly procoagulant", *Circulation*, vol.96, n. 10, pp3534–3541, 1997

- [4] Berckmans R J, Nieuwland R, Böing AN, “Cell- derived microparticles circulate in healthy humans and support low grade thrombin generation”, *Thieme Thrombosis and Haemostasis*, vol.85, n.4, pp. 639–646, 2001
- [5] Kireev D A, Popenko N Y, Pichugin A V, Panteleev M A, Krymskaya O V et al., “Platelet microparticle membranes have 50- to 100-fold higher specific procoagulant activity than activated platelets”, *Thrombosis and Haemostasis*, vol. 97, no.3, pp. 424-435, 2007
- [6] Wang Z T, Wang Z, Hu Y W, “Possible roles of platelet-derived microparticles in atherosclerosis”, *Atherosclerosis*, vol. 248, pp 10-16, 2016
- [7] Nieuwland R et al., “Cell-Derived Microparticles Generated in Patients During Cardiopulmonary Bypass Are Highly Procoagulant”, *Circulation*, vol. 96, no. 10, pp. 3534-3541, 1997
- [8] Suades R, Padro T, Vilahur G, Badimon L. Circulating and platelet-derived microparticles in human blood enhance thrombosis on atherosclerotic plaques. *Thrombosis and Haemostasis*, vol. 108, pp. 1208-19, 2012
- [9] Ramacciotti E, Hawley A, Farris D, Ballard N, Wroblewski S, Myers D, Henke P, Wakefield T, “Leukocyte- and platelet-derived microparticles correlate with thrombus weight and tissue factor activity in an experimental mouse model of venous thrombosis”, *Thrombosis and Haemostasis*, vol. 101, n. 4, pp.748-754, 2009
- [10] Suades R, Padró T, Vilahur G, Martín-Yuste V, Sabaté M, Sans-Roselló J, Badimon L, “Growing thrombi release increased levels of CD235a+ microparticles and decreased levels of activated platelet-derived microparticles. Validation in ST-elevation myocardial infarction patients.”, *Journal of Thrombosis and Haemostasis*, vol. 13, n. 10, pp. 1776-1786, 2015
- [11] Leytin V, Allen D J, Mykhaylov S, Mis L, Lyubimov E V, Garvey B, Freedman J, “Pathologic high shear stress induces apoptosis events in human platelets”, *Biochemical and Biophysical Research Communications*, vol. 320, no. 2, pp. 303-310, 2004
- [12] Miyazaki Y, Nomura S, Miyake T, Kagawa H, Kitada C, Taniguchi H, Komiyama Y, Fujimura Y, Ikeda Y, Fukuhara S "High Shear Stress Can Initiate Both Platelet Aggregation and

Shedding of Procoagulant Containing Microparticles" *Blood*, Vol. 88, No. 9, pp: 3456-3464, 1996

[13] Sheriff J, Tran P L, Hutchinson M, DeCook T, Slepian M, Bluestein D, Jetsy J, "Repetitive Hypershear Activates and Sensitizes Platelets in a Dose-Dependent Manner", *Artificial Organs*, vol. 40, no. 6, pp. 586-595, 2016

[14] Consolo F, Valerio L, Brizzola S, Rota P, Marazzato G, Vincoli V, Reggiani S, Redaelli A, Fiore G, "On the Use of the Platelet Activity State Assay for the In Vitro Quantification of Platelet Activation in Blood Recirculating Devices for Extracorporeal Circulation", *Artificial Organs*, vol. 40, no.10, pp 971-80, 2016

[15] Jesty J, Bluestein D, "Acetylated prothrombin as a substrate in the measurement of the procoagulant activity of platelets: elimination of the feedback activation of platelets by thrombin", *Analytical Biochemistry*, vol. 272, pp. 64-70, 1999

[16] Einav S, Dewey C F, Hartenbaum, H, "Cone-and-plate apparatus: a compact system for studying well-characterized turbulent flow fields", Springer, *Experiments in Fluids*, vol. 16 ,pp. 196–202, 1994

[17] Girdhar, G, Bluestein D, "Biological effects of dynamic shear stress in cardiovascular pathologies and devices", *Expert Review of Medical Devices*, vol. 5, n. 2, pp. 167–181, 2008

[18] Sims J P, Wiedmer T S, Esmon C T, Weissll H J, Shattil S J, "Assembly of the Platelet Prothrombinase Complex is Linked to Vesiculation of the Platelet Plasma Membrane", *Journal of Biological Chemistry*, vol. 264, no. 29, pp. 17049-17057, 1989

[19] Girdhar G et al., "Dynamic Shear Stress Induced Platelet Activation in Blood Recirculation Devices: Implications for Thrombogenicity Minimization", *American Society of Mechanical Engineers*, pp. 231–232, 2009

# Sommario

Nell'ultima decade, l'interesse per le micro-particelle piastriniche (PMPs) è aumentato in quanto alleate decisive per la prevenzione e il trattamento di disordini cardiovascolari. L'obiettivo di questo lavoro è verificare se le micro-particelle derivanti dalla membrana delle piastrine (PMPs) si comportino come agonisti dell'attivazione piastrinica e nel comparare il loro potenziale pro-coagulante con altri attivatori

## Introduzione

Le piastrine giocano un ruolo centrale nella normale emostasi, trombosi, emorragie e molte malattie cardiovascolari [1]. Si è scoperto che anche le micro-particelle generate dalla membrana piastrinica hanno un contributo pro-coagulante. Infatti, i livelli fisiologici di PMPs aumentano in diversi disturbi pro-trombotici ed infiammatori cronici e si sta indagando quali siano gli effetti su soggetti sani. La concentrazione di PMPs presenti comunemente nel sistema circolatorio, espressa come rapporto PMP/piastrine (PMP / PLT) è  $1 / 300 - 1 / 3000$ . Il ruolo delle PMPs nella trombosi è stato studiato come possibile marker al fine di identificare pazienti a rischio di disturbi vascolari [2]. Per questa ragione, negli ultimi decenni, ricercatori medici e biomedici si sono focalizzati sulle PMPs. [6] [5] [4] [7]. Comunque, un loro utilizzo clinico non è ancora stato stabilito dal momento che mancano metodologie standardizzate per l'analisi delle PMPs.

## Stato dell'arte

Diversi studi hanno mostrato che le PMPs, formatesi durante l'attivazione piastrinica, sono potenziali pro-coagulanti [3] [4]. Berckmans et al. [4], hanno dimostrato che, aggiungendo alte concentrazioni di PMPs nel plasma autologo, incrementa notevolmente la produzione di trombina. Infatti, Kireev et al. [5], dimostrarono che l'attività pro-coagulante della membrana delle PMPs è approssimativamente dalle 50 alle 100 volte più alta rispetto a quella delle piastrine attivate. Le PMPs, *in-vivo*, partecipano alla formazione del trombo. In uno studio clinico Nieuwland et al. dimostrarono che le PMPs formatesi in vivo supportano la formazione di trombina [7]. Difatti, Le PMPs giocano un ruolo rilevante anche nell'arteriosclerosi

promuovendo l'adesione delle piastrine sul sito endoteliale lesionato e promuovendo la placca arteriosclerotica all'interno del vaso ematico [6]. Fu riscontrato che le PMPs incentivano il deposito di fibrina sul vaso arteriosclerotico [8]. In particolare, le PMPs promuovono l'adesione e il deposito delle piastrine sul sito lesionato, in condizioni di alti sforzi di taglio, contribuendo alla crescita del trombo [9]. In fine, Suades et al., riscontrarono che il numero di PMPs è correlato positivamente al peso del trombo. Questi risultati suggeriscono che un'alta concentrazione di PMPs nel sangue promuove la coagulazione piastrinica, e confermano il coinvolgimento delle PMPs nella formazione dei trombi [10]. Analizzando gli effetti delle forze idrodinamiche sull'attivazione delle piastrine e sulla loro apoptosi, Leytin et al., dedussero che uno sforzo di taglio patologico ( $>117$  dyne/cm<sup>2</sup>) indusse l'attivazione delle piastrine e quindi la formazione delle PMPs. Invece, uno sforzo di taglio fisiologico (10–44 dyne/cm<sup>2</sup>) non indusse all'attivazione piastrinica [11]. Allo stesso modo, in uno studio condotto da Nomura et al. fu mostrato che l'esposizione delle piastrine ad alti sforzi di taglio ( $>108$  dyne/cm<sup>2</sup>) causò il rilascio delle PMPs. Al contrario, l'esposizione di queste a bassi sforzi di taglio (12 dyne/cm<sup>2</sup>) non causò alcun rilascio o aggregazione piastrinica. Inoltre, fu riportato che il livello di aggregazione piastrinica e il numero di particelle non mostrano differenze se testati con sangue intero o con piastrine lavate.

Sheriff et al. dimostrarono che lo sforzo di taglio oltre il quale si verifica l'attivazione piastrinica e il rilascio delle PMPs è intorno ai 60-70 dyne/cm<sup>2</sup>. Secondo questo studio, l'attività protrombinase registrata durante gli esperimenti di stimolazione meccanica fu causata maggiormente dalla presenza delle PMPs formatesi durante uno stimolo breve ed intenso e durante uno stimolo basso e duraturo [13].

### **Scopo del lavoro**

Lo scopo di questa tesi è stata l'analisi dell'impatto delle PMPs sull'attivazione piastrinica *in vitro*. Per raggiungere questo obiettivo sono stati messi a punto diversi e specifici protocolli per la rilevazione, produzione ed isolamento delle micro-particelle derivanti dalle piastrine. Una volta che le PMPs sono state isolate, è stata valutata l'interazione tra PMPs e piastrine. In seguito, è stata comparata l'attività delle PMPs in presenza di adenosin difosfato (ADP) e con sforzi di taglio differenti.

## **Materiali e Metodi**

**Preparazione delle piastrine:** 30ml di sangue di un volontario adulto furono raccolti tramite prelievo venoso. Il sangue fu poi centrifugato (Beckman GS-6R Centrifuge) con 270 RFC per 15 minuti collezionando il plasma arricchito di piastrine (PRP). Le piastrine, filtrate con il gel (GFP), furono ottenute tramite il sistema di cromatografia filtrazione-gel.

**Preparazione delle PMPs:** La sonicazione e la calcimicina sono state utilizzate sulle piastrine per promuovere la vescicolazione delle PMPs. Un sonicatore Brandson Model 4C15 fu usato per 10 secondi a 10 Watt su 350  $\mu$ l di GFP. La calcimicina A23187 [5 $\mu$ M] è stata aggiunta a 350  $\mu$ l di GFP. Un microscopio a scansione elettronica (SEM) e un microscopio a forza atomica (AFM) furono usati per accertare la presenza di PMPs. Le PMPs sono state isolate utilizzando una micro-centrifuga Eppendorf 5415 C; 1 ml di GFP sonicato è stato centrifugato con due differenti velocità in sequenza: 4000 rpm (1310 RFC) per 20 minuti, 6000 rpm (2940 RFC) per 20 minuti. La citometria a flusso (BD FACS Canto™) è stata impiegata prima dell'isolamento per verificare la presenza di PMPs e dopo l'isolamento per una conta delle PMPs. Il protocollo di rilevazione è stato ottimizzato tramite l'utilizzo di beads fluorescenti e la marcatura con Annessina V e antigene CD41.

**Platelet Activity State (PAS) Assay:** Il saggio PAS misura in tempo reale la formazione di trombina.

Il PAS è eseguito con GFP e utilizza pro-trombina acetilata (Ac-FIIa) come substrato per la trombina. Il metodo di protrombinase modificata permise una correlazione lineare tra lo stimolo applicato e la produzione di trombina, che è l'indice dell'attivazione piastrinica [14] [15]. I reagenti necessari per attuare questo saggio sono: una soluzione tube che contiene Fattore II acetilato, HBS:BSA, Cloruro di calcio ed una soluzione well che contiene HBS:BSA EDTA, Cromozina-TH. Il campione (25  $\mu$ l) è incubato con la soluzione tube (70  $\mu$ l) e fattore X (5  $\mu$ l) e dopo, aggiunto alla soluzione well (150  $\mu$ l) e rilevato da uno spettrofotometro (versamax).

**Hemodynamic Shearing Device (HSD):** L'HSD è uno strumento utilizzato per la generazione di sforzi di taglio specifici, uniformi e costanti sulle piastrine. L'HSD è geometricamente progettato per generare uniformi sforzi di taglio su ogni particella e combina la geometria di un cono (cone) con un viscosimetro piano (plate) e un viscosimetro Couette (ring) coassiale

cilindrico, come mostrato in **Figura I**. L'HSD è stato impiegato per generare sforzi di taglio fino a 70 dyne/cm<sup>2</sup> al fine di mantenere un flusso laminare, assenza di flussi secondari e garantire minimi effetti inerziali in regime dinamico [16] [17].

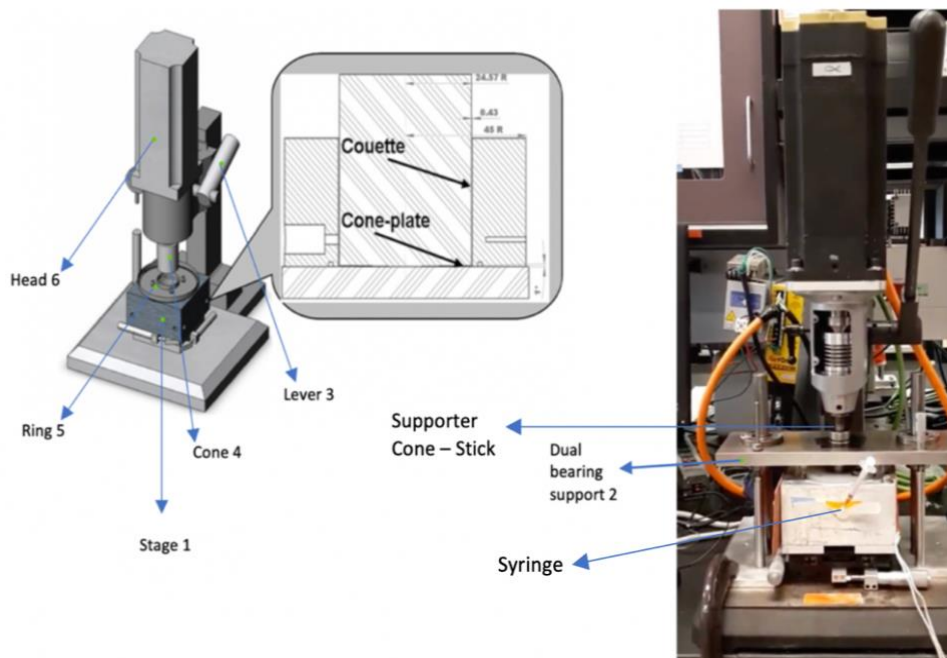


**Figura I: Presentazione schematica dell'HSD (sinistra), assemblaggio dell'HSD (destra). Cono, ring e plate sono fatti di UHMWPE**

### Esperimenti statici

**Effetti delle PMPs sull'attivazione piastrinica :** le PMPs furono aggiunte al GFP (piastrine a riposo) in due differenti rapporti di concentrazione PMP / PLT: 1 / 1000 (alta) e 1 / 5000 (bassa). Comunemente, la concentrazione di PMPs presente nel sistema circolatorio, espressa come rapporto PMP/piastrine (PMP / PLT) è 1 / 300 – 1 / 3000. Le PMPs da sole (PMP-only) furono diluite con platelet buffer (PB) con la stessa concentrazione in assenza di GFP. I campioni furono incubati per 0, 10, 30 e 60 minuti a 37°C. Infine, il saggio PAS fu utilizzato per stimare l'attivazione delle piastrine. Il GFP puro (GFP-only) fu usato come controllo negativo mentre il GFP sonicato come controllo positivo. I valori furono normalizzati rispetto alla massima produzione di trombina (GFP sonicato).

**Effetti delle PMPs sulla attivazione piastrinica in confronto a quelli dell'ADP:** l'ADP in quanto attivatore fisiologico fu usato come ulteriore controllo dell'attività delle PMPs. L'ADP fu comprato dalla Sigma Alderich (USA), aliquotato a 1mM e conservato a -20°C. GFP + PMPs, GFP + ADP, GFP + ADP + PMPs furono comparati per valutare il ruolo delle PMPs sull'attivazione piastrinica rispetto all'ADP. Le PMPs furono aggiunte al GFP-only (20'000 PLT/ $\mu$ l) in due differenti rapporti di concentrazione PMP / PLT: 1 / 1000 (alta) e 1 / 5000 (bassa). PMP-only furono diluite con platelet buffer (PB) con la stessa concentrazione in assenza di GFP. L'ADP fu aggiunta al GFP (20'000 PLT/ $\mu$ l) in due differenti concentrazioni: 10  $\mu$ M e 20  $\mu$ M. I campioni furono incubati per 0, 10, 30 e 60 minuti a 37°C. Infine, il saggio PAS fu utilizzato per stimare l'attivazione delle piastrine. Il controllo positivo e negativo furono rispettivamente il GFP sonicato e il GFP-only. I valori furono normalizzati rispetto alla massima produzione di trombina (GFP sonicato).

**Esperimenti dinamici:** le PMPs furono aggiunte al GFP-only (20'000 PLT/ $\mu$ l) in due differenti rapporti di concentrazione PMP / PLT: 1 / 1000 (alta) e 1 / 5000 (bassa). GFP + PMPs furono esposti, utilizzando l'HSD, a due differenti sforzi di taglio:

- Esperimento 1: 1: 30 dyne/cm<sup>2</sup> per 120 secondi
- Esperimento 2: 70 dyne/ cm<sup>2</sup> per 120 secondi

Anche in questo caso i campioni furono incubati per 0, 10, 30 e 60 minuti a 37°C. Infine, il saggio PAS fu utilizzato per stimare l'attivazione delle piastrine. I controlli per questo esperimento furono GFP sonicato, GFP-only e GFP+PMP non stimolato. I valori furono normalizzati rispetto alla massima produzione di trombina (GFP sonicato).

**Analisi statistica:** L'analisi statistica sui risultati ottenuti è stata eseguita con GraphPad Prism 8 (GraphPad Software, Inc., CA, USA). È stata verificata la distribuzione normale dei dati con un test di normalità Shapiro-Wilk. In caso di normalità della distribuzione, il test di analisi della varianza (ANOVA) a una via è stato utilizzato per verificare le differenze statisticamente significative. In caso contrario, il test di Brown-Forsythe e Welch (non parametrico) è stato utilizzato. La significatività statistica è considerata tale se il valore p è minore di 0.05.

## **Risultati**



**Attivazione piastrinica:** Le acquisizioni del SEM di piastrine trattate con sonicazione e calcimicina sono mostrate in **Figura II**. Mentre in **Figura 3** è presente un'acquisizione con l'AFM del campione prima dell'isolamento.

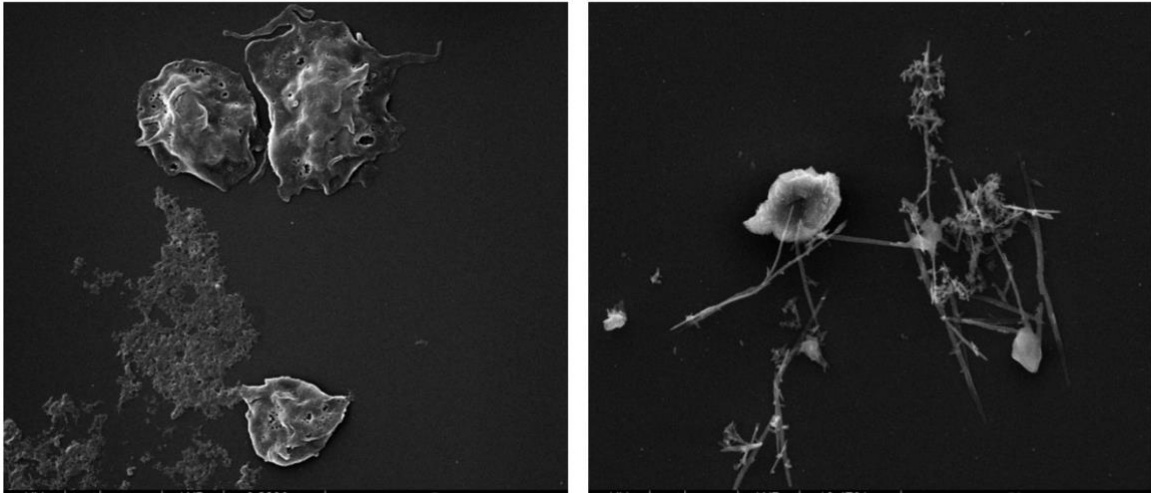


**Figura II:** Le piastrine sono attivate tramite sonicazione (sinistra), le piastrine sono attivate tramite Calcimicina (destra)

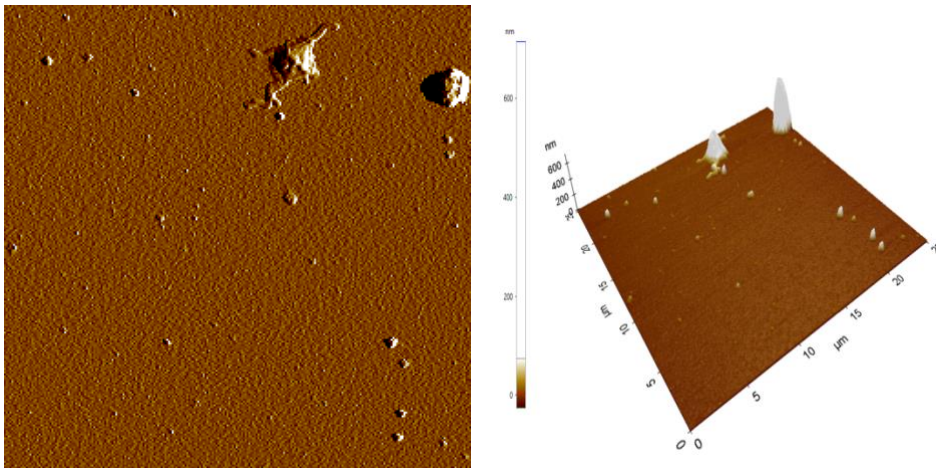


**Figura III:** Acquisizione tramite AFM con il metodo no-contact. Gli elementi più grandi sono le piastrine attivate, circondate da micro-particelle diffuse (sinistra). La stessa immagine con le scale di misura: 25x25x0.6  $\mu\text{m}$  (destra)

La sonicazione è risultata essere il miglior metodo per l'attivazione piastrinica. Infatti, la calcimicina rimarrebbe in soluzione anche dopo l'isolamento delle PMPs andando ad influenzare l'attivazione delle piastrine negli esperimenti successivi.

### Esperimenti statici:

#### Effetti delle PMPs sull'attivazione piastrinica

*rapporto di concentrazione 1 / 1000 e 1 / 5000 PMP / PLT:*

Un'analisi statistica fu condotta tra GFP + PMPs / PMP-only e il controllo negativo (GFP-only) ed è mostrata in **Figura IV**.

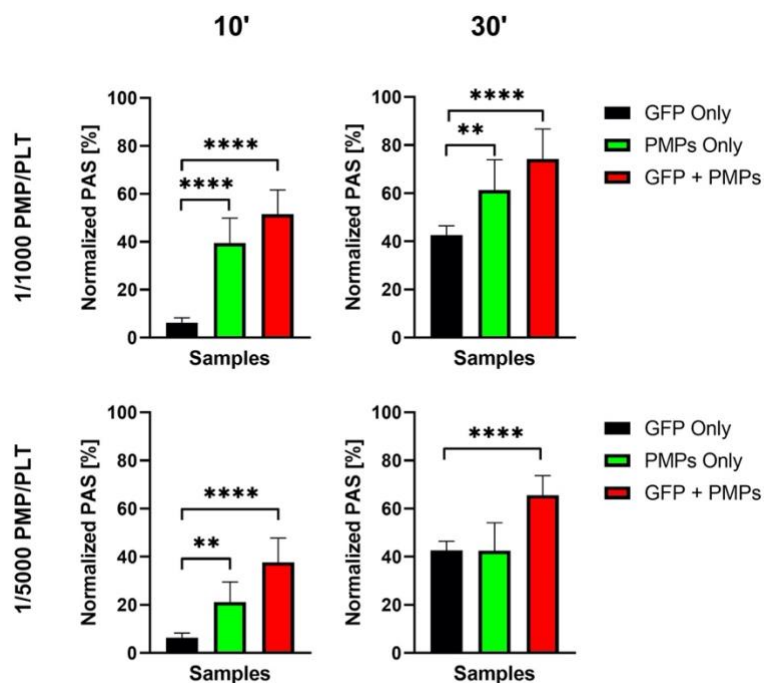


**Figura IV: Valori medi del saggio PAS (N=7,n=14). I dati sono mostrati come media ± DS.**

**Furono analizzati usando Brown-Forsythe e Welch ANOVA test.**

**\*p<0.05, \*\* p<0.01,\*\*\*\* p<0.0001**

Dopo 10 e 30 minuti di incubazione GFP + PMPs e GFP-only mostrarono differenze statistiche per entrambe le concentrazioni PMP / PLT utilizzate. Le PMP-only mostrarono significativa differenza rispetto al GFP-only dopo 10 minuti per entrambe le concentrazioni utilizzate, mentre

solo per la più alta concentrazione di PMPs fu riscontrata una differenza significativa rispetto al GFP-only dopo 30 minuti.

*Andamento della produzione di trombina nel tempo:* in **Figura V** sono mostrati gli andamenti della trombina prodotta dai diversi campioni nel tempo, per le due diverse concentrazioni di PMPs analizzate.

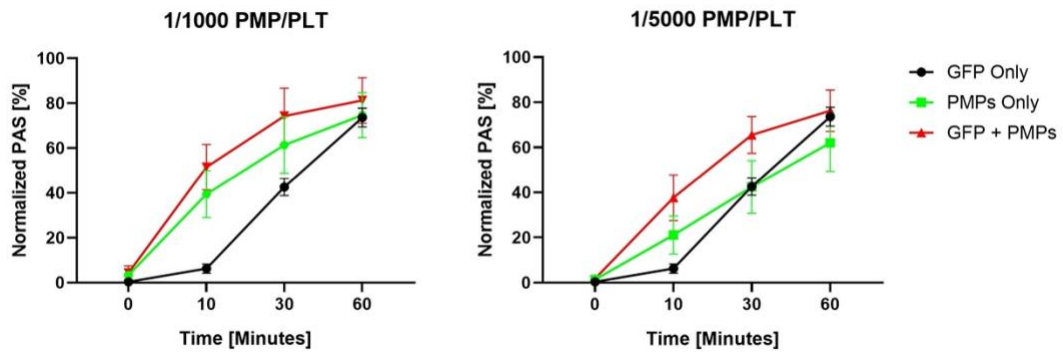
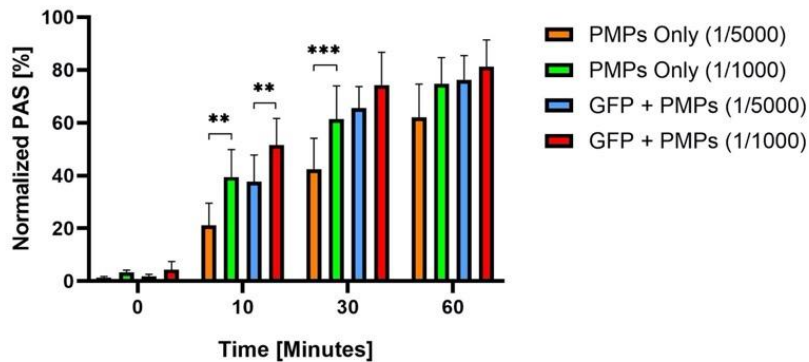


**Figura V: Produzione di trombina tracciata in funzione del tempo (N=7, n=4)**

A 60 minuti di incubazione il tasso di produzione di trombina tende a raggiungere lo stesso valore per tutti i campioni a causa dell'esaurimento dei reagenti la produzione. Ad ogni modo, la presenza di PMPs, da sole o in soluzione con il GFP, portano ad un più rapido raggiungimento della massima produzione di trombina.

*Confronto fra 1 / 1000 e 1 / 5000:* un'analisi statistica fu condotta fra i due diversi rapporti di concentrazione 1 / 1000 e 1 / 5000 PMP / PLT (**Figura VI**).



A 10 e 30 minuti fu stata riscontrata una differenza significativa tra le PMPs-only nei due diversi rapporti di concentrazione. GFP + PMPs mostrarono una differenza significativa tra 1 / 1000 e 1 / 5000 solo a 10 minuti. Il tasso di produzione della trombina è quindi dipendente dalla concentrazione di PMPs utilizzate.

### Effetti delle PMPs sulla attivazione piastrinica in confronto a quelli dell'ADP

*Rapporti di concentrazione 1 / 1000 e 1 / 5000 PMP / PLT:* Siccome le PMPs si dimostrarono essere procoagulanti, il loro effetto pro-coagulante fu messo a confronto con e in combinazione

**Figura VI: Confronto fra PMP / PLT 1 / 1000 e 1 / 5000 (N=7, n=14). I dati sono mostrati come media ± DS.**

**Furono analizzati usando Brown-Forsythe e Welch ANOVA test. \*\* p<0.01,\*\*\* p<0.001**

a quello dell'ADP. Un'analisi statistica fu condotta fra GFP + PMPs, GFP+ADP e GFP + PMPs + ADP. I risultati sono mostrati in **Figura VII**.

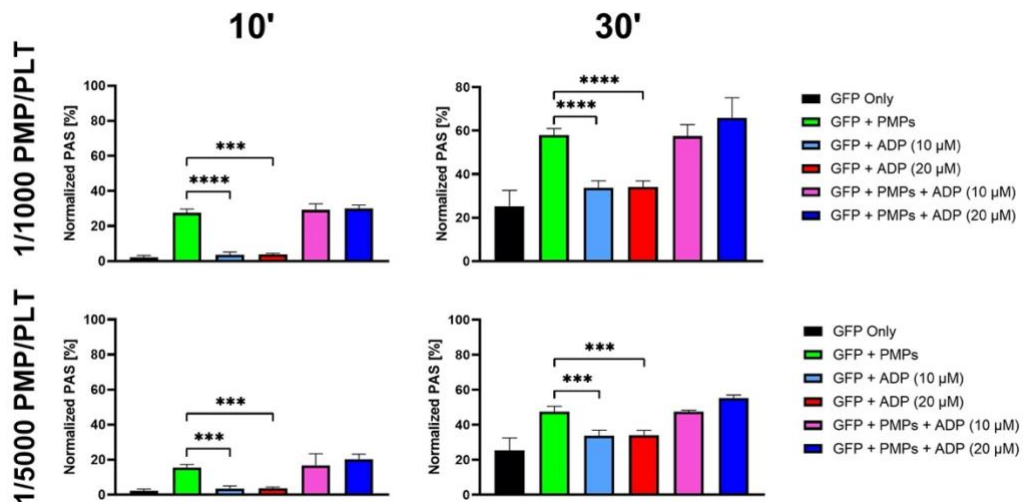


**Figura VII: Medie dei valori del saggio PAS (N=5, n=10). I dati sono mostrati come media ± DS.**

**Furono analizzati usando Brown-Forsythe e Welch ANOVA test. \*\*\* p<0.001,\*\*\*\* p<0.0001**

A 10 e 30 minuti differenze significative furono riscontrate tra GFP + PMPs (1 / 1000 and 1 / 5000) e GFP+ADP [10 2 20 μM]. GFP + PMPs indusse ad una produzione di trombina maggiore di quella di GFP+ADP.

### Esperimenti dinamici

*Comportamento pro-trombotico delle PMPs in presenza di sforzi di taglio:* GFP + PMPs, in rapporto di concentrazione 1 / 1000 e 1 / 5000 PMP / PLT, furono soggetti a differenti sforzi di taglio per replicare condizioni fisiologiche e patologiche. Un'analisi statistica fu condotta tra i campioni stimolati e non stimolati, e tra campioni soggetti a differenti shear. I risultati sono riportati in **Figura VIII**.

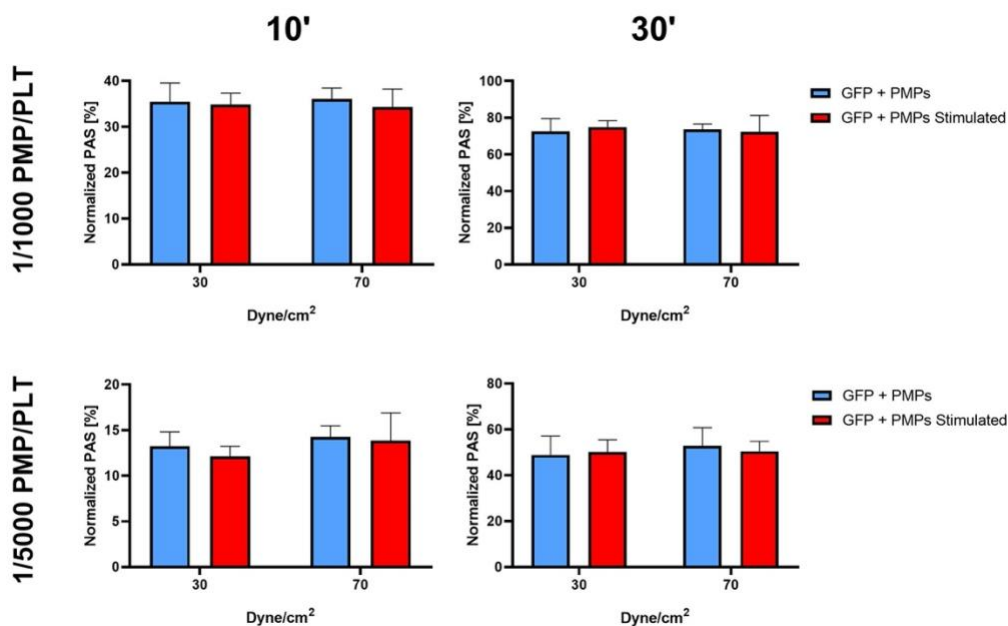


**Figura VIII: Medie dei valori del saggio PAS (N=5, n=10). I dati sono mostrati come media ± DS. Furono analizzati usando Brown-Forsythe e Welch ANOVA test.**

Per nessuna delle concentrazioni utilizzate furono riscontrate differenze significative fra campioni stimolati e non stimolati. Inoltre, nessuna differenza significativa è stata riscontrata fra GFP + PMPs stimolato a 30 dyne/cm<sup>2</sup> e stimolato a 70 dyne/cm<sup>2</sup>, per entrambe le concentrazioni di PMPs utilizzate.

### Discussione

*Trombogenicità testata in condizioni statiche:* le PMPs, in soluzione con le piastrine, sono in grado di generare un tasso di trombina maggiore di quello generato dalle piastrine a riposo. La trombina prodotta dalle PMPs risultò essere dipendente dalla concentrazione di PMPs e dal tempo di incubazione. I nostri risultati trovarono un riscontro in letteratura [4] [6] [7]. Un altro risultato interessante è stato il fatto che la produzione di trombina risultò dipendente dalla

concentrazione di PMP. Lo stesso risultato è stato raggiunto da Kireev et al. [5]. Infatti, notarono che la produzione di trombina aumentava rapidamente con l'aumento della concentrazione di PMPs aggiunte.

*Trombogenicità delle PMPs confrontata con un attivatore fisiologico:* l'attività pro-coagulante delle PMPs si dimostrò essere superiore a quella promossa dall'ADP sull'attivazione delle piastrine. Secondo P.J Sims et al., l'ADP è un agonista debole della attivazione piastrinica [18]. Questo ci porta a supporre che le PMPs siano degli attivatori forti capaci di sormontare l'attività pro-coagulante dell'ADP in queste condizioni.

*Trombogenicità delle PMPs testate in condizioni dinamiche:* sforzi di taglio costanti furono applicati per simulare condizioni dinamiche. 30 dyne/cm<sup>2</sup> simula uno sforzo di taglio fisiologico mentre 70 dyne/cm<sup>2</sup> simula uno sforzo oltre le condizioni fisiologiche (range fisiologico venoso-arterioso 1-50 dyne/cm<sup>2</sup>) [19]. Piastrine a contatto con le PMPs, stimolate e non, non mostrano differenze significative nel tempo per entrambi gli sforzi applicati. Secondo Leytin et al., uno sforzo di taglio fisiologico (30 dyne/cm<sup>2</sup>) non porta all'attivazione delle piastrine [12].

Nel caso non fisiologico fu assunto che l'effetto dello sforzo applicato, 70 dyne/cm<sup>2</sup>, era troppo basso per essere distinto dall'azione delle PMPs già presenti. Infatti, Sheriff et al., documentarono che la soglia di attivazione per l'attivazione delle piastrine è intorno ai 70 dyne/cm<sup>2</sup> e che il numero di piastrine attivate è proporzionale dall'intensità dello sforzo applicato [12]. Perciò le PMPs create per l'effetto dello sforzo di taglio applicato non diedero un contributo significativo all'azione delle PMPs aggiunte prima della stimolazione.

In conclusione, dal primo esperimento abbiamo determinato che l'azione delle PMPs è pro-coagulante. Successivamente, dimostrammo che le PMPs hanno un'alta attività pro-coagulante rispetto a quella dell'ADP. In condizioni dinamiche, fu stabilito che l'attivazione piastrinica, in presenza di una concentrazione di PMPs aggiuntiva, non fu influenzata dalla presenza di uno sforzo di taglio costante, fino a 70 dyne/cm<sup>2</sup>.

## **Conclusioni**

Nell'ultima decade il ruolo delle PMPs è cambiato da secondario a fondamentale nell'ambito cardiovascolare. Inoltre, nuove funzioni sono continuamente affibbate alle PMPs. In questo progetto la funzione di elementi pro-coagulante è stata indagata. Il nostro studio ha mostrato che:

- (1) Le PMPs agiscono come fattori pro-coagulanti
- (2) Il potenziale trombogenico delle PMPs è superiore rispetto a quello dell'ADP
- (3) La presenza di un'alta concentrazione di PMPs rende l'effetto degli sforzi di tagli trascurabile fino a 70 dyne/cm<sup>2</sup>

La maggiore limitazione di questo progetto è che il nostro approccio è in vitro, usando GFP, il quale non replica completamente le condizioni fisiologiche. Inoltre, il saggio PAS non permise di testare concentrazioni di PMPs maggiori (patologiche) a causa della rapida saturazione.

Tra i progetti futuri pianificammo di fare una comparazione fra l'effetto dello stimolo meccanico sulle piastrine e l'effetto delle PMPs sulle piastrine e confrontare i due stimoli separatamente. Inoltre, siccome in patologie come gravi stenosi o in presenza di device impiantati (MCS) gli sforzi di taglio raggiungono picchi di 1000 e 2000 dyne/cm<sup>2</sup>, pianificammo di replicare tali stimoli al fine di ricreare simili situazioni patologiche. Questi due set di esperimenti furono temporaneamente rimandati a causa dell'inevitabile situazione causata dal COVID-19.

#### **Bibliografia:**

- [1] A. D. Michelson, "Platelet Function Testing in Cardiovascular Diseases," *Circulation*, vol. 110, no. 19, pp. 489–93, 2004
- [2] Perrotta PL, Parsons J, Rinder HM, Snyder EL, "Platelet Transfusion Medicine" In *Platelets*, Elsevier, pp 1275-1303, 2013
- [3] Nieuwland R, Berckmans R J, Rotteveel-Eijkman R C, et al., "Cell-derived microparticles generated in patients during cardiopulmonary bypass is highly procoagulant", *Circulation*, vol.96, n. 10, pp3534–3541, 1997
- [4] Berckmans R J, Nieuwland R, Böing AN, "Cell- derived microparticles circulate in healthy humans and support low grade thrombin generation", *Thieme Thrombosis and Haemostasis*, vol.85, n.4, pp. 639–646, 2001
- [5] Kireev D A, Popenko N Y, Pichugin A V, Panteleev M A, Krymskaya O V et al., "Platelet microparticle membranes have 50- to 100-fold higher specific procoagulant activity than activated platelets", *Thrombosis and Haemostasis*, vol. 97, no.3, pp. 424-435, 2007

- [6] Wang Z T, Wang Z, Hu Y W, “Possible roles of platelet-derived microparticles in atherosclerosis”, *Atherosclerosis*, vol. 248, pp 10-16, 2016
- [7] Nieuwland R et al., “Cell-Derived Microparticles Generated in Patients During Cardiopulmonary Bypass Are Highly Procoagulant”, *Circulation*, vol. 96, no. 10, pp. 3534-3541, 1997
- [8] Suades R, Padro T, Vilahur G, Badimon L. Circulating and platelet-derived microparticles in human blood enhance thrombosis on atherosclerotic plaques. *Thrombosis and Haemostasis*, vol. 108, pp. 1208-19, 2012
- [9] Ramacciotti E, Hawley A, Farris D, Ballard N, Wroblewski S, Myers D, Henke P, Wakefield T, “Leukocyte- and platelet-derived microparticles correlate with thrombus weight and tissue factor activity in an experimental mouse model of venous thrombosis”, *Thrombosis and Haemostasis*, vol. 101, n. 4, pp.748-754, 2009
- [10] Suades R, Padró T, Vilahur G, Martin-Yuste V, Sabaté M, Sans-Roselló J, Badimon L, “Growing thrombi release increased levels of CD235a+ microparticles and decreased levels of activated platelet-derived microparticles. Validation in ST-elevation myocardial infarction patients.”, *Journal of Thrombosis and Haemostasis*, vol. 13, n. 10, pp. 1776-1786, 2015
- [11] Leytin V, Allen D J, Mykhaylov S, Mis L, Lyubimov E V, Garvey B, Freedman J, “Pathologic high shear stress induces apoptosis events in human platelets”, *Biochemical and Biophysical Research Communications*, vol. 320, no. 2, pp. 303-310, 2004
- [12] Miyazaki Y, Nomura S, Miyake T, Kagawa H, Kitada C, Taniguchi H, Komiyama Y, Fujimura Y, Ikeda Y, Fukuhara S "High Shear Stress Can Initiate Both Platelet Aggregation and Shedding of Procoagulant Containing Microparticles" *Blood*, Vol. 88, No. 9, pp: 3456-3464, 1996
- [13] Sheriff J, Tran P L, Hutchinson M, DeCook T, Slepian M, Bluestein D, Jetsy J, “Repetitive Hypershear Activates and Sensitizes Platelets in a Dose-Dependent Manner”, *Artificial Organs*, vol. 40, no. 6, pp. 586-595, 2016
- [14] Consolo F, Valerio L, Brizzola S, Rota P, Marazzato G, Vincoli V, Reggiani S, Redaelli A, Fiore G, “On the Use of the Platelet Activity State Assay for the In Vitro Quantification of



Platelet Activation in Blood Recirculating Devices for Extracorporeal Circulation”, *Artificial Organs*, vol. 40, no.10, pp 971-80, 2016

[15] Jesty J, Bluestein D, “Acetylated prothrombin as a substrate in the measurement of the procoagulant activity of platelets: elimination of the feedback activation of platelets by thrombin”, *Analytical Biochemistry*, vol. 272, pp. 64-70, 1999

[16] Einav S, Dewey C F, Hartenbaum, H, “Cone-and-plate apparatus: a compact system for studying well-characterized turbulent flow fields”, Springer, *Experiments in Fluids*, vol. 16 ,pp. 196–202, 1994

[17] Girdhar, G, Bluestein D, “Biological effects of dynamic shear stress in cardiovascular pathologies and devices”, *Expert Review of Medical Devices*, vol. 5, n. 2, pp. 167–181, 2008

[18] Sims J P, Wiedmer T S, Esmon C T, Weissll H J, Shattil S J, “Assembly of the Platelet Prothrombinase Complex is Linked to Vesiculation of the Platelet Plasma Membrane”, *Journal of Biological Chemistry*, vol. 264, no. 29, pp. 17049-17057, 1989

[19] Girdhar G et al., “Dynamic Shear Stress Induced Platelet Activation in Blood Recirculation Devices: Implications for Thrombogenicity Minimization”, *American Society of Mechanical Engineers*, pp. 231–232, 2009

# 1. Introduction

The blood circulating in the human body contains also cell membrane microparticles derived from platelets, blood cells and endothelial cells, called also microvesicles. Microparticles (MPs) are sub-micrometer sized vesicles released from cell membranes in response to activation or apoptosis. Among them, platelet-derived MPs (PMPs) are believed to account for the majority of circulating MPs in healthy subjects [1]. In 1967 Peter Wolf first identified the PMPs [2]. Platelets release microparticles whether they are stimulated with agonists such as thrombin, collagen, or calcium ionophore A23187 or whether exposed to high-stress shear forces [3]. A non-physiological shear stress is often verified in presence of mechanical circulatory support (MCS). Platelets activated by these mechanisms release PMPs which could be involved in high incidence of thromboembolic events in MCS devices [4]. PMP level increases also in several prothrombotic and inflammatory disorders. Commonly, the number of PMPs circulating in the human blood system are in the concentration ratio PMPs /platelets equal to 1/300 – 1/3000, considering an average of 300'000 platelets/ $\mu$ l in physiological conditions. PMPs are also detectable in the serum of healthy donors, thus it is not excluded that PMPs have effects also in healthy subjects.

In these clinical settings, PMP count and metrics to detect their interaction with platelets may be useful for identifying patients at risk for vascular disorders [5]. For this reason, medical and biomedical research has focused on PMPs in the last decade. However, their clinical use is not fully established, because standardized methodologies for PMP analysis are lacking [6]. The present thesis project aims to investigate the role of PMPs on platelet activation and therefore their thrombogenic effect in static and dynamic conditions. In addition, we explored methods for producing, locating, isolating and storing the PMPs.

In this study we have developed an experimental protocol to induce production and to detect the PMPs by using the sonication and the flow cytometry respectively. The protocol was optimized with the use of beads to distinguish PMPs from platelets based on size and with markers as

specific antibodies and annexin V to precisely gate the PMPs. PMPs were isolated from platelets by centrifugation. Isolated PMPs were incubated in solution with quiescent platelets in static condition. The activation level of platelets was measured by means of thrombin production using the Platelet Activity State (PAS) assay. The results were observed after different incubation periods of the solution and then compared with different nature of control: quiescent platelets, maximum activation platelets and platelets activated by ADP.

Later on, the hemodynamic shearing device (HSD) was instead used to produce a constant and homogeneous shear on platelets in solution with the PMPs. Two different shear levels acted on platelets and PMPs to simulate physiological and non-physiological environment in dynamic conditions. PAS assay was utilized to measure the level of activation induced by stimulated and non-stimulated samples. Significant differences were then investigated by performing statistical analysis.

## 2. Clinical background

### 2.1 Blood

Human blood is a liquid mixture composed of cellular elements, colloids and crystalloids [7] with a temperature of around 38°C; one degree higher than body temperature [8]. The average human adult with a weight of 70 kg (154 lb) has more than 5 liters circulating around the body [8] [9].

It is also composed by different cell types, each of which is responsible for specific tasks. These cells can be isolated into three layers by the process of centrifugation given their different density values. These isolation of blood components was developed in 1960 [5], and centrifuge protocols have become highly standardized within laboratories, where two principal variables can be varied: relative centrifugation force (RCF) and spinning time [10] [11].

By using this method, it is possible to separate the cell types according to their density as follows **(Figure 1)**:

- i) The red layer on the bottom contains Red Blood Cells (RBCs)
- ii) The middle white layer is composed by White Blood Cells (WBCs). It is also known as Buffy Coat.
- iii) The straw-colored fluid on the top is the plasma and platelets (around 60% of blood)

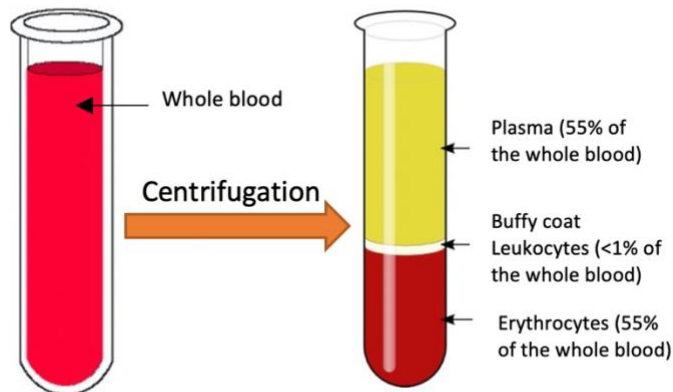


**Figure 1: Blood three layers after the centrifuge process**

- RBCs, also known as erythrocytes, are biconcave discoid shape cells without a nucleus or mitochondria. These characteristics allow RBCs to store hemoglobin, the oxygen-binding protein [9] [12]. They have a diameter ranging from 7.5 to 8.7  $\mu\text{m}$ , and a thickness of around 1.7 to 2.2  $\mu\text{m}$ . RBCs are extremely deformable and elastic, as they are exposed to shear forces while traveling through the vascular system [12] [13]. They are highly abundant in the bloodstream, reaching a concentrations of 4.3-5.9 million/ $\mu\text{l}$  in males and 3.5-5.5 million/ $\mu\text{l}$  in females [3], for a total number of circulating RBCs of approximately  $2.5 \times 10^{13}/\mu\text{l}$  [14]. It is no surprise that RBCs are essential not only for gas transport and cellular respiration, but also for inflammation and coagulation [12].
- WBCs, also known as leukocytes, are immune cells that play a fundamental role in battling infection. Their normal concentration in blood can vary between 4000 and 10000/ $\mu\text{L}$ . There are different types of WBCs characterized by different sizes, properties and functions. Broadly, they are divided into two groups according to the presence or absence of granules in their cytoplasm:
  - i) Granulocytes; including basophils, eosinophils and neutrophils.
  - ii) Agranulocytes; including lymphocytes (T cells, B cells and natural killer cells) and monocytes.

In terms of these study, we will focus on platelets, which will be described in more detail in the next section.

## **2.2 Platelets**

Platelets, also called thrombocytes, were first described as disk-like structures by Osler in 1873 [15]; their anatomical structure and role in hemostasis and experimental thrombosis was first described by Giulio Bizzozero in 1882 [16]. They are small subcellular fragments with a dimension of 1 to 4  $\mu\text{m}$ . Their typical inactivated discoid form is given by an internal coil, formed by rigid and hollow polymers called microtubules. These microtubules are composed of 13 heterodimeric tubulin subunits ( $\beta 1$ ,  $\beta 2$ ,  $\beta 4$  and  $\beta 5$ ) arranged in a head-to-tail alignment, called protofilaments [17]. Furthermore, platelets have a half-life of 7-10 days and their concentration in blood is between 150 and  $450 \times 10^9/\text{L}$  [18][19].

Platelets originate from megakaryocytes (MKs) at a rate of around  $1 \times 10^9$  platelets/day [20][21]. MKs have a single multi-lobulated and polyploid nucleus [20][21], and they are one of the largest and scarcest cells in the bone marrow. MKs diameters range from 50 to 150  $\mu\text{m}$  [21] and according to Nakeff and Maat (1974), they represent about 0.01% of nucleated bone marrow cells [22]. In addition to bone marrow, they have also been found in the lungs and peripheral blood, and in the fetal liver and yolk sac in early development during megakaryopoiesis [23]. The mechanism by which platelets are formed and released from MKs cell is not fully understood. However, several models of platelet production have been proposed; platelet budding, cytoplasmic fragmentation via the demarcation membrane system (DMS) and proplatelet formation.

In terms of their function, platelets play a role in several processes such as inflammation, tumor metastasis, infection and other cellular modulations. They primarily function as regulators of hemostasis and participants in the coagulation process, which will be described thoroughly next.

### **Platelets Granules**

In particular, platelets influence inflammatory process and have interactions with the immune cells, particularly monocytes (through chemokines CCL [24]) and neutrophils (through chemokines CXCL [21]). In order to perform this function, platelets are able to release three types of granules:  $\alpha$ -granules, dense granules and lysosomal granules [25].

Each platelet contain around 50-80  $\alpha$ -granules with a diameter of 200-500 nm [25] [26].  $\alpha$ -granules contain many proteins and peptides involved in coagulation, platelet adhesion and aggregation, and inflammatory and immune responses [16]. One of the most important components of  $\alpha$ -granules is P-selectin, which is stored in resting platelets and moves quickly to platelet surface in case of activation (a similar mechanism happens in endothelial cells [27]) [28]. Once exposed on the surface, P-selectin is able to bind to its receptor on the monocyte and neutrophil surface, called P-selectin glycoprotein ligand-1 (PSGL-1). This binding allows for the recruitment and activation of leukocytes [26] [29] [30]. The number of binding sites for platelet P-selectin present on neutrophils has been estimated to be 10000-20000/cell [28]. In addition,  $\alpha$ -granules also contain chemokines such as PF4 (also known as CXCL4) and  $\beta$ -

thromboglobulin, which have a key function in inflammation; they are able to recruit and activate neutrophils, and inhibit neutrophil apoptosis [32] [33].

Another important component of platelets are dense granules. They appear as dense bodies on electron microscopy because of their great quantity of calcium and phosphate [26]. There are thought to 3 or 4 dense granules in each platelet [25], and have a diameter of 150 nm [26]. Dense granules contain more than 200 small molecules [25], including nucleotides (ATP and ADP), serotonin and cations ( $\text{Ca}^{2+}$  and  $\text{Mg}^{2+}$ ). One of these components, ATP, modulates inflammatory pathways by activating dendritic cells, while ADP is responsible for the positive feedback mechanism that activate platelets. Serotonin recruits neutrophils at inflammatory site, and cations support signal transduction processes [26].

Lastly, the third granules present in platelets are the lysosomal ones. They have a diameter of 200-250 nm and are involved in the inflammatory potential of platelets [26] and in proteins degradation [25].

As key parts of the immune system, they are key contributors in fighting infections. In particular, they can be used as a biomarker for infection, as many infections are associated with thrombocytopenia [34] [35]. Platelets are also able to interact with different kinds of cells, such as WBCs, and serve as a link between the immune cells and the complement system [33]. Platelets are characterized by the presence of Toll-like receptors (TLRs), which are capable of recognizing pathogens and granules, e.g.,  $\alpha$ , dense and lysosomal, and releasing many bactericidal proteins, e.g., kinocidins and defenses, that attack (directly or with the help of WBCs) micro-organisms [34].

### **Platelets in Tumors**

Platelets are also involved in tumor angiogenesis, metastasis and chemo-resistance [36]. This is a longstanding concept, as their critical role in tumor progression has been analyzed for more than 50 years and it has been shown that they have both positive and negative effects.

According to some studies, platelet count may be used as a tumor biomarker [37] [38]. It has been reported that patients with thrombocytosis in primary care have higher risk of cancer, and

patients with a platelet count greater than  $3.5 \times 10^{11}/L$  have an increase in risk of more than 3% for tumor formation after one year of observation [38].

On the other hand, platelets are not only a clinical ally in tumor formation, but have also non-beneficial roles in tumor angiogenesis, metastasis and chemotherapy. Platelets can be activated by tumors through tissue factors (TF). This activation can cause platelet-derived pro-angiogenic regulators to be higher, and platelets themselves can deliver angiogenic signals [38]. Furthermore, platelets also have relevant role in tumor metastasis by protecting cancer cells from several possible harm, such as shear stress and immune response by NK cells [38]. Finally, they are able to increase chemo-resistance in patients by secreting growth factors that can fight the anti-proliferative effects of chemotherapeutic drug and by maintaining tumor vasculature [36].

### 2.3 Coagulation process

Coagulation is a dynamic process [39] composed of a series of proteolytic events that are, for the most part, highly dependent on vitamin K (VK) [40] binding to the surface of activated platelets [41]. The concept of *coagulation cascade* or *waterfall* was introduced by Davie, Ratnoff and Macfarlane in 1964 which described this process like a cascade of proenzymes leading to the activation of downstream enzymes [42] [43].

Under normal conditions, the coagulation process is regulated by two pathways: pro-coagulant, which leads to clot formation, and anti-coagulant, which inhibits the cascade initiation. Anti-coagulant process is controlled by several inhibitory agents, among which the two most important ones are:

- **Antithrombin (AT)**. It is a heparin cofactor produced mainly in the liver. Primarily the molecule that is directly involved in inhibition during the coagulation cascade is Antithrombin III, whose name was reduced to Antithrombin [44]. Its principal effect in the coagulation cascade is the inhibition of the activation of several coagulation factors: factor IIa (first target), factor Xa, factor IXa and factor VIIa [45] [46]. Its action is increased by binding to glycosaminoglycans (GAG) of the endothelial surface, which carries heparin-like effects. A deficiency of AT leads to a reduction of thrombin and factor Xa inhibition, which in turn increases susceptibility to clot formation [45].



- = Protein C (PC). It is located on the surface of the endothelial cells, although its proenzyme is synthesized in the liver and circulates in plasma at 4 µg/ml. PC is a K-dependent coagulation factor and its physiological activation requires the binding of thrombin to thrombomodulin (TM), and binding of protein C to the endothelial protein C receptor (EPCR) [45]. Activated PC (APC) is able to maintain blood flow, safeguarding the integrity of the vasculature against injury and preventing thrombus formation [47]. To perform this task, APC assembles in macromolecular complexes with its cofactors, such as protein S [45], and cell receptors. In particular, they inactivate factors Va and VIIIa, thereby reducing the rate of thrombin and fibrin formation [45].

The balance between anti- and pro-coagulation mechanisms is disrupted whenever the pro-coagulation factors increase or the anti-coagulation factors decrease their activity. In addition, other causes of disrupted hemostasis are hypoxia, hyperthermia, metabolic acidosis, extracorporeal circulation, physiological disturbances, disturbances in primary/secondary hemostasis, the blood-foreign material interaction, vasculature injury, perioperative period, during critical illness or abnormalities in blood or plasma [39].

In these situations, two main processes occur at the same time: primary hemostasis and secondary hemostasis. The former refers to platelet adhesion, aggregation and platelet plug formation, while the latter refers to the insoluble fibrin deposition due to the coagulation cascade, which forms a mesh-like structure around the platelet plug [48].

Primary hemostasis starts immediately when there is damage to a vessel. It triggers vasoconstriction, which is the early response (within 30 minutes) used to stop blood flow and is localized to the injured area [49]. After injury, subendothelial extracellular matrix is exposed to the blood, and platelets adhere to it and limit the hemorrhage. This matrix contains different macromolecules such as collagen, von Willebrand factor (vWF), laminin and fibronectin, which serve as ligands for different platelets receptors [39] [50]. Among all of these, collagen type I and III are by far, the most potent mediators for platelet adhesion.

In the first phase, vWF, an adhesive protein [49] secreted by activated endothelial cells, is deposited on collagen fibers exposed at injury site [51] and acts as a bridge between endothelial collagen and platelet surface G-protein receptors, embedded in the phospholipid bilayer leading to the adherence of the platelets to the exposed sub-endothelium, with the contribution of

calcium ions [39]. The interaction between platelets and subendothelial cells is strongly dependent on local rheological conditions; at shear rate levels lower than 1000/s (e.g., in veins or larger arteries), platelet adhesion involves mainly collagen, fibronectin and laminin [50] [52]. However, at shear rates higher than 1000/s (e.g., in small arteries or capillaries) platelets bind directly to vWF (A1 domain) resulting in definitive arrest of platelets and the consequent thrombus formation [50] [52]. These platelet adhesion phenomenon involves tethering, rolling and stable adhesion, as it initiates a signaling cascade of tyrosine kinases, also with the support of several receptors for activation, such as thrombin receptors, ADP receptors, thromboxane receptors and GPIIb/IIIa [52]. In this way, the adhesion guides the platelet activation and the granule release, which in turn leads to the further activation of platelets [50].

Simultaneously, platelets are activated by several chemical and mechanical stimuli, called agonists [55]. During their activation phase, platelets undergo degranulation of  $\alpha$ - and  $\delta$ - (or dense) granules that release cytoplasmatic granules containing serotonin, platelet activating factors, adenosine diphosphate (ADP), adenosine triphosphate (ATP), thromboxane (TXA<sub>2</sub>) and calcium [39] [49] [54]. At the same time, the GPIIb/IIIa and P-selectin move from the  $\alpha$ -granules membrane towards the platelet membrane and support platelet aggregation [49] and anionic phospholipids in the platelet membrane move from the internal part of the platelet membrane to the external one causing their morphological change through extensive formation of pseudopods, as shown in **Figure 2** [57] [49].

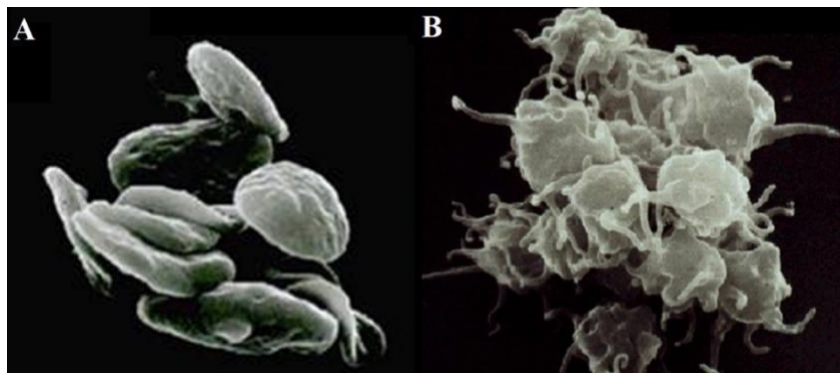


**Figure 2: Platelet conformational change occurring during the activation. The figure shows: inactivated discoid platelets (A) and activated platelets with pseudopods (B).**

Once platelets become activated and form pseudopods, they aggregate especially due to thromboxane A2 and ADP, which increase platelet aggregation and pseudopods themselves [39]. In particular, the ADP receptor interacts with specific receptors called P2Y1 and P2Y2, detected on platelet surface. In addition, the generation of thrombin enhances platelet aggregate formation [49] and the formed platelet plug can be made more stable by the deposition of fibrin.

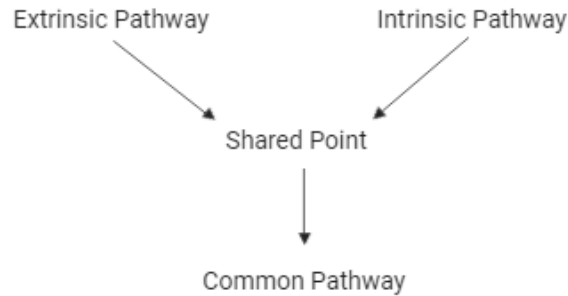


**Figure 3: Schematic representation of the three coagulation pathways**

Simultaneously, secondary hemostasis, also called coagulation cascade, has both an extrinsic and intrinsic pathway, depending on the trigger that causes it, with a shared point to continue coagulation (common pathway) (**Figure 3**). Although new insights demonstrate that this division is not so clear, the intrinsic-extrinsic pathway classification is still valid [39].

All three pathways occur on multiple spatial and temporal scales. The process involves element with different dimensions (from angstrom, micrometers, millimeters and centimeters) and happens with different timing (from microseconds, milliseconds, minutes and hours) [55]. They are based on the zymogens (inert enzyme precursors) indicated by Roman numerals, while the associated activated enzymes with the same Roman numeral joined the lowercase letter “a” to indicate the activated form. In addition, zymogens are produced mainly in the liver, with some exceptions like FIII, FVIII (both produced by endothelial cells) and FIV (or calcium ions that are free in plasma) [56]. Before their activation, they are inert pro-cofactors that are activated via limited proteolysis and are converted into their activated forms, the enzymes.

All the three different pathways are characterized by specific factors [56].

The extrinsic pathway includes:

1. Factor III, also called Tissue Factor (TF)
2. Factors VII, also known as stabilizing factor

The intrinsic pathway includes:

3. Factor XII, also known as Hageman factor
4. Factor XI, called also plasma thromboplastin antecedent

Finally, the common pathway includes:

5. Factor X, called also Stuart-Prower factor
6. Factor VIII or antihemophilic factor A
7. Factor V, known also as proaccelerin
8. Factor IX, named also Christmas factor
9. Factor II, named also prothrombin
10. Factor I or fibrinogen
11. Factor XIII, known also as fibrin-stabilizing.

Another important classification of coagulation factors relates to their family. This division is presented in **Table 1**:

Fibrinogen family	Vitamin K dependent	Contact family
<b>Fibrinogen</b>	Factor II	Factor XI
<b>Factor V</b>	Factor VII	Factor XII
<b>Factor VIII</b>	Factor IX	High molecular weight kininogen
<b>Factor XIII</b>	Factor X	Prekallikrein

**Table 1: The table represents the coagulation factor family classification**

Beyond the mentioned factors, vital roles are played by Vitamin K and Calcium (or FIV) during the coagulation process.

Vitamin K is fundamental in the formation of both the prohemorrhagic factors, ie., factor II (common for extrinsic and intrinsic pathways), VII (extrinsic pathway), IX (extrinsic pathway) and X (common for extrinsic and intrinsic pathways), and also for the antithrombotic ones, ie.,

protein C and protein S [58]. These factors, called K-vitamin coagulation factors (VKCFs), are characterized by multiple  $\gamma$  carboxyglutamic acid ( $\gamma$ -Gla) residues and undergo a post-translational modification which allows them to bind calcium and other bivalent positive ions, taking part in the coagulation process. Furthermore, Vitamin K is essential for the correct modification [39].

Regarding calcium, it is required for multiple steps in all three coagulation pathways [56]. Its contribution will be explored with all the three pathway (intrinsic, extrinsic and common) descriptions.

The extrinsic pathway is also known as Tissue Factor (TF) pathway and it is triggered by vessel damage. Upon vessel injury, blood is exposed to the transmembrane protein tissue factor (TF) that is normally not expressed by cells in direct contact with blood, but it is activated through a process in case of vessel trauma [59] [60]. The overall process is not fully understood, but it is thought that it could be caused by the expression of negatively charged phospholipids on the vessel walls.

The main extrinsic pathway modulator is the integral-membrane protein Tissue Factor, also called Thromboplastin, Coagulation Factor III, CD142 or Tissue Thromboplastin [41] [60]. It binds to the glycosylated protein FVIIa (that is activated by FT itself) with the contribution of  $Ca^{2+}$  ions forming the TF:VIIa complex [58] which acts as a strong enzyme with an activation potential higher than for the free FVIIa [59].

Then, the complex TF:VIIa allows the activation of two fundamental substrates, FIX into FIXa and FX into FXa [60]. In addition, these adhere to the membrane of activated platelets and increase the proteolytic activity of the complex itself [41]. In order to propagate the coagulation cascade, FXa and FIXa attach to cell membrane surfaces with their respective co-factors, FVa for the former and FVIIIa for the latter. This last step of the extrinsic pathway leads to a massive thrombin production, starting from prothrombin, and is the common point with the intrinsic pathway [60].

On the other hand, the intrinsic pathway is also known as plasma kallikrein-kinin system or contact pathway because it is due to the contact between blood and a foreign material, and the activation of zymogens is provoked by the contact with artificial, negatively charged surfaces [60] [61]. Its biological role is to participate in the pathophysiological responses to injury.

It is initiated by the conversion of FXII to FXIIa with a process that involves also nonenzymatic cofactor high-molecular-weight kininogen (HK) and plasma prekallikrein (PK). In more detail, when blood comes into contact with a foreign material, FXII is subject to a conformational change resulting in its activation. FXIIa in turn facilitates the passage from prekallikrein into kallikrein and a positive feedback process takes place: FXIIa activates PK and kallikrein activates FXII [60]. Thanks to the positive feedback loop and the contribution of calcium ions, the activation of factor XI to FXIa occurs which further activates the conversion of FIX into FIXa and, as consequence, the activation of FX (FXa). Finally, FXa leads to a massive thrombin generation (as a point in common with extrinsic pathway) [60].

A schematic representation of the contact pathway (until the conversion of prothrombin to thrombin) is reported in **Figure 4**.

Finally, the two pathways (extrinsic and intrinsic ones) meet each other in a common point from which the common pathway starts.

In particular, FXa and FVa interact with each other through an unknown process [62] and form the prothrombinase complex that leads to the conversion of prothrombin to thrombin (FII to FIIa). This in turn mediates the transformation of fibrinogen into insoluble fibrin through both enzymatic and non-enzymatic steps [59] [63]. In particular, the conversion is composed of different processes in which the first one is the formation of fibrin monomers and then their association into protofibrils. The subsequent aggregation of protofibrils into fibers allows the development of a fibrin meshwork that is fundamental for blood clot stability [64]. Furthermore, this last step also involves the activation of factor XIII (XIIIa) that covalently crosslinks fibrin polymers [39].

The fibrin generation process is strongly influenced by several aspects. The most common are [64]:

1. Thrombin concentration. A high concentration of thrombin leads to a dense and highly branched fibrin fiber network; on the other hand, a low concentration of thrombin leads to a coarse and unbranched fibrin fiber network.
2. Concentration of procoagulants.

3. Concentration of anticoagulants.
4. Concentration of metal ions; Henderson and colleagues reported that zinc released by activated platelets is able to bind fibrin (fibrinogen) and attenuates fibrinolysis; in addition, calcium ions lead to a more stable platelet-fibrin plug [54]).
5. Blood flow conditions.
6. Cell-derived microvesicles.

A schematic representation of the common pathway (until the conversion of prothrombin to thrombin) is reported in **Figure 4**.

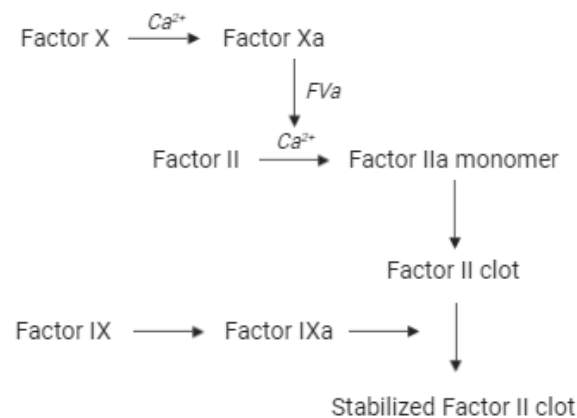


**Figure 4: Schematic representation of the common pathway**

## 2.4 Platelet-derived microparticles (PMPs)

Platelets play important roles in hemostasis. After vessel wall damage, platelets rapidly adhere, aggregate, and secrete compounds that activate other platelets. This results in the formation of a platelet plug (primary hemostasis). In addition, activated platelets support the formation of insoluble fibrin (coagulation, secondary hemostasis) that strengthens the platelet plug. In the 1940s it was known that platelets support clotting, because platelet-containing plasma clotted faster than platelet-poor plasma (PPP). High-speed centrifugation of PPP further prolonged the clotting time, suggesting that PPP contained another (subcellular) factor that facilitated clotting [65][66]. In 1967, Wolf demonstrated the presence of “coagulant material in minute particulate form,” which was present in “normal plasma, serum and fractions derived therefrom.” This material originated from platelets and was initially called *platelet dust* [67]. The ability of

platelets and platelet dust to facilitate coagulation was known in the early literature as platelet factor 3 (also called tissue factor or CD142) activity. We now know that platelet dust consists of small vesicles that are mainly platelet derived (PMPs). Especially during the last decade, there has been renewed interest in the potential role of PMP in health and disease. [68]

## 2.5 Origin of PMPs

Our current knowledge of the mechanisms underlying PMPs formation is still fragmentary. PMPs are formed upon platelet activation, during platelet aging and platelet destruction, and possibly directly from megakaryocytes. Activated platelets release PMPs *in vitro* when agonists (first messengers), e.g., collagen and thrombin, bind to their surface receptors. The process through which the PMPs are created is called *Vesiculation*; either *Shedding* or *Budding* (**Figure 5**). These receptors then transduce signals across the cell membrane and generate changes in levels of intracellular second messengers such as release of PMPs.

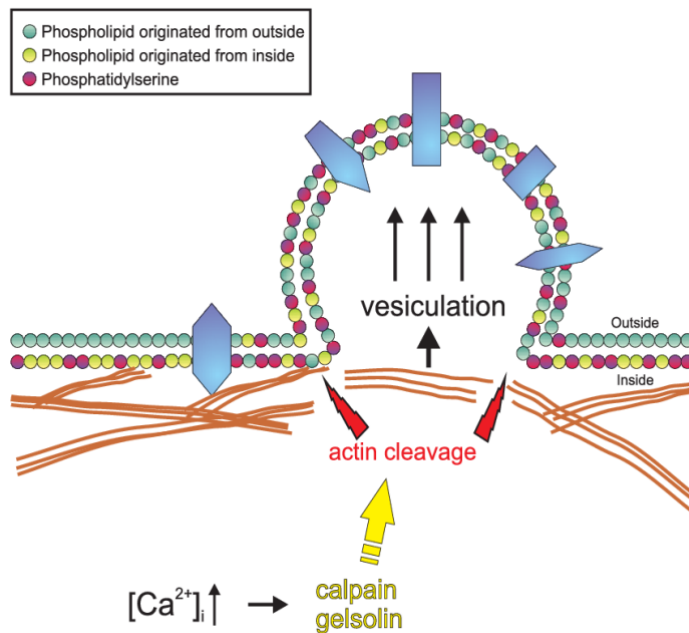


Figure 5: During platelet activation or apoptosis the cell membrane



Alternatively, platelets release PMPs when compounds are added that directly affect second messenger levels, e.g., calcium ionophores A23187 or ionomycin and phorbol esters.

PMPs release also occurs when platelets are activated in response to high shear conditions[69] [70], contact with surfaces of foreign bodies, complement system, or low temperatures [71] [72] [73]. Integrin  $\alpha$ IIBb3 is essential for interaction between platelets and the elevation of cytosolic calcium ( $\text{Ca}^{2+}$ ) levels is essential for the activation of platelets and release of PMPs. This  $\text{Ca}^{2+}$  elevation is a prerequisite for PMPs release during activation, and results in the activation of several enzymes that are calcium-dependent for their activity, such as calpains and protein kinase C (PKC).

## 2.6 Structure of PMPs

In steady state, the cell membrane is asymmetric regarding the composition and the distribution of phospholipids in its inner and outer layers; phosphatidylcholine and sphingomyelin are located in the outer layer, while phosphatidylserine (PS) and phosphatidylethanolamine (PE) are present in the inner layer. This asymmetric distribution of phospholipids in the membrane is maintained by a three-piece enzyme system: *flippase*, *floppase* and *scramblase*. The flippase translocates PS and PE from the outside to the inside of the bilayer membrane. The floppase translocates PS and PE from the inside to the outside of the bilayer membrane, while the scramblase transports of phospholipids between the two monolayers of the cell membrane. Successive mechanisms initiate PMPs formation during cell activation or other cell processes including apoptosis and senescence:

1. Calcium is released by the endoplasmic reticulum.
2. Calcium inactivates flippase and activates floppase and scramblase.
3. Calcium release leads to activation of two enzymes, *calpain* and *gelsolin*, which disrupt the anchorage between proteins and cytoskeleton.

This therefore results in membrane budding and microparticles shedding. The main mechanism of PMPs formation is thus calpain dependent [74]. PMPs enriched in PE and PS exposed on their outer surface are released [75].

Platelets and PMPs share glycoprotein (GP) receptors, such as GPIb (CD42b) platelet–endothelial cell adhesion molecule-1 (CD31), and the integrin  $\alpha$ IIb $\beta$ 3 (GPIIb-IIIa, CD41/CD61). In addition, subpopulations of PMPs can expose activation markers, including P-selectin (CD62P), and may bind fibrinogen [64]. The antigenic composition of PMPs and their functions are dependent on the mechanisms underlying their release. For example, PMPs released from platelets activated by collagen and thrombin expose integrin  $\alpha$ IIb $\beta$ 3 that binds fibrinogen, whereas PMP from complement C5b-9- activated platelets expose  $\alpha$ IIb $\beta$ 3, which does not bind fibrinogen [72] [75].

Activated platelets release two types of membrane vesicles — PMP, which are budded from the surface membrane, and exosomes (**Figure 6**). PMPs are heterogeneous in size, ranging between 0.1  $\mu$ m and 1.0  $\mu$ m. Their upper size limit may therefore be almost that of a platelet. Exosomes are smaller on average than PMPs and range in size between 40 nm and 100 nm. They are stored within  $\alpha$ -granules and become released during the secretion response.

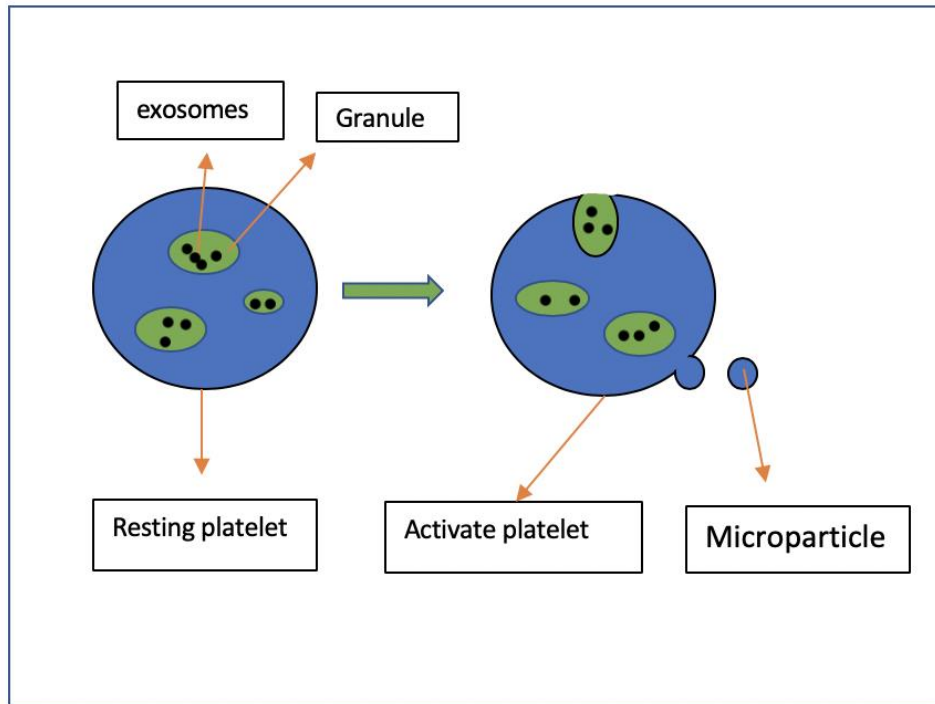


**Figure 6: PMPs and exosomes. A resting platelet (left) contains  $\alpha$  granules in which exosomes are stored. Physiological platelet agonists like thrombin, ADP or collagen, as well as non-physiological agonists such as calcium ionophores, activate the platelet (right)**

The activated platelet releases microparticles which are ‘blebbed’ from the plasma membrane. When the activated platelet secretes its granule contents, granule membranes fuse with the plasma membrane and their contents, including the exosomes, are released.

## **2.7 Functions of PMPs**

The number of PMPs from both platelets and other cells in circulation, and their composition and function are, at least in part, disease dependent. PMPs are supposed to be involved in different process such as coagulation, inhibition of coagulation, adhesion, carrier functions and clinical disorders. Studies show how PMPs can play an ulterior thrombogenic role in a pre-existing disease condition [78] [79], while others show how PMPs and platelets are involved in the inactivation of the factor V and factor VIIIa when vitamin C is activated [80]. PMPs bind

integrin  $\alpha$ IIBb3 *in vitro* and promote the platelets and leukocyte adhesion *in vitro* and flow condition [81] [82]. PMPs contains bioactive lipids such as arachidonic acid and platelet activating factor that can be transferred to endothelial cells. Thus, PMPs could activate other cells or modulate the activation status of a target cell.

## 2.8 Clinical disorder related to PMPs

Disorders associated with PMPs can be both *inherited disorders* or *acquired disorders*, and both *nonimmune mediate disorder* and *immune mediate disorder*. The most known inherited disorders are the “Scott Syndrome and Castaman Syndrome” and “Wiskott–Aldrich Syndrome” (WAS). The first disease, now referred to as *Scott Syndrome*, is an inherited disorder that is characterized by an impaired scrambling of phosphatidylserine [83], impaired release of PMPs [84] [85], a reduced number of binding sites for factor Va, and a decrease ability to support tense and prothrombinase complex formation. In the second case, WAS patients suffer from severe bleeding resulting from thrombocytopenia and aberrantly small platelets. Isolated WAS platelets release large numbers of PMPs, and platelets have strongly elevated levels of  $Ca^{2+}$ , compared with control. The aberrant increase in  $Ca^{2+}$  is thought to underlie both exposure of PS and release of PMPs [86]. There are different non-immune disorders relate to the PMPs: *Immune Thrombocytopenic Purpura (ITP)*, *Heparin-Induced Thrombocytopenia (HIT)*, *GPIIb-IIIa Antagonist-Induced Thrombocytopenia*, *Paroxysmal Nocturnal Hemoglobinuria (PNH)* and *Miscellaneous*.

In the first disease, ITP patients have decreased a platelet count, but elevated numbers of PMPs. It has been suggested that PMPs are involved in hemostasis, but ITP patients with additional neurological complications have higher PMPs levels than patients without these complications, suggesting that these patients are at risk for thromboembolic complication [87] [88].

Heparin-Induced Thrombocytopenia is a second well-known example of an acquired immunological disease associated with PMPs. Some patients, who receive heparin as an anticoagulant, produce antibodies directed against complexes of heparin and platelet factor 4. These antibodies, when bound to the heparin-platelet factor 4 complex, activate platelets via FC

receptors. The platelet aggregates secrete their granule contents, and release PMPs. HIT patients have low number of platelets, but elevated levels of procoagulant PMPs compared to healthy subjects, and these elevated levels have been associated with thrombotic complications [89].

GPIIb-IIIa Antagonist-Induced Thrombocytopenia is a third example of an autoantibody-induced thrombocytopenia with concurrent PMPs formation. About 0.2% of patients treated with the GPIIb-IIIa antagonis, i.e., eptifibatide or integrin, develop acute thrombocytopenia. When control blood is incubated with eptifibatide in the presence of either patient or control plasma, platelets bind IgG and release PMPs only in the presence of patient plasma [90].

The most well-known non-immune mediated disease is the Paroxysmal Nocturnal Hemoglobinuria (PNH). PNH is an acquired stem cell disorder, characterized clinically by hemolytic anemia and a hypercoagulable state that often leads to venous thrombosis in liver, abdominal organs, cerebrum, and skin. Blood cells of these patients partially or completely lack glycolipid-anchored membrane proteins. Two of these proteins, CD55 and CD59, are cell-surface complement inhibitors. *In vitro*, platelets from PNH patients generate approximately 10-fold more procoagulant PMPs when incubated with the complement C5b-9 complex compared to control platelets. The elevated numbers of PMPs in these patients have been associated with their hypercoagulable state [91].

Another non-immune condition is the *Miscellaneous*. Evidence that PMPs trigger coagulation directly *in vivo* is still scarce. Isolated PMPs from pericardial wound blood of patients undergoing cardiac surgery strongly initiate thrombus formation in a rat venous stasis model [92]. Also, PMPs infused into rabbit bloodstream shortened bleeding times [93]. In most study, however, only associations between changes in levels of circulating PMPs and the risk for thromboembolic events have been reported. Available research regarding PMPs is still reduced, but there is an increasing in research and clinical interest in the physiological role played by PMPs. Most of the research regarding PMPs is especially targeted to methods and protocol design for PMPs manipulations (to locate, count, and isolate PMPs).

## 3. State of the art

### 3.1 PMP detection

#### 3.1.1 Flow cytometry

Flow cytometry is undoubtedly the mostly used instrument to detect PMPs. Originally developed in the late 1960s, flow cytometry is a popular analytical cell-biology technique that utilizes light to count and profile cells in a heterogenous fluid mixture. Modern flow cytometers (Figure 7) are able to analyze many thousand particles per second in "real time" thanks specific optical properties on a cell-by-cell basis.

A flow cytometer has five main components:

1. Flow cell;
2. Measuring system;
3. Detector
4. Amplification system;
5. Computer for analysis of the signals.

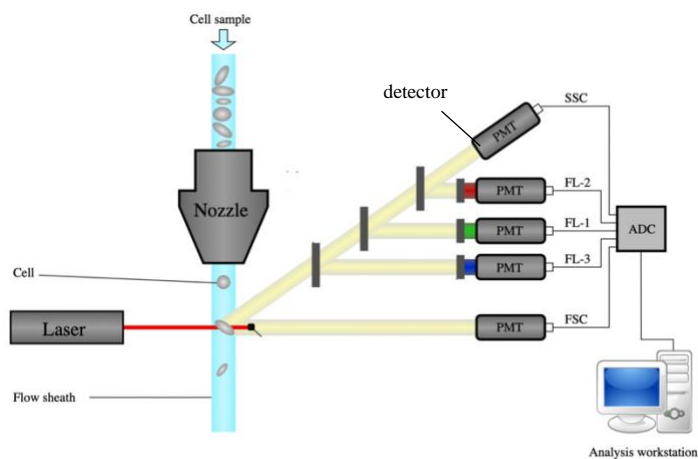


Figure 7: Schematic diagram of a flow cytometer, from sheath focusing to data acquisition

The **flow cell** has a liquid stream (sheath fluid), which carries and aligns the cells so that they pass single file through the light beam for sensing. In order to create a single file of cells, the suspension is injected in or sucked by the machine through a narrow tube.

The **measuring system** commonly uses measurement of impedance (or conductivity) and optical systems: lamps (mercury, xenon); high-power water-cooled lasers (argon, krypton, dye laser); low-power air-cooled lasers (argon (488 nm), red-HeNe (633 nm), green-HeNe, HeCd (UV)); diode lasers (blue, green, red, violet) resulting in light signals. Optical filters and dichroic mirrors are used to filter and move light to the detectors such as photomultiplier tubes (PMTs).

The **detector** and analog-to-digital conversion (ADC) system converts analog measurements of forward-scattered light (FSC) and side-scattered light (SSC) as well as dye-specific fluorescence signals into digital signals that can be processed by a computer.

The **amplification system** can be linear or logarithmic.

The process of collecting data from samples using the flow cytometer is termed 'acquisition'. Acquisition is mediated by a **computer** physically connected to the flow cytometer, and the software which handles the digital interface with the flow cytometer. The software is capable of adjusting parameters (e.g., voltage, compensation) for the sample being tested, and also assists in displaying initial sample information while acquiring sample data to ensure that parameters are set correctly.

A fluidics cart holds large fluid tanks necessary to operate and maintain the instrument. For sample acquisition, positive-pressure pumps in the fluidics cart send sheath fluid past a about 0.2- $\mu\text{m}$  filter to a pressurized interior reservoir inside the instrument called the *plenum*. The plenum maintains a nearly constant fluid level and dampens pump pulsation using a new dynamic feedback pressure control system designed to regulate the pressure. As a result, sheath flow rate does not vary with the level of fluid in the sheath cubitainer, and the reservoir automatically removes small air bubbles from the sheath supply. A high flow rate is generally used for measurements such as immunophenotyping, for which data is less resolved but is acquired more quickly. A lower flow rate is generally used in applications for which optimal resolution and sensitivity are critical (**Figure 8**).

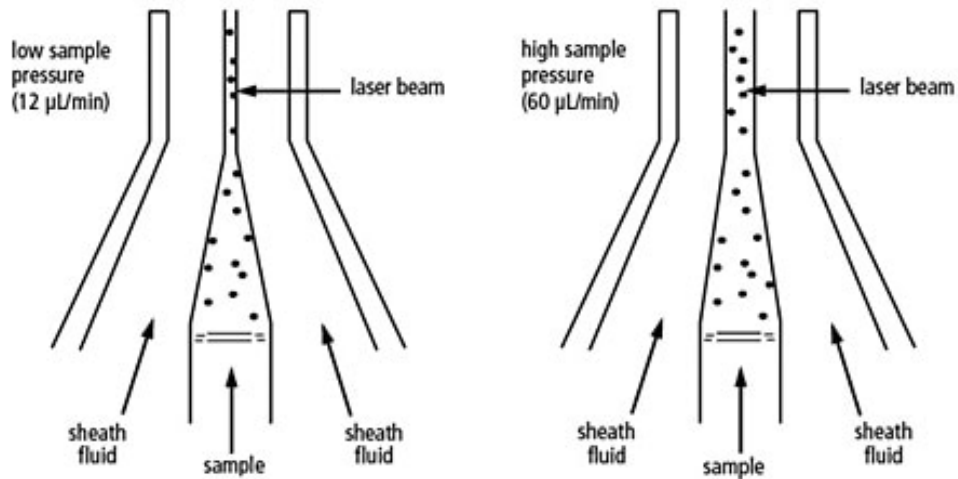


**Figure 8: Comparison of low and high sample pressure in flow cytometer**

Markers are used to detect specific cell population. To highlight platelets and PMPs different markers are used: Annexin A5 (Annexin V), Glycoprotein IIb/IIIa(antigen CD41), P-Selectin (antigen CD62P), Glycoprotein IIIa (antigen CD61), Glycoprotein Ib (antigen CD42). The mostly used are:

- Fluorescent conjugates of Annexin V are commonly used to identify activated platelets. The human vascular anticoagulant Annexin V is a 35–36 kDa,  $Ca^{2+}$ -dependent phospholipid-binding protein that has a high affinity for the anionic phospholipid phosphatidylserine (PS). In normal healthy platelets, PS is located on the cytoplasmic surface of the cell membrane. However, during the apoptosis and activation process, the cell membrane undergoes structural changes that include translocation of PS from the intracellular side of the plasma membrane to the outer leaflet (extracellular side) of the plasma membrane. On the PMPs the PS is commonly exposed. Thus, by detection of annexin V we are able to locate activated platelets and PMPs.
- Glycoprotein IIb/IIIa (GP IIb/IIIa or antigen CD41+) is an integrin complex found on platelets. It is a heterodimer composed of a heavy  $\alpha$ -chain and a light  $\beta$ -chain, which are linked by a single disulfide bond. Activated platelets present a conformational change in



GP IIb/IIIa that induces binding to fibrinogen. Thus, it is a convenient marker for the identification of platelets and PMPs.

- P-selectin (antigen CD62P) is a protein that acts as a cell adhesion molecule in activated platelets. It is stored in Weibel-Palade bodies and  $\alpha$ -granules and then, in response to inflammatory cytokines, translocated to the plasma membrane. P-selectin plays an essential role in the recruitment and aggregation of platelets at areas of vascular injury. Platelet activation result in “membrane flipping” where the inner walls of the granules are exposed on the outside of the membrane. P-selectin promotes platelet aggregation through platelet-fibrin and platelet-platelet binding.

The flow cytometer commonly used in laboratory activities is not able to detect elements smaller than 0.5  $\mu\text{m}$  [94]. To overcome to this issue there have been find tricks and methods. In the 2015, Poncelet et al. have published a review which sums up the smartest tricks to detect microparticles [95]. To provide the concentration or absolute count of MPs in a sample, counting beads of a known brightly fluorescent are commonly employed, across a wide range of excitation and emission wavelengths. When they are used as internal standard, the beads are added to each sample before the flow cytometry measurement. When used as external standard, the counting beads are processed as a sample at the same flow cytometry settings/conditions used for the samples. [96] [97]

### **3.1.2 Scanning Electron Microscopy (SEM)**

PMPs and exosomes can be visualized by electron microscopy. Through this methodology is possible to characterize the PMPs under a dimensional aspect [98]. A scanning electron microscope (SEM) is a type of electron microscope that produces images of a sample by scanning the surface with a focused beam of electrons. The electrons interact with atoms in the sample, producing various signals that contain information about the surface topography and the chemical composition of the sample with spatial resolution and surface sensitivity down to few nanometers [99]. The electron beam is scanned in a raster scan pattern, and the position of the beam is combined with the intensity of the detected signal to produce an image. In the most common SEM mode, secondary electrons emitted by atoms excited by the electron beam are

detected using a secondary electron detector. More in detail, accelerated electrons in an SEM carry significant amounts of kinetic energy, and this energy is dissipated as a variety of signals produced by electron-sample interactions when the incident electrons are decelerated in the solid sample. These signals include secondary electrons (that produce SEM images), backscattered electrons (BSE), diffracted backscattered electrons (EBSD that are used to determine crystal structures and orientations of minerals), photons (characteristic X-rays that are used for elemental analysis and continuum X-rays), visible light (cathodoluminescence--CL), and heat. Secondary electrons and backscattered electrons are commonly used for imaging samples: secondary electrons are most valuable for showing morphology and topography on samples and backscattered electrons are most valuable for illustrating contrasts in composition in multiphase samples (i.e. for rapid phase discrimination). X-ray generation is produced by inelastic collisions of the incident electrons with electrons in discrete orbitals (shells) of atoms in the sample. As the excited electrons return to lower energy states, they yield X-rays that are of a fixed wavelength (that is related to the difference in energy levels of electrons in different shells for a given element). Thus, characteristic X-rays are produced for each element in a mineral that is "excited" by the electron beam. SEM analysis is considered to be "non-destructive"; that is, x-rays generated by electron interactions do not lead to volume loss of the sample, so it is possible to analyze the same materials repeatedly. It is usually applied because of its ability to resolve smaller structures at a higher magnification than other techniques like light microscopy [100]. The scales of micrometer and nanometer are those we are interested in to map and analyze platelets and their microparticles.

### **3.1.3 Atomic Force Microscopy (AFM)**

Atomic force microscopy is a type of scanning probe microscopy that creates 3-dimensional topographic images with sub-nanometer resolution. The image is created by scanning the surface with a sharp tip with or without physical contact commonly indicated as contact mode and non-contact mode [101]. The AFM belongs to a series of scanning probe microscopes invented in the 1980s. This series started with the scanning tunneling microscope (STM), which allowed the imaging of surfaces of conducting and semiconducting materials. With the STM it

became possible to image single atoms on “flat” surfaces. The AFM has become the most important scanning probe microscope. The AFM allowed the imaging of the topography of conducting and insulating surfaces with atomic resolution. The AFM reaches 30 nm as lateral resolution and about 0.1 nm as vertical resolution. Almost any sample can be imaged, be it very hard (ceramic material) or very soft (human cells, individual molecules of DNA). In the non-contact mode, AFM provides a 3D profile of the surface on nanoscale, by measuring weak forces (Van der Waals forces, dipole-dipole interactions, electrostatic forces) between a sharp tip (<10 nm and connected to the cantilever) and the surface at very short distance (0.2-10 nm probe-sample separation). The tip is supported on a flexible cantilever (**Figure 9**).

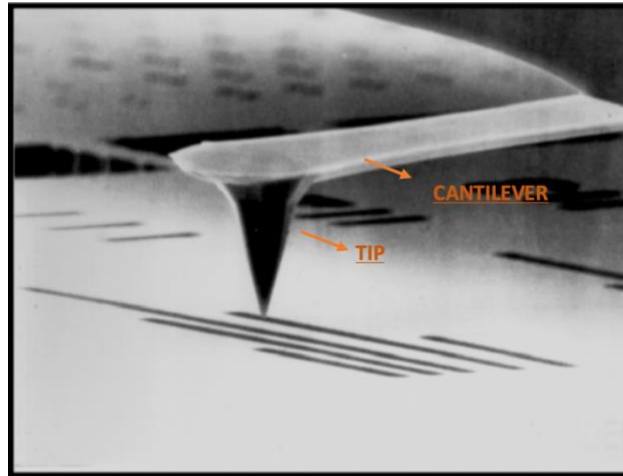


**Figure 9: SEM image of a cantilever and a tip**

The AFM tip “gently” approaches the surface and records the small force between probe and surface. Forces between the tip and the sample lead to the deflection of the cantilever according with the Hooke’s law. Indeed, we can model the cantilever as a spring. The amount of force between probe and sample depends on spring constant (the stiffness of the cantilever) and the distance between the probe and the sample. A laser diode hits for all the duration of the acquisition the cantilever (**Figure 10**). Then, the laser beam is reflected by the back side of the cantilever and acquired by the detector that is a segmented photodiode. The direction of the laser

beam depends on the cantilever deflection caused by the force between the tip and the sample. The feedback loop includes all the structural elements that are required to hold the probe at a fixed distance from the sample. Finally, the controller records and processes displacements recreating the surface topography.

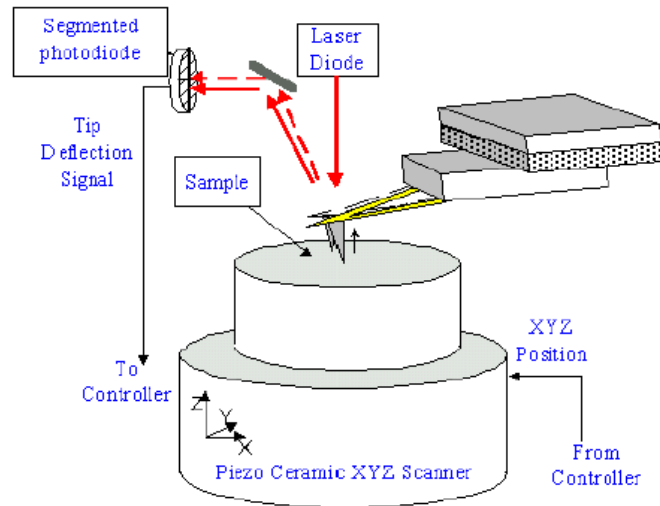


Figure 10: Schematization of AFM working model

### 3.1.4 Enzyme-Linked Immunosorbent Assay (ELISA)

The enzyme-linked immunosorbent assay (ELISA) is a commonly used analytical biochemistry assay, first described by Engvall and Perlmann in 1971 [102]. The assay uses a solid-phase enzyme immunoassay (EIA) to detect the presence of a ligand (commonly a protein) in a liquid sample using antibodies directed against the protein to be measured. ELISA has been used as a diagnostic tool in medicine, plant pathology, and biotechnology, as well as a quality control check in various industries. Performing an ELISA involves at least one antibody with specificity for a particular antigen. The sample with an unknown amount of antigen is immobilized on a solid support (usually a polystyrene microtiter plate) either non-specifically (via adsorption to the surface) or specifically (via capture by another antibody specific to the same antigen, in a

"sandwich" ELISA). After the antigen is immobilized, the detection antibody is added, forming a complex with the antigen. The detection antibody can be covalently linked to an enzyme or can itself be detected by a secondary antibody that is linked to an enzyme through bioconjugation. PMPs can also be detected by enzyme-linked immunosorbent assay (ELISA). For example, by coating ELISA plates with annexin V or cell-specific monoclonal antibodies, PMPs can be captured from plasma samples [103], [104]. Other investigators have captured PMP by coating ELISA plates with kistrin, a disintegrating for which integrin  $\alpha$ IIb $\beta$ 3 has a much higher affinity than for fibrinogen or arginine-glycine-aspartic acid (RGD) peptides [105].

## **3.2 Isolation of PMPs**

Regarding the isolation there are different strategies. The centrifugation and the filtration are the most used methods to isolate the microvesicles from bigger particles.

### **3.2.1 Centrifugation**

The classical method for EV isolation utilizes the separation of particles according to their dimension and density by centrifugation [106]. At the present time, the large majority of the teams working on microparticles use a centrifugation protocol to eliminate cells or debris [106].

From the literature it follows that for PMPs a definitive working protocol has not been characterized yet. Commonly, platelets-free-plasma (PFP), platelets-poor-plasma (PPP) or platelets-rich-plasma (PRP) are the initial centrifuged sample used to reach the PMPs isolation. [105] The optimal type of samples for the isolation of microparticles is still under investigation. Several studies have demonstrated platelet-derived microparticles presence in PRP, PPP and PFP but did not compare different sample types in PMPs isolation.

Generally, two or more centrifuge steps are required to isolate PMPs. A first passage is made to pellet platelets and big cells fragments (range: 2'000 – 10'000 RCF for 10 – 30 minutes at 20°C/room temperature). A second passage, with a higher centrifugation speed, is used to ensure the absence of platelets in the solution (10'000 – 25'000 RCF for 20 – 60 minutes at 20°C /room temperature). Sometimes, a further step is performed to spin down the PMPs. In this case very

high velocity is required [107] [108]. When interpreting the data, potential contamination of PMP samples by platelet exosomes of 40–100 nm, which originate from multivesicular bodies and have a distinct molecular content, should be kept in mind [109].

### **3.2.2 Microfiltration**

The currently available commercial membrane filters have pores of various diameters with a narrow range of pore size distribution, which simplifies isolation of the particles with a specified size. In particular, ultrafiltration may alternate successive ultracentrifugation stages [110] [111] or it can be an additional step in gel filtration chromatography [112]. However, micro- and ultrafiltration alone are also applicable for PMPs isolation [113] [114]. The diversity of isolation protocols used by different researchers considerably complicates comparison of the results obtained by different laboratories. When isolating PMPs by microfiltration, the filters with pore diameters of 1.22, 0.8, 0.45, 0.22, and 0.1  $\mu\text{m}$  are typically used; such filters retain the particles with diameters of over 1220, 800, 450, 220, and 100 nm. Larger particles are removed first and the particles with a size smaller than the target PMPs are separated from the filtrate at the next stage. Thus, the PMPs fraction of a specified size is concentrated. The microfiltration protocol uses commercially available hydrophilized poly vinylidene difluoride (VVLFP) filter (Millipore, United States) with a low affinity for proteins [115].

## **3.3 New techniques for PMPs detection**

### **3.3.1 Proteomic Analysis**

Mass spectrometry (MS)-based proteomic analysis provides an opportunity to characterise the protein composition of PMPs. Generally, this method requires extraction, separation, trypsin digestion, MS analysis, and identification of proteins. Cell-surface antigens are generally of high molecular weight and hydrophobic [117] [118]. Therefore, an ionic/non-ionic detergent or a high-pH is used for the extraction of the membrane proteins prior to the gel separation and MS analysis [118] [119]. Finally, each MS spectrum is used to search the protein database for matched peptides [117] [120]. Proteomic analysis has been used by several groups to investigate

the protein content of PMPs [121] [122]. For instance, PMPs isolated from the supernatant of ADP-stimulated platelets contained membrane surface proteins derived from platelets (GPIIIa, GPIIb, and P-selectin), chemokine ligand 4 (CXCL4), pro-platelet basic. protein (CXCL7), and RANTES (CCL5). Proteins from the alpha granules (fibrinogen, vWF, FV and FXIII, thrombospondin, and protein S) were also found [122].

### **3.3.2 Impedance Based Flow cytometry**

Unlike the conventional flow cytometer, impedance-based flow cytometry is based on the Coulter principle to detect simultaneously changes in electrical impedance produced by particles in suspension. These changes can be measured as a voltage pulse or a current pulse. The pulse height is proportional to the volume of the sensed particles [123]. For PMPs measurement, this system is calibrated using fluorescent polystyrene microspheres of uniform size. Subsequently, PMPs can be detected directly in PPP by using fluorescently labelled antibodies.

Zwicker et al. [124] have compared the measurement of PMPs, calibrated microspheres (0.78  $\mu\text{m}$ ), and platelets in frozen-thawed PPP, both by impedance- and light scatter-based flow cytometry. The size of platelets and PMPs is poorly characterized by the light- scatter based flow cytometry and both populations overlap with the 0.78  $\mu\text{m}$ -microspheres. Conversely, the impedance-based flow cytometer could resolve the populations of PMPs, calibrated microspheres, and platelets. In impedance-based flow cytometry, the size detection limit of the measurement depends on the diameter of the flow cell. Post- market installation of smaller flow cells with diameters of 25 and 40  $\mu\text{m}$  is required to analyze particles between 0.3 and 1.0  $\mu\text{m}$  in diameter [124]. Thus, PMPs below 0.3  $\mu\text{m}$  in diameter might not be detected by using these flow cells. Using fluorescently labelled antibody, the size distribution of PMPs can theoretically be determined from the amplitude of the fluorescent signal under the assumption that the signal is either proportional to the volume or the surface of the particles (in the case of surface labelling). In addition, the size distribution is calculated assuming a spherical shape. In the case of fluorescent labelling one generally assumes that the labelling efficiency is independent of the particle shape and (surface) composition.

### **3.4 New techniques for counting PMPs and study PMPs size distribution**

Dynamic light scattering (DLS) and nanoparticle tracking analysis (NTA) measure Brownian motion of MPs [125] in liquid suspension and from this movement the particle size can be calculated using the Stokes-Einstein equation [126]. NTA measures the movement of each particle through image tracking analysis, whereas DLS measures all particles at the same time and produces an average particle size.

Two DLS systems, the Zetasizer Nano S (Malvern Instruments Ltd, Worcestershire, UK) and the N5 Submicron Particle Size Analyzer (Beckman Coulter) were used to examine the size distribution of MPs in frozen-thawed plasma [117]. It was found that PMPs with sizes ranging from 50–1,000 nm could be detected by the N5 instrument utilizing a 30.1° angle of measurement, whereas the Zetasizer detected some particles considerably larger than those identified by the N5. The main disadvantage of DLS for measuring PMPs is that it performs best in studying monodisperse particles while cell-derived PMPs are clearly polydisperse. This makes that the size distribution of PMPs measured by DLS is biased towards the presence of small numbers of large particles or contaminants as they scatter light more intensely than the smaller particles. The Zetasizer Nano S uses the back scattered light to increase the sensitivity of the method, while the N5 system can use up to six different scattering angles. The scattering angles of both instruments do not overlap. This problem seems not to occur with the NTA approach because a microscope and a CCD camera track and visualize the individual particles by using particle tracking image analysis software. Harrison, et al. [127] used an NTA system, known as Nanosight LM10 (Nanosight, Amesbury, UK) to measure PMP distributions in isolated MPs and in PPP diluted in PBS (1:40–1:60). They found that PMPs have a polydisperse distribution up to 1,000 nm, but with a predominant population from lower than 50 nm to above 300 nm. They estimated that PPP contains  $\sim 200\text{--}260 \times 10^9$  MPs/l which is 1,000-fold higher than previous estimates based on using flow cytometry. As mentioned before, NTA can accurately size particles in a sample, but unfortunately the presence of a few larger particles will reduce the number of small particles detected by the software. This has been demonstrated by



Filipe et al [128] by mixing 60-nm/ 100-nm beads in a ratio 4:1. The NTA analysis of this mixture showed two distinct size populations, but it detected more 100-nm beads than 60-nm beads due to the masking effect of the larger beads over the smaller beads. For MP measurements the NTA approach has some disadvantages when compared to the DLS approach. The operation of NTA is not yet as user friendly as that of DLS. This is due to the fact that several parameters need to be adjusted carefully by a skilled operator prior to the NTA measurement. These parameters include the settings for the video capture and analysis, which are essential to obtain accurate and reproducible measurement results. As the Brownian motion of a particle in a solution depends on the viscosity and temperature of the solution, these parameters should also be defined prior to PMP measurement in (diluted) plasma. NTA and DLS may be unable to differentiate PMPs from other particles present in plasma like (lipids/lipoproteins). Recently, Nanosight has launched a fluorescence-NTA, the NS500. This instrument enables the detection of individual quantum dots, fluorescent nanoparticles with a diameter of 2–10 nm, with minimal background interference of other particles in the solution. This will hopefully enable the detection of specific subsets of PMPs, for example by using quantum dot-labelled antibodies.

### **3.5 PMPs pro-coagulant activities**

There is now set of experimental preclinical and clinical evidence to suggest that the presence of PMPs in blood components is associated with a haemostatic effect and also with potentially severe acute disease.

Several works showed that PMPs formed during platelet activation are potentially procoagulant. The principal lines of evidence are the following:

- PMPs are formed by platelets upon activation, and hence their membrane should possess all properties of the activated platelet membrane;
- PMPs can bind components of procoagulant complexes such as factors V(Va) and VIII(VIIIa); moreover, the binding-site densities for these proteins on PMP membranes even exceed those on platelet membranes;

Berckmans et al., demonstrate that by adding high concentration of isolating PMPs to PMP-free plasma the production of thrombin increases with respect the negative control [129]. (**Figure 11**).

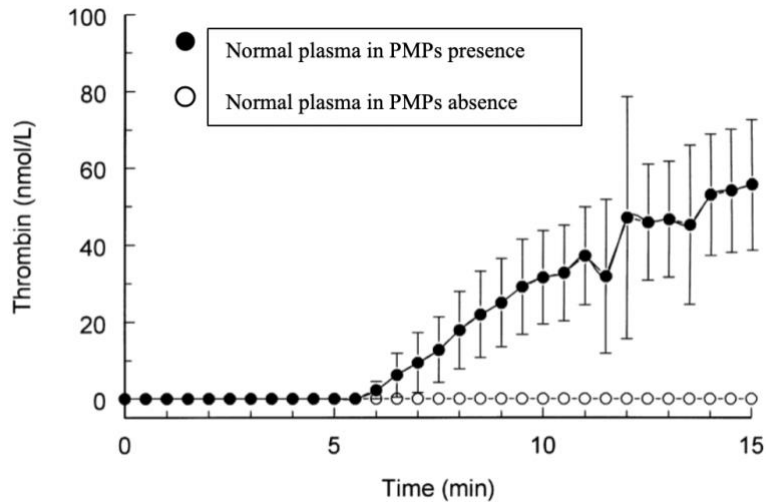


**Figure 11: Thrombin generation by microparticles from healthy individuals**

It has been supposed that PMPs can contribute to the development of thrombotic complications in the pathologic states associated with the increase of their blood concentration. In 2007 Kireev et al. [130], compared procoagulant properties of calcium ionophore A23187-activated platelets and PMPs using several in-vitro models of hemostasis. The principal conclusion of this study was that abilities of an activated platelet and a PMP to support coagulation are very similar. In addition, they noticed that the maximal thrombin production rapidly increased with the increase of the concentration of PMPs added.

Taking into account an approximately 100-fold difference in their surface area (platelets and PMPs), it can be concluded that specific procoagulant activity of the PMP membranes is approximately 50- to 100-fold higher than that of activated platelets.

Although the level of platelet-derived microparticles is elevated in a variety of diseases, including cardiac surgery, many aspects about their functions in vivo are unknown.

Platelets and platelet-derived microparticles (PMPs) play important roles in cardiovascular diseases, especially atherosclerosis. It influences atherosclerosis through inducing adherence of

platelets and other cells to endothelial cells in endothelial lesion site, promoting the lesion plaque clotting in the arterial wall and participating in the inflammatory responses, as well as lipid deposition. When destabilized lipid-rich plaque in the arterial wall ruptured, the myocardial infarction and stroke, which are the important reasons causing the death of cardiovascular patients, will be triggered [132]. According to Christersson et al., PMPs expressing P-selectin might be a promising biomarker for predicting future cardiovascular events. Indeed, they promote a study in 2017 about PMPs number variation during long-term follow-up after acute myocardial infarction. It resulted that the concentrations of PMPs in whole blood increased during the time period for patients with non-ST-elevated myocardial infarction (MI). Furthermore, higher concentrations of PMPs early after MI were associated with an increased risk of cardiovascular events during follow-up [133].

The aim of Nieuwland et al. study was to investigate the procoagulant properties of PMPs generated *in vivo*. They addressed the question whether pericardial blood, obtained from patients undergoing coronary bypass surgery, may contain cell-derived microparticles that support coagulation. Their results show that pericardial blood is indeed rich in platelet-derived generated during coronary bypass surgery which support coagulation. Data indicate that the *in vivo* generated microparticles support thrombin generation [131].

PMPs participate to clot formation in *in vivo* condition. It was found that PMPs enhance platelet and fibrin deposition on the atherosclerotic vessel wall [134]. Suades et al. showed that, using fluorescence-tagged PMPs, under high shear rate conditions PMPs localize within the growing platelet thrombi on exposed collagen. In particular, PMPs bind to adhered platelets under high shear rate conditions stimulating further platelet deposition and so, thrombus growth [135].

Finally, studies on animals were conducted to assess the PMPs relevance in thrombus formation. Ramacciotti et al. isolated and re-injected PMPs in two groups of mice: wild types or genetically modified (deletion of E- and P-selectin) [136]. They found that re-injections of PMPs, and so PMPs number, correlate positively with thrombus weight. These results suggest that a high level of PMPs in blood promotes platelet coagulation and support their involvement in clot formation.

### **3.6 Microparticles released as consequence of applied high shear**

*In vivo* and *in vitro* pathologic high shear stresses induce fragmentation of platelets into microparticles. For analyzing effects of hydrodynamic forces on platelet activation and apoptosis, Leytin et al. [137], exposed platelets to different shear stresses, ranging from physiologic arterial and arterioles levels (10–44 dyne/cm<sup>2</sup>) to pathologic high levels (117–388 dyne/cm<sup>2</sup>), occurring in stenotic vessels. They found that pathologic shear stresses (>117 dyne/cm<sup>2</sup>) induce platelet activation and then PMPs formation. Instead, physiologic shear stresses (10–44 dyne/cm<sup>2</sup>) did not affect the platelet responses. In a study conducted by Nomura et al., it was documented that the exposure of washed platelets to high shear stress (>108 dyne/cm<sup>2</sup>) caused the release of microparticles. In particular, significant release of microparticles occurred within 30 seconds of the application of shear stress and the number of microparticles continued to increase as the shear time was prolonged. In contrast, exposure of washed platelet to low shear stress (12 dyne/cm<sup>2</sup>) did not cause either platelet aggregation or microparticle formation. They also investigated the release of microparticles from platelets in whole blood. Both platelet aggregation and the number of microparticles released showed no significant differences between whole blood and washed platelet [138]. Sheriff et al. conducted a study in which purified platelets were exposed to brief (5–40 s) periods of high-shear stress, and then exposed to longer periods (15–60 min) of low shear. They demonstrated that the threshold of shear for platelets activation and the microparticles release is around 60-70 dyne/cm<sup>2</sup>. According to this study it was also clear that a substantial proportion of the total prothrombinase activity recorded was due to microparticle formation, both immediately after high-shear exposure and after extended low-shear exposure. Significantly, the proportion of activity due to PMP remained approximately the same throughout, suggesting that microparticle formation continued throughout the low-shear activation phase [139].

### **3.7 Platelets activity state (PAS)**

Among platelet activation assays the PAS has been often chosen [139] [140]. By using a modified prothrombinase method, the PAS assay, developed in 1999 by Bluestein, Jesty and colleagues [140].

The modification of the prothrombinase method allows to obtain a linear quantitative measurement of the initial platelet activity state. This linearity allows, in turn, for a 1:1 correlation between the applied stimulus and thrombin generation, which is then index of induced activation.

Platelets, once activated, expose anionic phospholipids on the outer leaflet of the cell membrane supporting the binding and activation of vitamin K-dependent protein of coagulation (factors VII, IX, X and prothrombin). Furthermore,  $\alpha$ -granules of platelets secrete Factor V, concomitantly activated in factor Va. Both anionic phospholipids and factor Va, bind to FXa, which is exposed on the cell membrane, forming the prothrombinase complex (Factor Xa + Va + anionic phospholipid) needed for prothrombin activation and thrombin formation.

Human prothrombin was acetylated to produce a modified prothrombin that upon activation by platelet-bound prothrombinase generates a form of thrombin that does not activate platelets but retains its amidolytic activity on a chromogenic peptide substrate. If normal prothrombin would be used in such an assay, the thrombin that is generated would activate the platelets in a feedback manner, accelerating the rate of thrombin generation and thereby preventing accurate measurement of the initial platelet procoagulant activity. Because the feedback action on the platelets is blocked, thrombin generation is linear, allowing quantitative measurement of the initial platelet activity state.

A schematic representation of acetylate prothrombin action is shown in **Figure 12**.

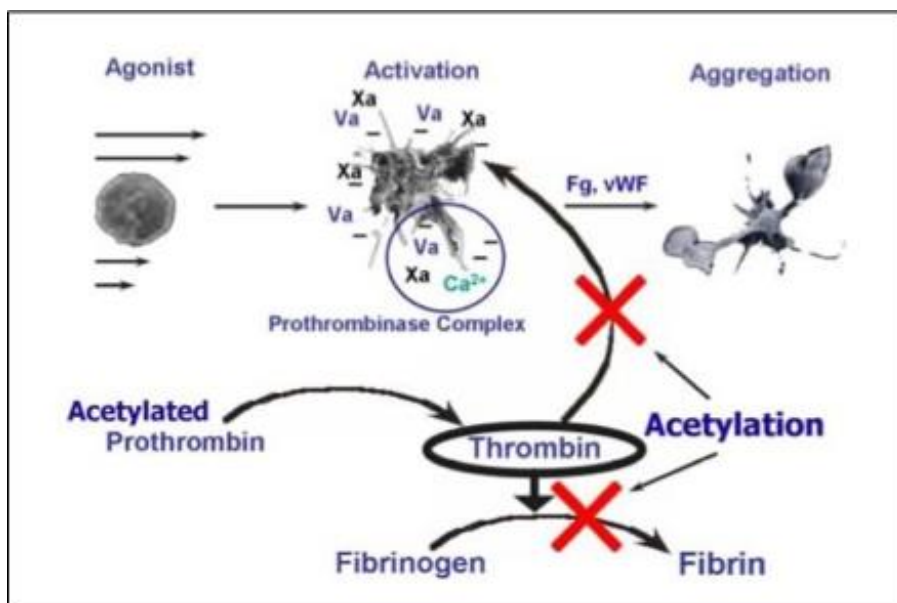


**Figure 12: Schematization of the effects Ac-FIIa, used in the PAS assay execution, on the coagulation process. Acetylation stops further platelet activation and fibrin formation**

The instrument that permits to execute the evaluation is the spectrophotometer (VersaMax<sup>TM</sup> absorbance Microplate Reader). It is able to measure molecular absorption of monochromatic electromagnetic radiations in the visible or ultraviolet field.

It is composed of:

- Light source: it is a quartz halogen lamp 6 V/10 W.
- Monochromator: it permits only the passage only to the wavelength chosen by the operator.
- Reading wells: they contain the sample during the analysis.
- Detector: it converts the electromagnetic radiation into electrical signal.
- Amplifier: it amplifies the electrical signal outgoing from the detector.
- Recorder: it provides the absorbance value.

The instrument is connected to a dedicated software through which it is possible to set all process parameters and monitor the absorbance variation dynamics in real time.



## 4. Materials and Methods

This chapter will present a brief description of the utilized instruments and the performed experimental tests.

### 4.1 Blood collection

About 30 ml of whole blood was collected from healthy voluntary donors by using a 21G butterfly needle (BD Vacutainer Safety-Lok). Blood was drawn into a falcon tube and gently mix with acid-citrate dextrose solution A (ACD-A). ACD-A was added to blood with a ratio of 1:10 acts as an anticoagulant by the action of the citrate ion chelating free ionized calcium, thus making calcium unavailable to the coagulation system. Moreover, it is the only anticoagulant product approved by the United States Food & Drug Administration (FDA) for the use in preparation of Platelet-Rich Plasma.

### 4.2 Platelets-Rich Plasma (PRP) preparation

PRP was collected by centrifugation. The centrifuge is an instrument capable of accelerating the separation process of elements with different densities and dimensions inside a solution.

In order to obtain a solution with high concentration of platelets, blood was centrifuged at 1300 rpm for 15 min. After centrifugation, RBCs and WBCs were deposited on the bottom of the falcon tube, while the plasma, the platelets and the coagulation factors remain of the top, forming the PRP. Later on, the PRP was gently aspirated with a Pasteur pipette in order not to activate the platelets and was poured in another 15 mL falcon tube.

### 4.3 Gel-Filtrated Platelets (GFP) collection

The extraction of GFP sample was performed by gel filtration chromatography. This technique involves two different components (**Figure 13**):

- the stationary phase (usually composed of a gel);



- mobile phase (usually composed of platelets buffer or PRP);

The column was loaded with a specific gel containing agarose beads (Sepharose 2B) with a diameter between 20-600  $\mu\text{m}$ . The agarose beads separate PRP into different components, slowing down smaller proteins and allowing platelets to advance down the column with ease. The process was aided by a peristaltic pump (Rainin Dynamax RP-1 Peristaltic Pump), allowing the column perfusion with a 1x HEPES-modified Tyrode's buffer, termed Platelet Buffer (PB), essential for filtration and platelet longevity.

To ensure that the PB was at a pH value of 7.40, the pH was checked by using a pH-meter (Corning pH meter 430), an electronic device that permits pH assessment of a solution by the use of a probe. The pH value was modifiable with the addition of Sodium Hydroxide [NaOH] to increase it, or hydrochloric acid [HCl] to decrease it.

Agarose beads are stored inside the column with Sodium Azide (SA) at a concentration of 0,05% to prevent bacteria growth. SA must be completely eliminated before GFP collection because of SA's cytotoxicity. It must be substituted with PB, at a concentration of 1x having a physiological pH ( $7.40 + 0.04$ ), in order to guarantee normal platelet functionalities. The substitution process was checked with the analysis of the refractive index (RI) of the two solutions through a refractometer (**Figure 14**); in particular, the instrument (American Optical) is able to measure values between  $0^\circ$  and  $32^\circ$  Brix and it is composed of:

- Prism: on the prism, a solution drop is deposited in order to analyze it
- Cover plate: it covers prism after the drop deposition
- Mirror tube: mirror that directs the light on the prism
- Setting screw: it allows the focus

- Eyepiece (with adjusting ring of diopter): it allows the RI reading

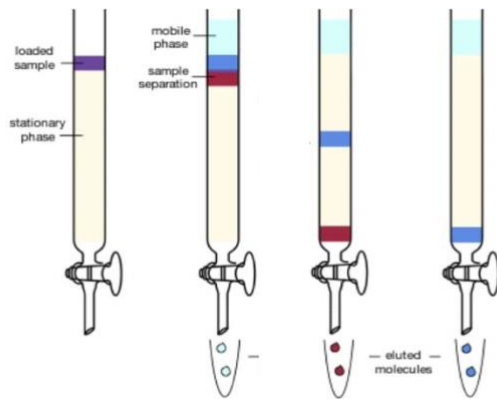


**Figure 13: Chromatography processes inside glass columns**

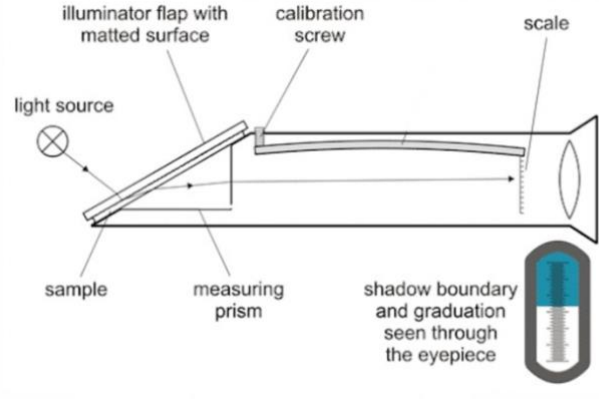


**Figure 14: Refractometer**

In order to measure an RI value, a drop was deposited on the prism and the specific value was read inside the eyepiece. It is known that the RI (expressed in Brix grades) of 0,05% SA is equal to 10, while the RI value for PB is 30. At regular interval (approximately every 30 minutes) the RI was checked; until the refractometer showed an RI equal to 30. At this point, the substitution process was completed and the gel filtration could be performed. The columns were loaded with 150 ml of gel so, that the PRP that was filtered in a single process was around 15 ml. It is important to pour the PRP along the column wall to avoid the impact between the sample itself and the agarose beads that could lead to platelet activation. During the gel filtration, the collection timing can be established in two qualitative ways; it is possible to place a beaker containing water below the column inferior tap in order to monitor the PRP drop density and the outgoing drop turbidity. Indeed, when the platelets get out from the column both increase: the drop appears more turbid and the platelet diffusion inside the water is clear.

#### 4.4 Platelet Count

After the gel filtration process, the next step was to obtain the platelet count in order to extrapolate platelet concentration of the GFP collection. Knowing the initial concentration was

fundamental because it was necessary to dilute the GFP sample to a specific concentration to standardize the test and compare the results with other laboratories. A Z1 Particle Counter was used in order to evaluate the sample platelet concentration. The Z1 Particle Counter makes use of the Coulter Principle to analyze particle size and count. A nonconductive aperture tube are immersed inside a cuvette containing 10 mL of isotonic solution and 10  $\mu$ L of GFP sample. Two electrodes (one inside and one outside the aperture tube) apply a potential difference; with an aspiration system, the GFP sample is forced to pass through the aperture tube and the platelet passage generates an impedance variation that is detected as a voltage or current impulse by the instrument. Once a particle dimension is set, the particle counter detects the particle number inside an aspired sample counting the generated impulse number. In order to evaluate the platelet concentration, five measurements were done for each experiment and the average value was determined.

Two different dilution were used to perform the experiments: 100 000 platelets/ $\mu$ l to isolate PMPs and 20 000 platelets/ $\mu$ l to analyze the PMPs thrombogenicity. The dilution of GFP was done with PB and Calcium Chloride ( $\text{CaCl}_2$ ) 50 mM, that dissociates in  $\text{Cl}^-$  and  $\text{Ca}^{2+}$  (that is essential in fibrin production) in aqueous medium.

In order to obtain the diluted sample, the first step was calculating the volume of the three components (GFP, PB and 50 mM  $\text{CaCl}_2$ ); the needed quantity of diluted GFP depended on the sample volume required for the specific experiment. Firstly, GFP was taken from the collected GFP by using a micropipette (in general, P1000) and were poured into a falcon tube. Then, the calculated volume of PB was added with a micropipette. Only few minutes before the experiment, the 50 mM  $\text{CaCl}_2$  volume was added to the GFP+PB, in order to prevent a possible platelet activation. Final concentration of  $\text{CaCl}_2$  was 3 mM.

#### **4.5 Scanning Electron Microscope (SEM)**

SEM resolution allows to detect platelets and PMPs. In this project the SEM was used on three different samples: solution containing platelets activated by sonication, solution containing

platelets activated by adding calcium ionophore and solution containing platelets which were not activated.

The samples needed to undergo several steps before being used for SEM acquisition. The preparation protocol took 24 hours. The first part provided the fixation phase: 100  $\mu$ l of biological sample was deposited on a glass coverslip (12 mm  $\varnothing$ ) and fixed by adding the same volume of Glutaraldehyde or Paraformaldehyde 4% (GA or PFA). The GA or PFA acted on the biological sample for 2 hours. Later on, it was washed with PBS (Phosphate Buffered Saline) and water. Each wash took 10 minutes and it was repeated three times, before with PBS and then with water. The sample was dehydrated by using ethanol in different concentration :35%, 50%, 70% for 5 minutes each step and 80%, 95%, 100% x2 for 10 minutes each step. Finally, to dry the sample, it took three steps of incubation with HMDS : Ethanol in: 1:2 solution; 2:1 solution; 100% HMDS solution x2. All the incubations lasted 20 minutes. The final step was to submerge the sample with 100% HMDS and leave it in the fume hood overnight. After one night if some liquid was still not evaporated, it was sucked by using a pipette. Then, samples were placed on specific metallic supports covered with carbon tape to make the glass adhere. Later on, because of the sample non-conductivity, samples were covered with a thin layer of metal. The metal used for sputtering samples was gold. This process was performed by Hummer 8.0 Sputter System (Anatech USA, **Figure 15**). In order to avoid charging problems in the SEM, as the electrons from the electron beam remain in the samples to form clouds of negative charges, copper tape was used to connect the support to the sample.



**Figure 15: Hummer 8.0 Sputter System used to gold coating on the samples**

For the sputtering the sample was placed inside a cylindrical chamber as shown in **Figure 16**. Once closed, the vacuum process was started. When the pressure reached a value less than 40 millitorr the chamber was filled by Argon. At this point the pressure value was reset to 70 millitorr manually using a knob. When it reached 70 millitorr, the voltage was turned on to reach a value of 15 milliamperes in plasma. Once the voltage reached the exact value, the current was discharged and gold coating process was performed.



**Figure 16: Gold coating process of the samples**

After that, samples were ready to be analyzed with SEM. The samples were loaded in the analysis chamber, which contains a maximum of 6 samples. Samples and standard (the support in the chamber) height had to be below 10 mm. If the samples were too high the “Z” knob on the outside of the stage door was adjusted to lower the sample stage to the appropriate height. Then, the pump, which creates vacuum in the chamber, was activated. The High Voltage was set at 30 kV and it increased until the image becomes an oval of uniform brightness. At this point we could find our gold particles surface of the standard sample and adjusting the position and the magnification. Once on the sample, the focus was set by creating a focus box in which it was possible vary the focus parameters until the proper ones were found. After the focus, the stigmation had to be adjusted using the gold particle standard sample with a magnification of 50,000X. So, stigmation was adjusted to be able to see small spherically shaped gold particles covering the surface. When stigmation was far out of alignment particles were not spherically shaped or sharp. Once the stigmation was set, it was possible move on the sample and look for

the interested area. Once located the area, the images were acquired. In order to obtain the desired quality of images, Magnification, Contrast, Brightness, Scan Speed and Resolution had to be adjusted. At each area of interest, these parameters had to be re-set and changed until the best image possible could be acquired.

#### **4.6 Atomic Force Microscopy (AFM)**

We used the atomic force microscopy to detect activated platelets and their PMPs. In particular the acquisitions were done before the isolation of PMPs from the platelets to ensure the presence of PMPs once platelets were stimulated.

24 hours before the acquisition by AFM, it was necessary to prepare the sample with a fixation protocol which provided several steps. 100 µl of biological sample was deposited on a glass coverslip (12 mm Ø) and fixed by adding the same volume of Glutaraldehyde or Paraformaldehyde 4% (GA or PFA). The GA or PFA acted on the biological sample for 2 hours. After that it was washed with PBS (Phosphate Buffered Saline) solution and water. Each wash took 10 minutes and it was repeated three times, before with PBS and then with water. The sample was dehydrated by using ethanol in different concentration :35%, 50%, 70% for 5 minutes each step and 80%, 95%, 100% x2 for 10 minutes each step. Finally, to dry the sample, it took three steps of incubation with HMDS : Ethanol in: 1:2 solution; 2:1 solution; 100% HMDS solution x2. All the incubation lasted 20 minutes. The final step required to submerge the sample with 100% HMDS and leave it in the fume hood overnight. After one night if some liquid still remained, it was suctioned out using a micropipette tip. Then, the glass cover slips were mounted directly into the AFM. This project used the Park NX20 AFM controlled by SmartScan software. For our setup we used a silicon probe in non-contact mode (HQ300 cantilever). Non-contact mode means that the tip and the sample surface never touch each other. Electrostatic interactions, as the Van Der Waals one, between surface and tip cause the bending of the cantilever. It ensures that both, the tip and the sample surface, remain intact. The proper way to assemble the tip and cantilever to the holder was an extremely important passage because of the fragileness of the tip. The holder was a removable part in order to make easier the placement of the probe (tip and cantilever). Once the holder was placed back with the probe it

was necessary to find the cantilever on the video screen, align it to the center and adjust the focus to make it sharp. To accurately measure surface topography with AFM, the laser had to be aligned onto the back of the cantilever at the AFM tip. The last step, in the alignment phase of imaging, was the adjustment of the position sensitive photo diode (PSPD). The sample moved with respect to the probe. When the area of interest was located, the distance between tip and sample surface was reduced taking every precaution to avoid any contact. Once the probe approached to the surface, it could only scan within a 100x100  $\mu\text{m}$  box. To move in a different area the probe had to be lifted up and repositioned. Then, it was necessary to set the image size area, the pixel density and adjust the contrast and brightness. At this point, enabling the line scan initiated the AFM to begin scanning back and forth (forward and reverse over a single area. It continued to do so indefinitely until it is told to scan or stop). The default scan size was 25x25  $\mu\text{m}$  and the scan size was decreased to 5x5  $\mu\text{m}$  to zoom on the sample. Three other important parameters were:

- Setpoint;
- Gain;
- Scan speed;

The **setpoint** determines how close to the surface the system will keep the cantilever, we used a range between 15 and 20 nm. The **gain** is how fast the system responds to features and it was generally set at 1 (dimensionless value). After setting the setpoint and gain, the **scan speed** had to be adjusted for the image. If it was difficult to get a good trace-retrace, the image scan could be slowed down through scan speed adjusting. The default scan speed was 1 Hz, we used the scan speed within a range of 0.5 and 1.5 Hz. The setpoint, gain and scan speed had to be reset for every acquisition. The data collected could be manipulated to a 2D or 3D image acquisition. It could also be used to measure the sizes of the features on three different axes.

## 4.7 Flow cytometry

In our project we used flow cytometry to detect PMPs and platelets before and after isolation. The Flow cytometry was also used for counting PMPs. The flow cytometer used is the BD FACSCanto™ with BD FACSDiva™ software integrated into the hardware. Samples containing PMPs only or platelets and PMPs were marked with the combination of Annexin V and antigen CD41+. Antigen CD41+ was diluted 10x with PB. Antibodies were added to 100 µl of sample: 5 µl of Annexin V (eBioscience™ Annexin V-FITC Apoptosis Detection Kit), 2 µl of antigen CD41+ (CD641 Monoclonal Antibody APC, MEM-O6). Samples were incubated for 30 minutes in the dark before being analyze through flow cytometry.

The flow cytometry protocol for PMPs was optimized using nano-flourescent size standard beads measuring 0.22, 0.45, 0.88 and 1.35 µm (Spherotech\_Nanoparticle\_Size\_kit 2) allowing to distinguish MPs based on their size. The dimension threshold imposed by the machine is 488 nm, the MPs with a diameter under this value were not considered by the flow cytometer. PMPs were subsequently detected by Annexin V and antigen CD41+. The samples were analyzed according to their size and phenotype in two different steps. Thanks to the beads, we discriminated a dimensional threshold shown in the **Figure 17** (left), as vertical line between 0.88 and 1.35 µm. Since platelets are from 1 to 4 µm in diameter and PMPs are in a range between 0.1 to 1 µm in diameter, the threshold imposed was chosen about 1 µm on forward scatter, indeed it is often suggested that forward scatter indicates cell size.

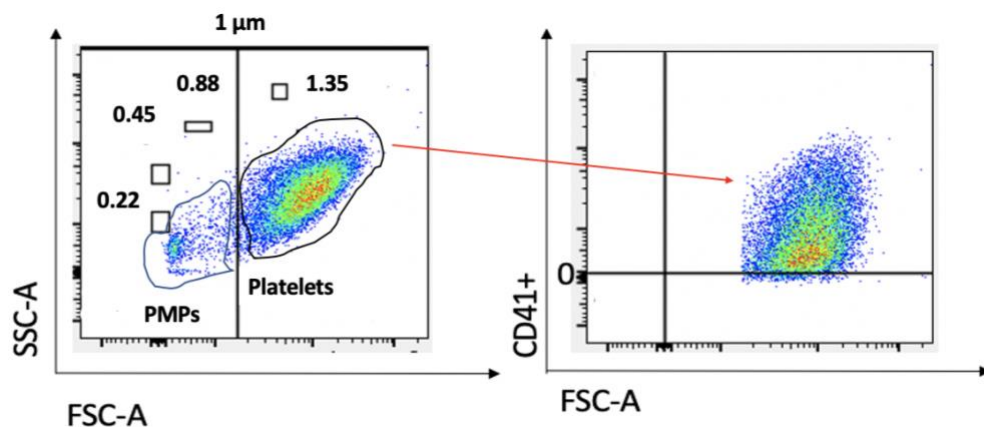


**Figure 17: Gating method to detect platelets. Forward scatter on the x-axis and side scatter on the y-axis. According to the vertical threshold, the platelets have been detected by gating those positive to antigen CD41**



On the right side of the threshold all the particles equal to and bigger than 1  $\mu\text{m}$  were gated. **Figure 18** (left) has a dividing threshold of 1  $\mu\text{m}$ . All the particles to the left are equal to or smaller than 1  $\mu\text{m}$ . Once the two populations, platelets and PMPs, were determined based on the size, they were further categorized according to their phenotype **Figure 18** (right). As we previously said, samples were marked with both antigen CD41+ and Annexin V, but to determine the difference antigen CD41+ was enough. The same protocol was applied to samples after-isolation (**Figure 18**).

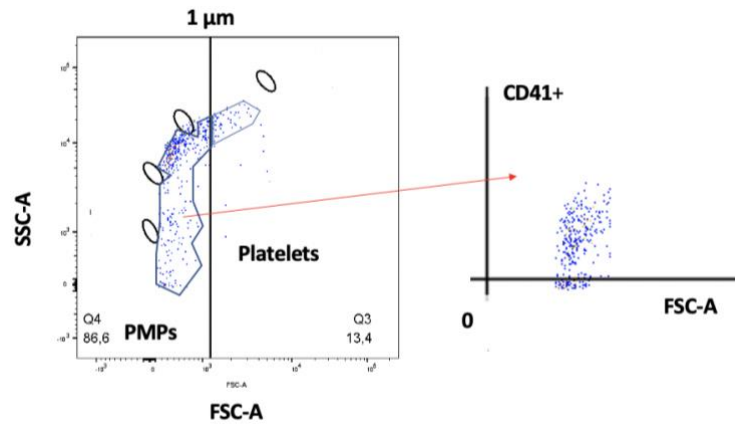


**Figure 18: Flow cytometry acquisition of PMPs sample after isolation. According to the vertical threshold the microparticles have been detected and classified as PMPs by gating those positive to antigen CD41**

To compute the concentration of PMPs/ $\mu\text{l}$  a mathematical method was used. Considering three parameters:

- $Q$ , the flow imposed by the flow cytometry machine to suction the liquid for acquiring data  $Q=12 \mu\text{l}/\text{min} \rightarrow Q=0.2 \mu\text{l}/\text{sec}$ ,
- $E$  the number of total events (particles) read;  $E = 1500$  events;
- $t$  the acquisition time, depending on the singular acquisition;

$$Q * t = \text{volume acquired } (V_a) [\mu\text{l}] \quad (\text{Eq. 1a})$$

$$\frac{E}{V_a} = \text{concentration of MPs} \quad (\text{Eq. 1b})$$

## 4.8 PMP Production, Isolation and Storage

### 4.8.1 PMP production

#### 4.8.1.1 Cold-Induced PMP Production

Inside our study, we explored the opportunity to store the platelets in order to induce production of PMPs and use frozen samples. The GFP was stored at different temperatures and over different periods of time. The GFP was diluted at 20'000 platelets/ $\mu\text{l}$ ; for the dilution, platelet buffer and Calcium chloride ( $\text{CaCl}_2$  [60 $\mu\text{l}$  each 1 ml of GFP]) was added to the solution. At the end of every storage period the sample was thawed for 30 seconds in a warm bath at 37°C, and compared with the same fresh sample previously analyzed. The comparison, between fresh and unfrozen sample, was performed to determine whether the number or/and the features of platelets and PMPs changed. Platelets and PMPs were assayed using a flow cytometer and cell-lineage specific monoclonal antibodies, annexin V and dimensional beads to identify platelets and PMPs. Tests were repeated for ten GFP samples obtained from ten healthy donors. GFP samples were stored for 24 hours, 3 days, 7 days and 10 days at 4°C, -20°C, -80°C. Furthermore, a negative control was provided by using no-antibodies marker sample to identify the background noise. (Figure 19).

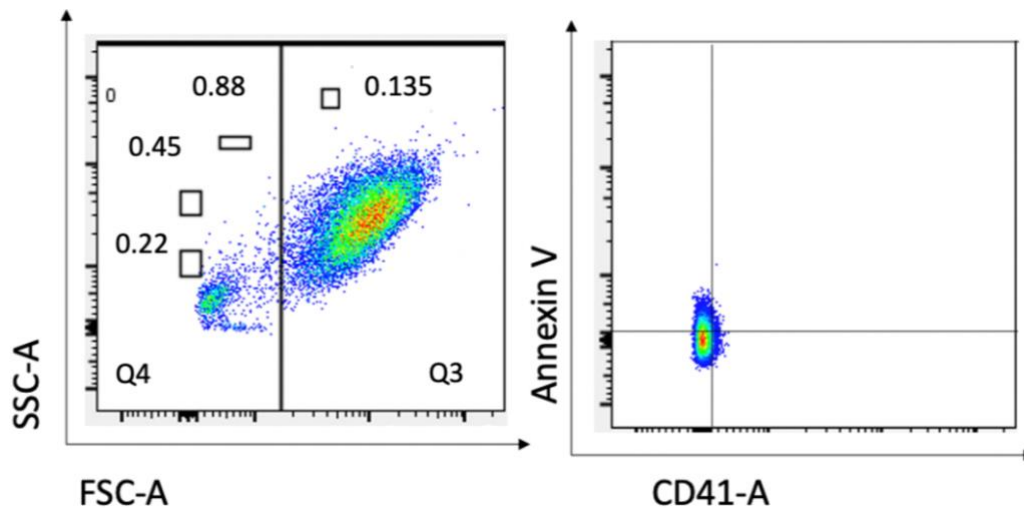


Figure 19: Flow cytometry acquisition. Background noise detected without the addition of markers

### 4.8.1.2 Agonist-Induced PMP production

#### *Sonication*

This process was fundamental because it allows to yield platelets with maximal prothrombinase activity and all PAS assay outputs can be normalized through it. Sonication activates platelets through ultrasounds, expansion and compression waves at high frequency. When the ultrasounds propagate inside a liquid, they create the needed conditions for several physical phenomena, such as cavitation. The cavitation happens in the preexisting weakest parts of the liquid, like the microbubbles. As the cavitation bubble is hit by the sound wave compression, the surrounding pressure, the superficial tension around the microbubble and the negative pressure inside the microbubble, provoke a collapse. This phenomenon leads to an elevated platelet activation and thus to PMPs release from platelets membrane. Sonication was performed by exposing 350  $\mu$ L of GFP (20'000 platelets/ $\mu$ l) to a microprobe sonicator.

The sonicator (Branson model 4C15, **Figure 20**) is equipped with:

- Current source: it provides the energy impulses at high tension and high frequency. It transforms the normal alternate current at 50 Hz to an electric energy at 10kHz.
- Converter: it converts the high frequency electric energy coming from the current source with a mechanical vibration into the specific frequency (around 10kHz). The oscillation of the converter piezo-electric crystals is transmitted and focused thanks to the microprobe.
- Microprobe: it amplifies the longitudinal vibration generated by the converter, producing a higher cavitation action and higher process efficiency.



**Figure 20: Sonicator. The microprobe is inserted in the tube to produce cavitation**

### *Calcium ionophore*

Calcium ionophore A23187 was used as non-physiological agonist for platelets activation. It is a mobile ion-carrier that forms stable complexes with divalent cations (ions with a charge of +2). Its action promotes platelets activation by increasing calcium ions concentration in the cytoplasmic environment [141]. Subsequently to their activation, platelets release PMPs. Calcium ionophore A23187 [5 mM] was added in solution with 350  $\mu$ l GFP (20'000 platelets/ $\mu$ l).

The number of PMPs produced by sonication and the number of PMPs produced by calcium ionophore were compared. Both the methods were correlated to resting platelets sample (not activated platelets).

## **4.8.2 PMPs isolation**

The following subparagraphs describes the methods used to isolate PMPs in this project.

### **4.8.2.1 Microcentrifugation**

Microcentrifugation is based on the differences in density and dimension between platelets and PMPs. We used an Eppendorf 1554 C micro centrifuge (**Figure 21**). The platelets sediment before then PMPs. The samples were loaded in the micro centrifuge, which can contain a maximum of 18 tubes with 11 mm of bore diameter and 45° of angle of bore. The micro centrifuge tended to warm the sample beyond room temperature; for this reason, the centrifuge was operated in a cold room at temperature of 4°C. At this point, each Eppendorf were inserted in the micro centrifuge. All the tubes were filled with a volume of 1 ml. Empty places were filled with water tubes at the same volume, in order to keep balance during rotation.

Different speeds were used sequentially: 4'000, 6'000 and 14'000 rpm (1310, 2940, 16 000 RCF). Three tubes were used to test: one to analyse the sample after 4000 rpm, one to analyse the sample after 4000 and 6000 rpm and one to analyse the sample after 4000, 6000 and 14000 rpm. At the beginning, samples were centrifuged for 20 minutes at 4'000 rpm. Then for 20 minutes at 6'000 rpm and finally for 40 minutes at 14'000 rpm. After the first 4000 rpm, 900  $\mu$ l from each tube was collected. The collected sample from 1<sup>st</sup> tube was put aside to be analysed, while the others two collected sample were inserted back in the centrifuge and a second step at 6000 rpm for 20 minutes was performed. After this, 900  $\mu$ l from each tube were collected. The collected sample from 2<sup>nd</sup> tube was put aside to be analysed and the 3<sup>th</sup> tube was centrifugated at 14'000 rpm for 40 minutes. Finally, the pellet from the last tube was collected, resuspended in platelet buffer and analysed.



**Figure 21: Microcentrifuge Eppendorf 5414**

#### **4.8.2.2 Microfiltration**

Microfiltration was the second method analyzed and compared to the previous one. A solution is forced to pass through a microfilter which allows the passage of particles smaller than its pores dimensions. Microfilter (Minisart® NML) shown in **Figure 22**, made of Surfactant-Free Cellulose Acetate (SFCA), was used with different pores sizes: 1.2 and 0.8  $\mu$ m of diameter. 10 ml of sample was loaded in a syringe after drawing a slight amount of air (at least 1 ml) into the syringe. This air volume was used to avoid a remaining sample volume inside the microfilter.

Then a microfilter was connected to the luer connector on the filled syringe. Sterile blister units were opened by peeling off the protective backing. An appropriate pressure was applied to press in the plunger of the syringe and force the passage of the solution through the microfilter. Firstly, the solution was forced to pass through a microfilter with pores of 1.2  $\mu\text{m}$  diameter and then through a microfilter with pores of 0.8  $\mu\text{m}$  diameter. The first step removed a high number of platelets. The second one removed any remaining platelets due to the little pores dimension.



**Figure 22: Microfilter with siringe inlet**

### **4.8.3 PMP storage**

All isolated samples were stored at 4°C [142] [143] [144] [145]. They were stored for 3, 7, 10 days. Flow cytometry was used to analyze the PMPs. PMPs were identified by dimension and chemical proprieties present on their surface. Beads of different sizes were used to determine the forward scattering threshold to distinguish particles littler than 1  $\mu\text{m}$ . Annexin V and antigen CD41+ were used as marker to highlight PMPs among all the particles. Stored samples were analyzed using flow cytometry and compared with a fresh sample. In particular, PMPs number was checked during storage time.

## **4.9 Platelet Activity State (PAS) assay**

The PAS assay was used to analyze the platelets activation response to an increment of PMPs for all the experiments run to test the PMPs thrombogenicity.

The first step was the preparation of the TUBES solution. Each tube was composed of:

- 50  $\mu\text{L}$  of HBS:BSA: it is a buffer solution containing 20 mM HEPES, 130 mM NaCl and 0.1% Bovine Serum Albumin (BSA)
- 10  $\mu\text{L}$  of 50 mM  $\text{CaCl}_2$  that is fundamental for the coagulation process
- 10  $\mu\text{L}$  of Ac-FII + HBS:BSA-PEG in relation 1:4: it is essential the usage of Ac-FII as thrombin (FIIa) substrate in order to obtain a linear relation between activated platelets level and thrombin generation

This solution had to be poured in Eppendorf and put in water bath for 10 minutes at  $37^\circ\text{C}$ .

Then, also the so-called WELLS solution had to be prepared. It was poured in the wells inside the spectrophotometer during the readings and each of them contained:

- 100  $\mu\text{L}$  of HBS:BSA – EDTA: it is essential because during the spectrophotometric analysis EDTA can sequester  $\text{Ca}^{2+}$  and block the conversion of FII into FIIa. In this way, only the thrombin produced during the stimulation process or the incubation is measured
- 50  $\mu\text{L}$  of CH-TH: it is needed because it is the chromophore used in order to evaluate the platelet activation. If platelets are activated and have produced thrombin, it emits a light wave; what the spectrophotometer measures is its absorbance value at a wavelength of 405 nm

In addition, also the Factor X (FX), that was essential for the generation of prothrombinase complex, had to be prepared. In order to do it, the needed reagents were:

- 10  $\mu\text{L}$  of FX
- 490  $\mu\text{L}$  of HBS:BSA – PEG

Human prothrombin acetylated was used in order to avoid platelets activation in a feedback manner. The feedback action on the platelets was blocked so that thrombin generation was linear, allowing quantitative measurement of the initial platelet activity state.

After reagents preparation, samples were prepared. PMPs were added to diluted GFP (20'000 platelets/ $\mu\text{l}$ ). 25  $\mu\text{l}$  of sample was collected and added to 70  $\mu\text{l}$  of TUBES solution. In order to allow thrombin production, 5  $\mu\text{l}$  of Factor X was added. This procedure was repeated for each

kind of sample. The samples were incubated at 37°C in order to let the platelets activate. Once the incubation phase was completed, each spectrophotometer well was loaded with 150 µL of WELLS solution and 10 µL of incubated sample. The spectrophotometric analysis allows to assess the variation of the specific sample absorbance during the established temporal interval. The slope of the curve absorbance-time [min] represents this variation that can be associated to the produced thrombin and to the platelet activation degree. Through a software (Softmax Pro 6.3), it was possible to set the parameters (reading speed, area of detection, number of readings) and process the collected data. Each acquisition lasted almost 7 minutes, during which 33 readings were performed.

#### 4.10 Hemodynamic Shearing Device (HSD)

The Hemodynamic Shearing Device (HSD) is an instrument which generates a known, uniform and constant value of shear on platelets. The HSD combines the geometry of a cone and plate viscometer (plate) and a cylindrical coaxial Couette viscometer (ring), as shown in **Figure 23**. HSD is driven by a highly accurate direct motor with very fast dynamic response that is controlled via a programmable interface. The HSD is geometrically designed to generate uniform levels of shear stress throughout the cone-plate and the Couette annular gaps.

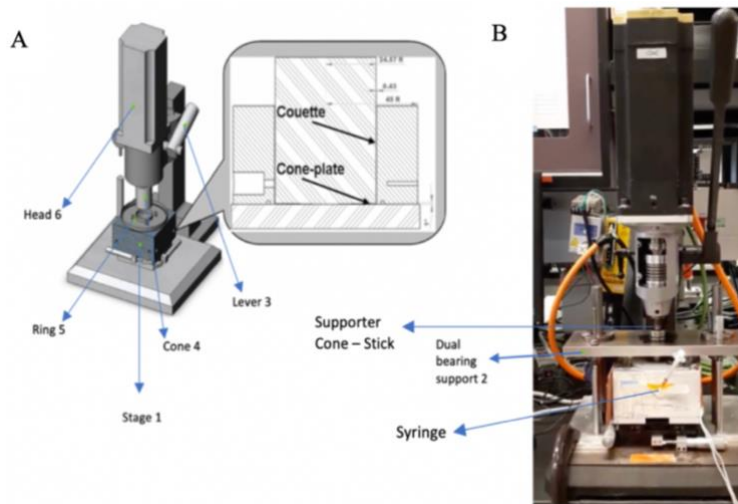


**Figure 23: The HSD combines the geometry of a cone and plate viscometer and a cylindrical coaxial Couette/ring viscometer where the cone and the cylinder gap are chosen such that all fluid is subjected to the same level shear stress**



According to the simplify mathematical model the stress tensor is symmetric and composed of six independent components. A common methodology employed in computational fluid dynamics studies of blood damage relies on the reduction in three-dimensional states of stress into one of its scalar invariants and frame indifference considerations [146]. Bludszuweit introduced the concept of assigning scalar stress values to path lines representing particle paths through the flow in blood recirculating devices, so that power law models could be employed [147]. The scalar stress  $\tau$  at each location and time of the path line of a fluid particle as it traverses the flow field is obtained by the **Equation 2**:

$$\tau = \left[ \frac{1}{6} \sum_{i,j=1}^3 (\sigma_{ii} - \sigma_{jj})(\sigma_{ii} - \sigma_{jj}) + \sigma_{ij}\sigma_{ij} \right]^{\frac{1}{2}} \quad \text{Eq. 2}$$

where  $\sigma_{ij}$  are the components of the stress tensor. It is assumed the fluid as a Newtonian one. Only one component of the deviatoric stress tensor is nonzero: the shear stress  $\tau = \tau(t)$  that the fluid is subjected to at time  $t$ . It is readily observed that the scalar stress resulting from **Eq. 2** for simple shear is the shear stress programmed in the HSD. The HSD was operated to generate a shear stresses up to 70 dyne/cm<sup>2</sup> such that flow remains laminar, inertial effects in the dynamic regime are minimal and secondary flow effects are not present [148] [149].

The assembly of the HSD is essential for the success of the experiment. The HSD is a highly sensitive instrument [150]. It is necessary to assemble the plate and the ring (couette, **Figure 23.A**) through two pins to create one unit; the unit, is insert inside the stage by two screws. The surfaces of Cone, Ring and Plate are made of UHMWPE and are designed to be as smooth as possible to minimize surface induced platelets activation. Platelet-surface interactions were then further minimized by coating the shear stress-generating surfaces with silicone. On the front side of the stage there is a channel which connects the inside of the ring with the outside. In the channel a syringe and polymeric tube are used to collect the sample at the end of the run. The stage is then, placed on the base and locked into place. Precise positioning of the cone height

above the base-plate (with respect horizontal line) is achieved with a dual-bearing-support and the couette gap between the cone and the ring is controlled with X-Y positioning micrometers. The platelets plus PMPs sample occupy the couette and the conical space. It is vital that the space between the base of the cone and plate is minimized as much as possible without making contact to ensure that the sample is between the walls during the cone rotation. If the base of the cone and plate come into contact frictional forces will weld both parts together and contaminate the sample. The same precaution of spacing has to be applied to the space between the ring walls and the cone walls. Once the proper alignment for the cone, with respect the ring and the plate along all axes, is achieved a volume of sample of 3 ml is added inside the ring and is distributed surrounding the cone. At the end we ensure the HSD by fastening all screws and bolts in the system. The cone supporter is connected to the motor mount (head) that is lowered by the lever. All screws and bolts must be tightly fasten in order to eliminate any vibrations that could damage the HSD. The device is controlled by Mint WorkBech: it is an integrated development environment (IDE) of MINT used to configure, query and program the controllers and drives. The viscosity  $\mu$  of the GFP is 1 cP (1 mPa\*sec).

## **4.11 Experiments**

The following sub-paragraphs describe which experiments were performed to study PMP procoagulant activity. In the static case, the procoagulant activity of PMPs was tested before with respect to quiescent platelets and consequently with respect to a physiologic activator. For dynamic experiments, HSD was instead employed. PAS assay was used to test the effective procoagulant potential of PMPs and consequently platelet activation. The experiments are listed in **Table 2** and **Table 3**.

### **4.11.1 Static Experiments**

#### **4.11.1.1 PMP effects on platelet activation**

PMPs were added to pure GFP (quiescent platelets, GFP-only), to test PMPs thrombogenicity, in three different concentration with respect to platelets. The concentrations were expressed as concentration ratio of PMP number over platelets (PLT) number:

- 1 / 100 PMP / PLT
- 1 / 1000 PMP / PLT
- 1 / 5000 PMP / PLT

The PMPs have been collected, isolated and used for the experiments. GFP + PMPs was obtained by adding 250  $\mu$ l of GFP (20 000 PLT/ $\mu$ l) to 250  $\mu$ l of PMPs diluted with PB (1 / 100, 1 / 1000, 1 / 5000 PMP / PLT).

In addition, PMPs alone (PMPs-only) were diluted with PB in same concentration in absence of GFP. Commonly, the number of PMPs circulating in the human blood system are in the concentration ratio PMPs /platelets equal to 1/300 – 1/3000, considering an average of 300'000 platelets/ $\mu$ l in physiological conditions.

Tube solution was incubated in a bath at 37°C for 5 minutes. Then 25  $\mu$ l of GFP + PMPs and 5  $\mu$ l of Factor X were added to 70 $\mu$ l of tube solution and incubate for different time-points: 0, 10, 30, 60 minutes. 0 minutes indicates that 10  $\mu$ l of sample were read immediately after the preparation of sample. The other samples were read at the end of each incubation time-step. For each sample, 10  $\mu$ L of solution were collected and inserted, with a micropipette, in a well plate with 150  $\mu$ l of WELLS solution. The well plate was read by a spectrophotometer (VersaMax™ absorbance Microplate Reader). Each acquisition lasted 7 minutes, during which 33 readings were performed. The PAS values were calculated as the slope of the linear fitting of the absorbance time data points through the software Softmax Pro 6.3, over the 7-min kinetic reading. PAS values were normalized against those obtained by sonicating GFP [145].

As control tests the following were used:

- Samples made by GFP- only (quiescent platelets) as negative control
- sonicated GFP (10 watt, 10 seconds) as positive control.

Negative and positive control were employed as upper and low limit and as reliability detectors of the assay.

#### **4.11.1.2 PMP effects on platelet activation compared with ADP**

ADP as physiological coagulation agonist were used as further control of PMPs activities. ADP interacts with platelets by binding to the receptor sites of the cells. Platelets undergo a conformational change, developing a spherical shape, enabling the release of granular contents (containing additional ADP) and thus further augmenting platelets aggregation.

ADP was purchased from Sigma Alderich (USA) and it was aliquoted at 1 mM and stored at -20 °C. The experiment provided a comparison of the following:

- GFP + PMPs;
- GFP + ADP;
- GFP + ADP + PMPs

in order to estimate the role of PMPs in platelet activation with respect the ADP.

PMPs have been added to GFP (20'000 platelets/ $\mu$ l), to test PMPs thrombogenicity, in two different concentration with respect to platelets. The concentrations were expressed as concentration ratio of PMP number over platelets (PLT) number:

- 1 / 1000 PMP / PLT
- 1 / 5000 PMP / PLT

GPF + PMPs was obtained by adding 250  $\mu$ l of GFP (20 000 PLT/ $\mu$ l) to 250  $\mu$ l of PMPs diluted with PB (1 / 1000, 1 / 5000 PMP / PLT). In addition, PMPs alone (PMPs-only) were diluted with PB in same concentration in absence of GPF.

Then, ADP has been added to the GFP (20'000 platelets/ $\mu$ l), to test PMPs thrombogenicity, in two different concentration:

- 10  $\mu$ M
- 20  $\mu$ M.

Tube solution was incubated in a bath at 37°C for 5 minutes. Then 25  $\mu$ l of each samples: GFP + PMPs, GFP + PMPs + ADP and GFP + ADP , were added to 5  $\mu$ l of Factor X and 70 $\mu$ l of tube solution and incubate for different time-points: 0, 10, 30, 60 minutes. 0 minutes indicates that 10  $\mu$ l of sample were read immediately after the preparation of sample. The other samples were read at the end of each incubation time-step. For each sample, 10  $\mu$ L of solution were

collected and inserted, with a micropipette, in a well plate with 150  $\mu$ l of WELLS solution. The well plate was read by a spectrophotometer (VersaMax<sup>TM</sup> absorbance Microplate Reader). Each acquisition lasted 7 minutes, during which 33 readings were performed. The PAS values were calculated as the slope of the linear fitting of the absorbance time data points through the software Softmax Pro 6.3, over the 7-min kinetic reading. PAS values were normalized against those obtained by sonicating GFP [145].

Positive and negative controls were provided:

- Samples made by GFP-only (quiescent platelets) as negative control
- sonicated GFP (10 watt, 10 seconds) as positive control.

Static Experiments	Samples tested	PMP / PLT concentration ratio	Incubation time [Min]
Pro-coagulant activity of PMPs	-PMPs only -GFP + PMPs	1 / 100	0
		1 / 1000	10
			30
		1 / 5000	60
Pro-coagulant activity of PMPs compared with ADP	-PMPs only -GFP + PMPs -GFP + PMPs + APD [10-20 $\mu$ M]	1 / 1000	0
			10
		1 / 5000	30
			60

**Table 2: Static experiments. Pro-coagulant activity of PMPs and comparison of PMPs activity with ADP**

#### 4.11.2 Dynamic experiments

We employed the HSD in our experiment to simulate a constant shear acting on platelets in combination with PMPs. PMPs were added to GFP before to undergo to constant shear by using HSD.

PMPs have been added to pure GFP (quiescent platelets, GFP-only), to test PMPs thrombogenicity, in two different concentration with respect to platelets. The concentrations were expressed as concentration ratio of PMP number over platelets (PLT) number:

- 1 / 1000 PMP / PLT
- 1 / 5000 PMP / PLT

GFP + PMPs was obtained by adding 250  $\mu$ l of GFP (20 000 PLT/ $\mu$ l) to 250  $\mu$ l of PMPs diluted with PB (1 / 1000, 1 / 5000 PMP / PLT).

The experiments have been performed with two different constant magnitude:

- Experiment 1: 30 dyne/cm<sup>2</sup> for 120 seconds
- Experiment 2: 70 dyne/ cm<sup>2</sup> for 120 seconds.

Tube solution was incubated in a bath at 37°C for 5 minutes. Then 25  $\mu$ l of each samples: GFP + PMPs stimulated and GFP + PMPs non-stimulated, were added to 5  $\mu$ l of Factor X and 70 $\mu$ l of tube solution and incubate for different time-points: 0, 10, 30, 60 minutes. 0 minutes indicates that 10  $\mu$ l of sample were read immediately after the preparation of sample. The other samples were read at the end of each incubation time-step. For each sample, 10  $\mu$ L of solution were collected and inserted, with a micropipette, in a well plate with 150  $\mu$ l of WELLS solution. The well plate was read by a spectrophotometer (VersaMax<sup>TM</sup> absorbance Microplate Reader). Each acquisition lasted 7 minutes, during which 33 readings were performed. The PAS values were calculated as the slope of the linear fitting of the absorbance time data points through the software Softmax Pro 6.3, over the 7-min kinetic reading. PAS values were normalized against those obtained by sonicating GFP [145].

The controls were:

- sonicated sample (positive control)
- GFP-only non-stimulated (negative control)
- GFP + PMPs non-stimulated.

<b>Dynamic Experiments</b>	<b>Samples tested</b>	<b>Applied shear levels</b>	<b>PMP / PLT concentration ratio</b>	<b>Incubation time [Min]</b>
<b>Pro-coagulant activity of PMPs under shear stress</b>	GFP + PMPs	Physiological 30 dyne/cm <sup>2</sup>	1 / 1000	0
				10
				30
				60
		Pathological 70 dyne/cm <sup>2</sup>	1 / 5000	0
				10
				30
				60

**Table 3: Dynamic experiments. Pro-coagulant activity of PMPs under shear stress**

#### **4.12 Statistical analysis**

Statistical analysis of the results obtained was performed with GraphPad Prism 8 (GraphPad Software, Inc., CA, USA). Normal distribution of data was tested with the Shapiro-Wilk normality test. The One-way Analysis of Variance (ANOVA) test was used when normality hypothesis was satisfied for all the groups being tested. Conversely, non-parametric Brown-Forsythe and Welch one-way ANOVA tests were performed. Finally, the Welch's t test was conducted between up to two groups. Statistical significance was assumed for p-values at least lower than 0.05.

## 5 Results

### 5.1 PMP Production, Isolation, and Storage

#### 5.1.1 PMP Production

##### 5.1.1.1 Cold-Induced PMP Production

As cold temperatures are known to activate platelets and to generate microparticles, cold storage of platelets was considered here as a method for producing PMPs for later experiments. The percentages of PMPs was calculated over the total number of particles acquired by flow cytometry. PMP percentages produced over time due to cold-induced platelet activation are shown in **Figure 24**.

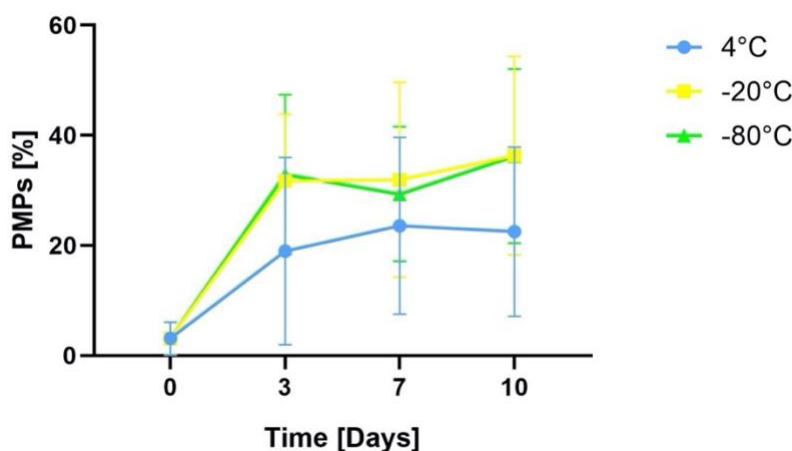


**Figure 24:** Percentage of PMPs produced by cold storage as a function of storage time, for different storage temperatures, N=10.

At low temperatures, PMP production increased with respect the fresh control (day 0). PMP production was temperature-dependent, such that the quantity of PMPs produced was greater when samples were frozen (-20°C and -80°C) rather than refrigerated (4°C). However, no difference was seen in PMP production between frozen samples at -20°C or 80 °C.

In addition, from the results we noticed that up to 3 days of storage, for each storage temperature, the number of PMPs produced increased dramatically and then flattened beyond the 3 days of storage.



To give a clearer image, in **Figure 25** it is shown an example of flow cytometry single acquisition of fresh, refrigerated and frozen GPF.

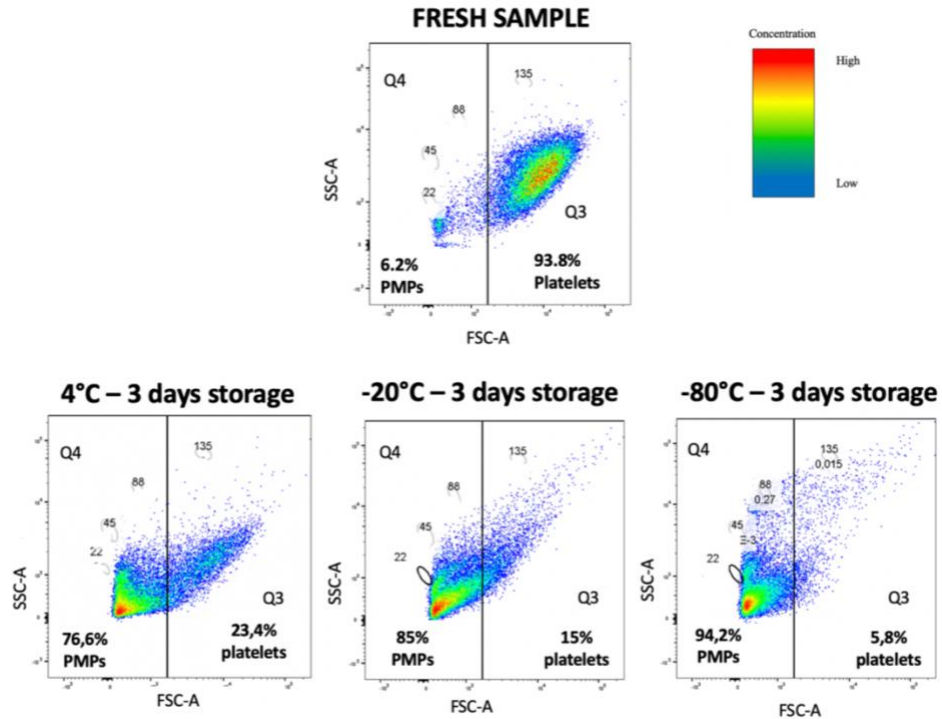


**Figure 25: SSC on y-axis and FSC on x-axis. Q4 and Q3 contain particles smaller and larger than 1  $\mu\text{m}$  respectively**

The images shown above display an example of how the temperature affected the activation of the platelets.

As the membrane of the platelets were cold-damaged, microparticles were generated increasing the particles number in quadrant Q4 (elements smaller than 1  $\mu\text{m}$ ).

Wide variances were recorded in generating PMPs using cold temperatures (**Figure 24**). As such, were quite difficult to obtain consistent results about the PMPs numbers, and cold temperature was thus avoided either as platelets activation or microparticle generation technique.

### 5.1.1.2 Agonist-Induced PMP production

Sonication and calcium ionophore are known platelet activators. We examined their ability to stimulate PMP production compared to resting samples (quiescent platelets) (**Figure 26**).

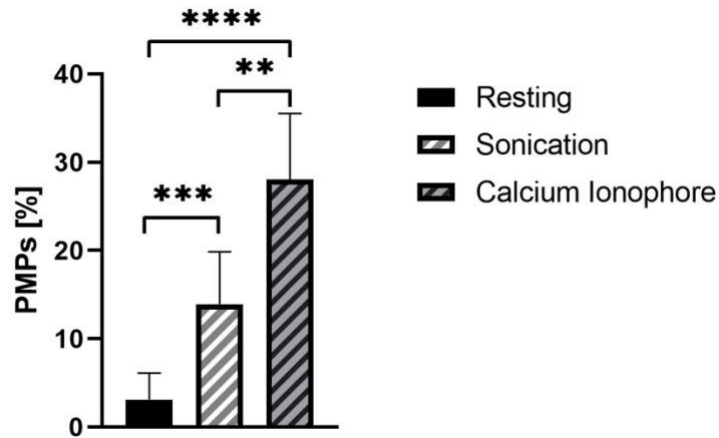


**Figure 26:**Percentage of PMPs over the total number of particles (N=8, n=16).

Data, shown as mean ± SD. \*\* p<0.01, \*\*\* p<0.001, \*\*\*\* p<0.0001

Both agonists were found to produce microparticles, with calcium ionophore producing a larger number of PMPs than sonication (\*\*, mean ± SD: 28 ± 7.5, 13.9 ± 5.9). A significant difference was found between sonication and resting sample with a p-value p<0.001 (\*\*\*, mean ± SD: 13.9 ± 5.9, 3.1 ± 3) and between calcium ionophore and resting sample with a p-value p<0.0001 (\*\*\*\*, mean ± SD: 28 ± 7.5, 3.1 ± 3).

The **Figure 27** shown an example of SEM of PMP production: inactivated platelets (a), calcium ionophore (b), and sonication (c).

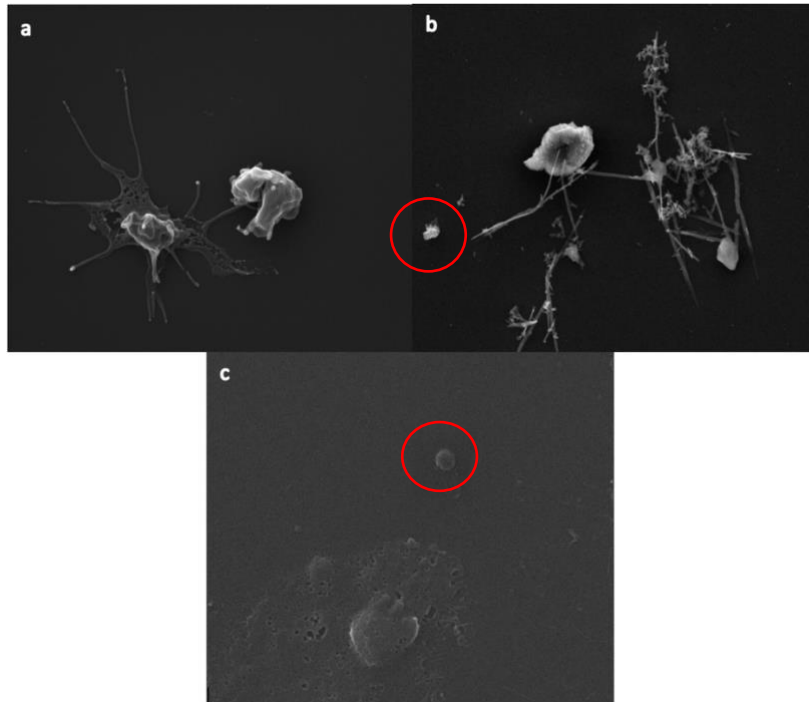


**Figure 27:** PMP production with different stimuli: no stimulus (a), calcium ionophore (b) and sonication (c). The elements circled in red are PMPs. Magnification is 20000x

An example of AFM output is shown in **Figure 28**. Platelets were stimulated by sonication.

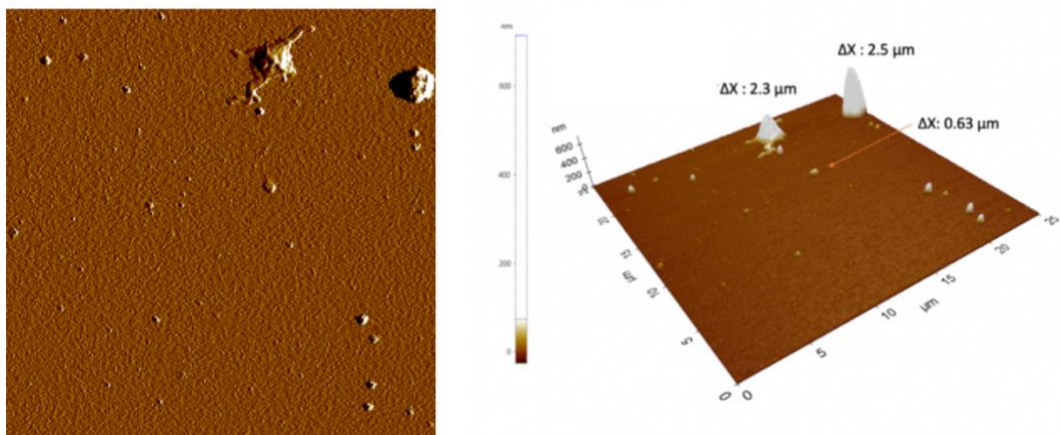


**Figure 28:** AFM acquisition of PMP produced by sonicated: raw image (left), background noise corrected 3D image (right). Scan dimension area :25x25x0.6μm

The larger size particles were identified as platelets activated by sonication. The small particles surrounding the activated platelets were identified as PMPs.

## 5.1.2 PMPs isolation

Two techniques were investigated for the isolation of PMPs produced by platelets: microcentrifugation and microfiltration. Microcentrifugation separates particles based on their differential densities, but requires optimization of centrifuge speeds, while microfiltration separates by size.

### 5.1.2.1 Microcentrifugation

Optimization of microcentrifugation speed was conducted in order to define the best protocol to collect the PMPs while avoiding platelet residues. Three sequentially centrifugation speeds 4000 rpm (1310 RCF), 6000 rpm (2940 RCF), 14 000 rpm (16 000 RCF) were operated and particle presence in the supernatant were evaluated.

**Figure 29** shows how the number of platelets and PMPs changes after each centrifugation step. The percentages were obtained over the total number of particles acquired by flow cytometry.

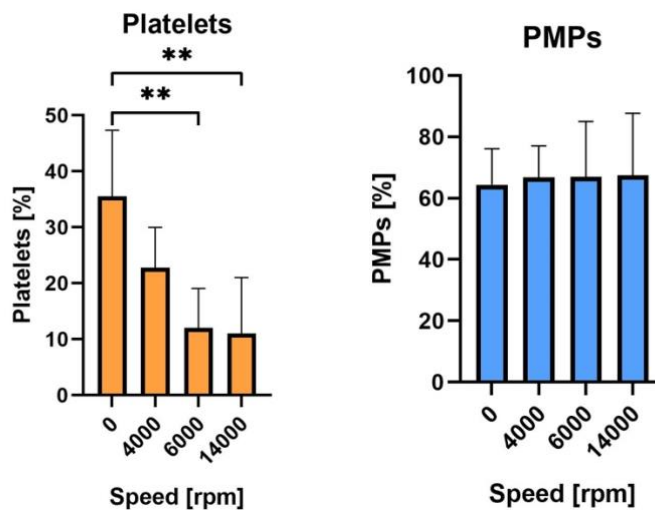


**Figure 29:** Percentages of platelets (left) and PMPs (right) as a function of the centrifugation speed (N=5, n=10). Data, shown as mean  $\pm$  SD. \*\* p<0.01

0 [rpm] indicates the sonicated GFP before the isolation by microcentrifuge. This sample was used as control to assess how the centrifugation speed and duration affected the number of platelets and PMPs.

Statistical analysis was performed between 0 [rpm] and the centrifugation steps for both platelet residues and PMP amount. After 1<sup>st</sup> centrifuge step (20 minutes at 4000 rpm), the number of platelet residues did not present a significant difference with respect the control (0 rpm). After 2<sup>nd</sup> centrifuge step (20 minutes at 4000 rpm and then 20 minutes at 6000 rpm) a decrease in the platelet residues was found, achieving a reduction of 23% with respect the control. The 3<sup>rd</sup> centrifuge step (20 minutes at 4000 rpm, 20 minutes at 6000 rpm and 40 minutes at 14 000 rpm) maintained approximately the same number of platelets residues recorded after 20 minutes at 4000 rpm and then 20 minutes at 6000 rpm. A significant difference was found by comparing the platelets number in the control (0 rpm) with the ones subjected to 2<sup>nd</sup> and 3<sup>rd</sup> centrifuge steps. Then, an analysis between 2<sup>nd</sup> and 3<sup>rd</sup> centrifuge steps was performed to compare the platelet residues and no significant difference was found.

The statistical analysis regarding the PMP loss demonstrates that the number of PMP was not changed significantly after the different centrifugation steps. In agreement with these results, it was chosen to perform two centrifugation speeds to isolate the PMPs: 4000 and 6000 rpm.

**Figure 30** shows a single flow cytometry acquisition of each centrifugation step.

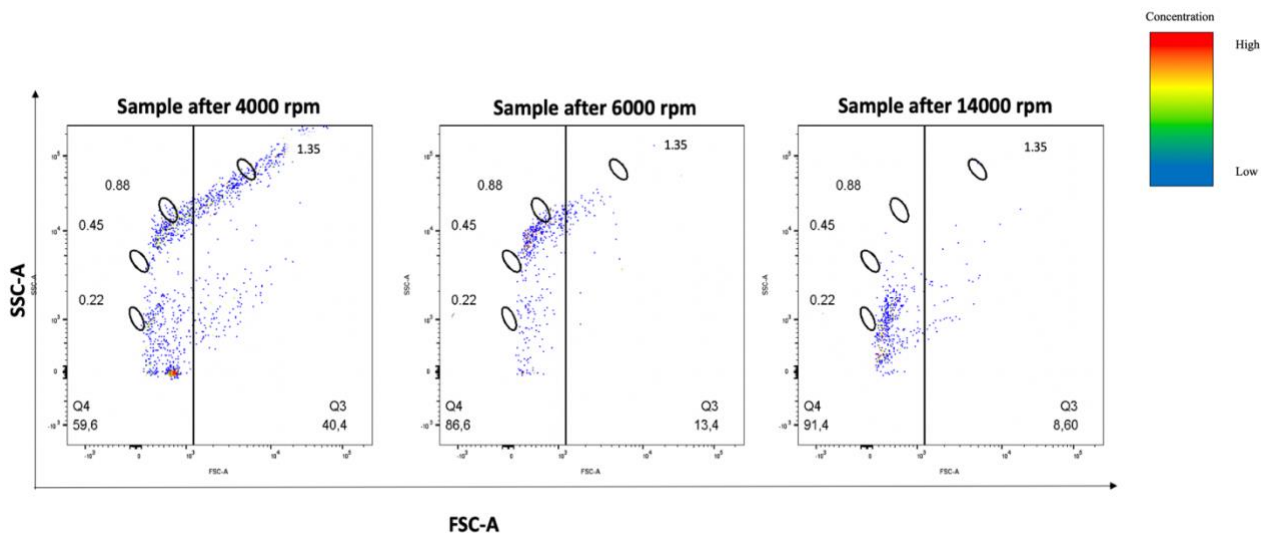


**Figure 30:** PMPs (Q4) and platelets (Q3) plotted as function of SSC (y-axis) and FSC (x-axis)

### 5.1.2.2 Microfiltration

In **Figure 31** the samples, collected after microfiltration, were analyzed to compare the elimination of platelets and retention of microparticles. A statistical analysis was performed between unfiltered and filtered samples. Platelet residues and PMP number were calculated as percentage over the total number of particles acquired by flow cytometry.

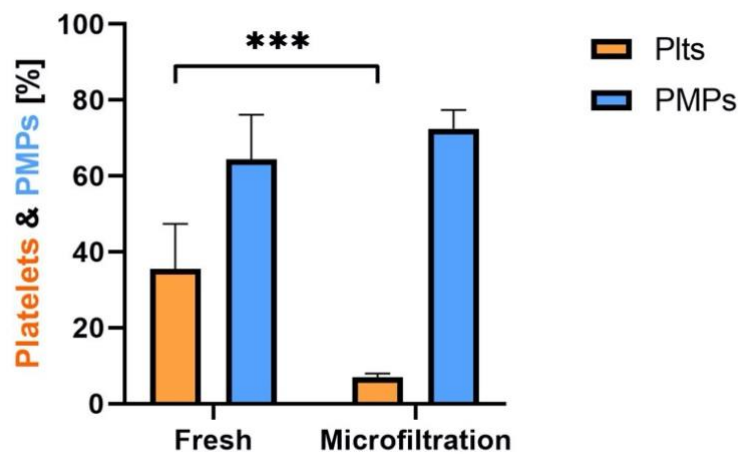


**Figure 31:** Platelet and PMP percentages over the total number of particles (N=4, n=8).

Data, shown as mean  $\pm$  SD. \*\*\* p<0.001

There is a significant difference between platelets quantity before and after the microfiltration with a p-value  $p < 0.001$  (\*\*\*). No statistical difference was reported regarding the PMP loss before and after the microfiltration. The low platelet concentration and the unchanged PMP concentration obtained after microfiltration (**Figure 31**) indicates a high efficiency of this isolation method.

Isolation was achieved by both microcentrifuge and microfiltration. However, microfiltration involved a loss of GFP due to the syringe loading and hold-up volume remaining in the inlet and outlet of the microfilter. As such, microcentrifugation was chosen as the preferred method of microparticle isolation.

### 5.1.3 PMP Storage

Establishing storage criteria improves usability of microparticles in the laboratory setting. The effect of storage duration at 4°C in the number of PMP was investigated. PMP number was compared with fresh sample (isolated PMPs) for each time-point. PMP number trend over time is shown in **Figure 32**.

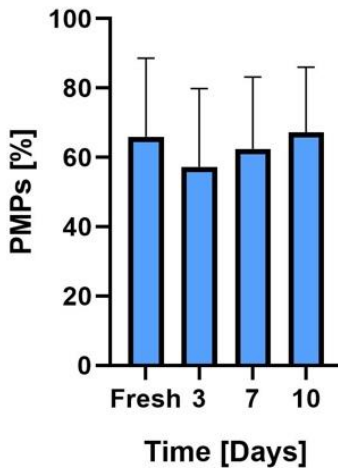


**Figure 32: PMP percentages as a function of storage time (N=10, n=5).**

Data, shown as mean  $\pm$  SD

According to the statistical analysis, PMP number was not affected by storage temperatures. Indeed, no significant differences between fresh sample and refrigerated samples were found. For these reasons, PMPs were stored up to 10 days.

## 5.2 Static experiments

### 5.2.1 PMP effects on platelet activation

To determine pro-coagulant potential of PMPs, platelets were incubated with microparticles under static conditions and examined for their ability to support thrombin generation. We investigated the effects of PMP concentration and incubation periods on platelet activation.

*1 / 100 PMP / PLT concentration ratio*

The first experiment was run with a concentration ratio PMP / PLT equal to 1 / 100. Outputs of the PAS assay, expressed as percentage of thrombin production, are shown in the **Table 4** and **Figure 33**.

Normalized PAS mean values [%]			
Time [Min]	GFP-only	PMPs-only	GFP + PMPs
<b>0</b>	0.40±0.4	33.50±10.7	15.15±6.3
<b>10</b>	6.35±2.6	96.50±22.6	84.80±23.4
<b>30</b>	34.75±12	103.75±20	95.80±90
<b>60</b>	66.60±15.7	97±21.5	94.10±19.7

**Table 4:** Normalized PAS values with respect to sonicated GFP, of static experiments with PMP / PLT concentration ratio equal to 1 / 100 (N=6, n=12)



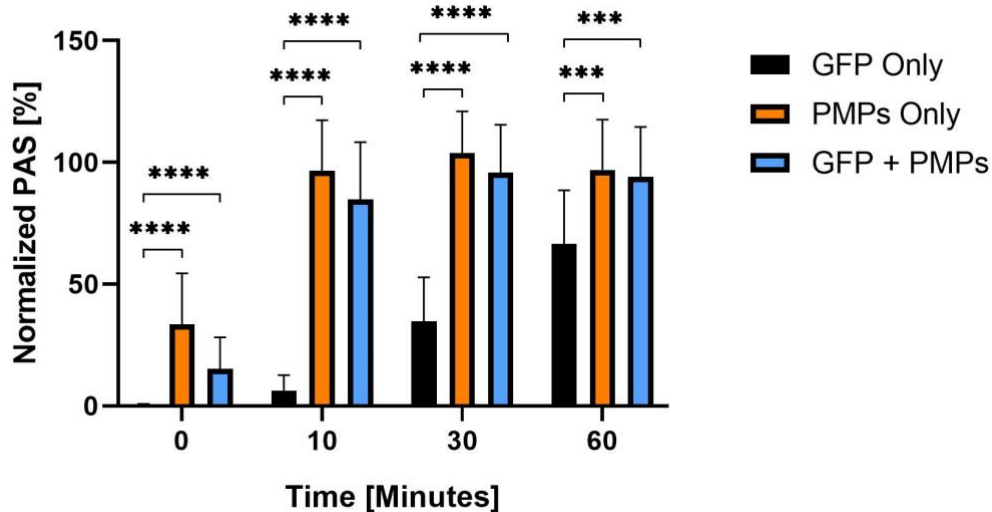


**Figure 33: Static experiments with PMP/platelet concentration ratio equal to 1 / 100 (N=6, n=12). Data, shown as mean  $\pm$  SD. \*\*\* p<0.001, \*\*\*\* p<0.0001**

Significant differences were observed between “GFP only” (negative control, quiescent platelets) and all the other samples, for all the incubation periods.

At 0 minutes, GFP-only showed a great significance with respect to PMPs-only and GFP + PMPs with a p-value  $p < 0.0001$  (\*\*\*\*). At 10 minutes the same p-value was found between GFP-only and PMPs-only and GFP + PMPs (\*\*\*\*). Significant difference with a p-value  $< 0.0001$  was also found at 30 minutes between GFP-only and PMPs-only and GFP + PMPs (\*\*\*\*). At 60 minutes a p-value  $< 0.001$  was found between GFP-only and PMPs-only and GFP + PMPs (\*\*\*).

No significant differences were found for all the incubation periods between PMPs-only or GFP + PMPs. PMPs-only thrombin production reached the saturation of the assay already after 10 minutes. Therefore, the added PMP concentration was too high for the assay used.

*1 / 1000 PMP / PLT concentration ratio*

Due to the saturation recorded in the previous experiment, PMPs were diluted with a concentration ratio PMP / PLT equal to 1 / 1000, and again examined for their ability to support thrombin generation. The PAS assay data, over time, are shown in **Table 5** and **Figure 34**.

<b>Normalized PAS mean values [%]</b>			
<b>Time [Min]</b>	<b>GFP-only</b>	<b>PMPs-only</b>	<b>PMPs + GFP</b>
<b>0</b>	0.40±0.1	3.35±0.7	4.38±3.5
<b>10</b>	6.26±2	39.43±10	51.50±10
<b>30</b>	42.60±3.8	61.34±6	74.25±8.4
<b>60</b>	73.59±4.2	74.72±10	81.25±9.9

**Table 5: Normalized PAS values with respect to sonicated GFP of static experiments with PMP / PLT concentration ratio equal to 1 / 1000 (N=7, n=14)**

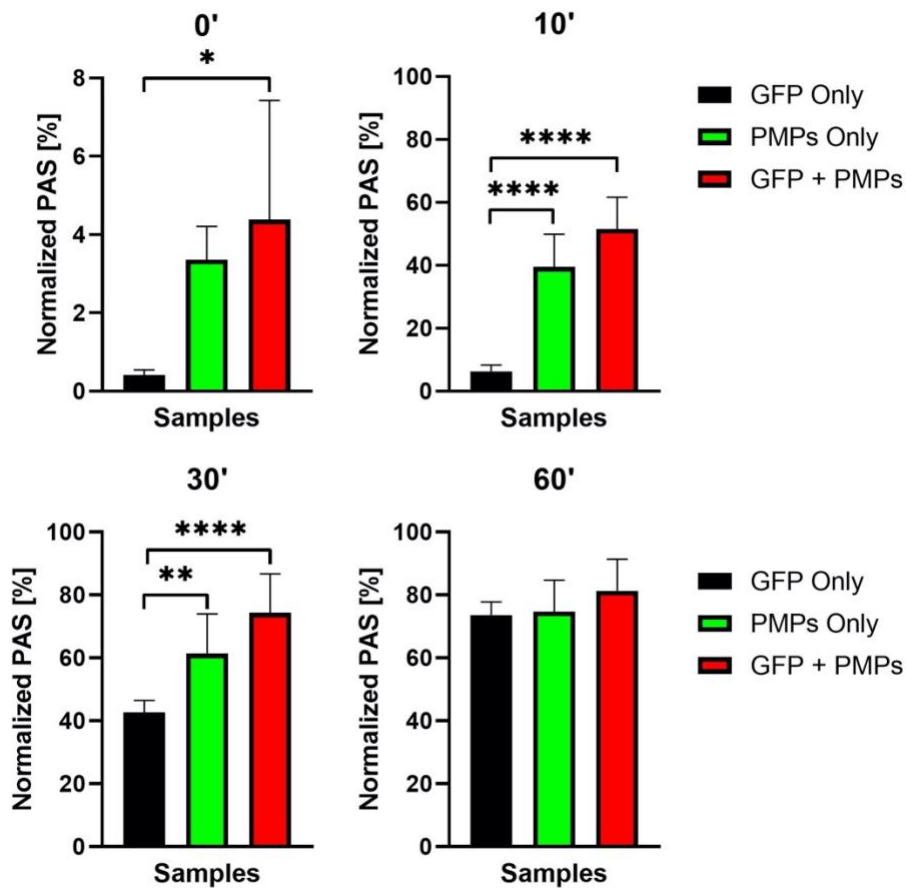


Figure 34: Static experiments with PMP / PLT concentration ratio equal to 1 / 1000 (N=7, n=14).

Data, shown as mean  $\pm$  SD. \* $p < 0.05$ , \*\*  $p < 0.01$ , \*\*\*\*  $p < 0.0001$

A statistical analysis was performed on results to establish whether there were some significant differences between GFP-only (negative control) and PMPs-only and between GFP-only and GFP + PMPs.

At 0 minutes the GFP-only and GFP + PMPs showed a  $p$ -value  $< 0.05$  (\*). Instead, no significant difference was found between PMPs-only and GFP-only. After 10 minutes of incubation the situation changed notably. Differences between the GFP-only and PMPs-only and between GFP-only and GFP + PMPs were significant. PMPs-only and GFP + PMPs showed a great significance with GFP-only,  $p < 0.0001$  (\*\*\*\*). After 30 minutes of incubation, GFP-only with GFP + PMPs showed a  $p$ -values  $< 0.0001$  (\*\*\*\*). The PMPs-only showed a significant

difference with GFP-only, with a p-values <0.01 (\*\*). After 60 minutes of incubation, both PMPs-only and GFP + PMPs almost reached the maximum thrombin production.

*1 / 5000 PMP / PLT concentration ratio*

PMPs were also diluted with a concentration ratio PMP / PLT equal to 1 / 5000, and again examined for their ability to support thrombin generation. The PAS assay recorded data over time are shown in **Table 6** and **Figure 35**.

<b>Normalized PAS mean values [%]</b>			
<b>Time [Min]</b>	<b>GFP-only</b>	<b>PMPs-only</b>	<b>PMPs + GFP</b>
<b>0</b>	0.40±0.13	1.34±0.5	1.82±0.8
<b>10</b>	6.26±2	21.13±8.4	37.68±10.1
<b>30</b>	42.60±3.8	42.45±11.6	65.54±8.1
<b>60</b>	73.59±4.2	62±12.6	76.32±9.1

**Table 6: Normalized PAS values with respect to sonicated GFP of static experiments with PMP / PLT concentration ratio equal to 1 / 5000 (N=7, n=14)**

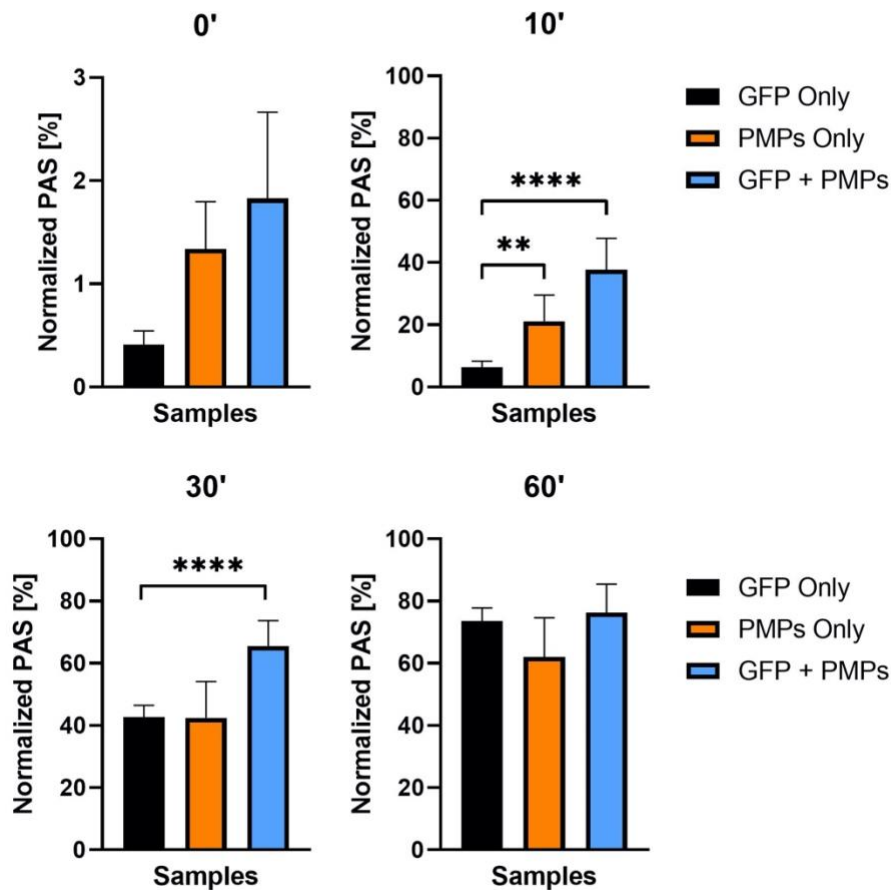


**Figure 35: Static experiments with PMP/platelet concentration ratio equal to 1 / 5000 (N=7, n=14). Data, shown as mean  $\pm$  SD. \*\* p<0.01, \*\*\*\* p<0.0001**

A statistical analysis was performed on results to establish whether there were some significant differences between GFP-only (negative control) and PMPs-only and between GFP-only and GFP + PMPs.

At 0 minutes no significant differences were found between GFP-only and PMPs-only and between GFP-only and GFP + PMPs.

After 10 minutes of incubation, significant differences between the GFP-only and the other samples (PMPs-only, GFP + PMPs) were found.

Indeed, the comparison between GFP-only and the PMPs-only showed a p-values <0.01 (\*\*). While GFP + PMPs showed a great significance with respect the GFP-only with a p-value

<0.0001 (\*\*\*\*). After 30 minutes of incubation, GFP-only and GFP + PMPs showed a p-values <0.0001 (\*\*\*\*). After 60 minutes of incubation, both PMPs-only and GFP + PMPs reached the maximum thrombin production.

Comparison between PMPs-only and GFP + PMPs

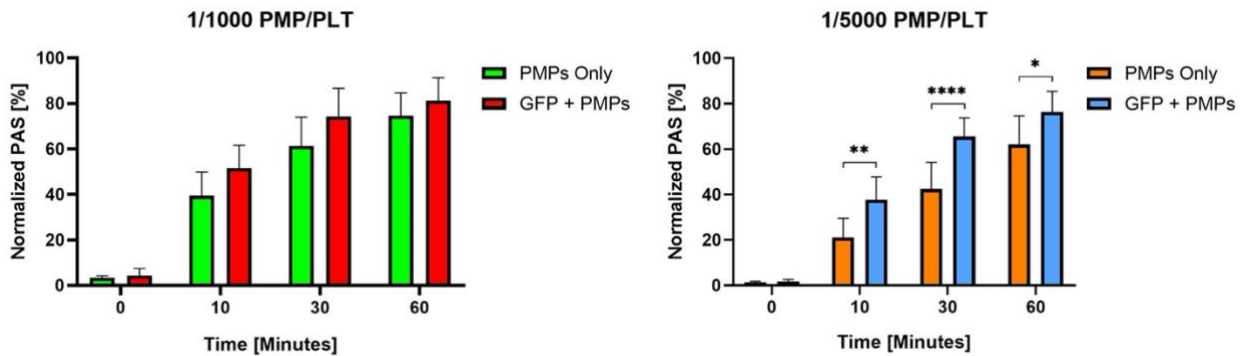
Based on the previous results, it could be reasonable to think that the increase in thrombin production of GFP + PMPs with respect PMPs-only is based on the additive effects of GFP and then of quiescent platelets. A statistical analysis was performed to compare GFP + PMPs and PMPs-only over time. The concentration ratios PMP / PLT used were 1 / 1000 and 1 / 5000 and the results of their comparison are shown in **Figure 36**.

No significant differences were found for higher concentration ratio, 1 / 1000 PMP / PLT; it suggests that the PMPs were responsible for most of the thrombin production.

At the contrary significant differences were found for lower concentration ratio, 1 / 5000 PMP / PLT, between PMPs-only and GFP + PMPs at 10, 30, and 60 minutes of incubation. It suggests that there is a significant contribution of platelets in thrombin production. At 10, 30 and 60

**Figure 36: PMPs-only and GFP + PMPs plotted as a function of time.(N=7, n=14).**

**Data, shown as mean ± SD. \* p<0.05, \*\* p<0.01, \*\*\*\* p<0.0001**



minutes of incubation, the significant difference between PMPs-only and GFP + PMPs showed

respectively a p-values  $<0.01$ (\*\*, mean  $\pm$  SD:  $21.1 \pm 8.4$ ;  $37.68 \pm 10.1$ ), a p-values  $<0.0001$ (\*\*\*\*, mean  $\pm$  SD:  $42.45 \pm 11.6$ ;  $65.54 \pm 8.1$ ), a p-values  $<0.05$ (\*, mean  $\pm$  SD:  $62 \pm 12.6$ ;  $76.32 \pm 9.1$ ). Hence, the thrombin increment in GFP + PMPs is due to additive effects.

### Dynamics of thrombin production over time

In **Figure 37** are shown the thrombin generation trends over time.

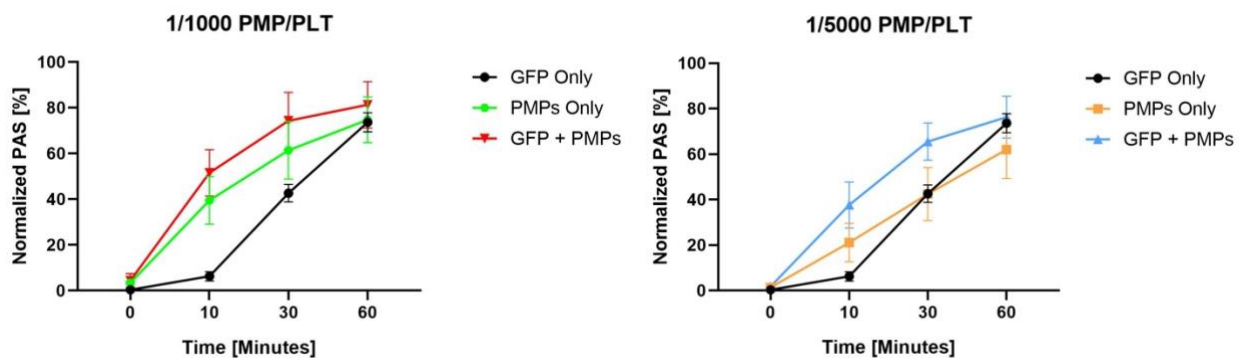


**Figure 37: Thrombin production plotted as a function of the time (N=7, n=14). Data are shown as mean  $\pm$  SD.**

**Figure 37** shows the trends of thrombin produced by each sample over the different incubation periods. Higher concentration ratio of PMPs, 1 / 1000, showed a high production of thrombin between 0 and 10 minutes for both samples: PMP-only and GFP + PMPs. While, between 10 and 30 minutes the slope growth of PMPs-only and GFP + PMPs slightly decreased.

Lower concentration ratio of PMPs, 1 / 5000, showed a linear production of thrombin for GFP + PMPs between 0 and 30 minutes and for PMP-only between 0 and 60 minutes. At 60 minutes of incubation the thrombin production tended to the same value for all the samples analyzed, due to reagents exhaustion. However, the presence of PMPs alone and in solution with platelets promoted a faster achievement of maximum thrombin production.

### Comparison of pro-coagulant activity between different PMP concentration

To test whether the pro-coagulant activity of PMPs was concentration dependent, a statistical analysis was performed between high and low PMP concentration ratios: 1 / 1000 PMP / PLT and 1 / 5000 PMP / PLT. PMPs were tested alone and in solution with GFP. The results are shown in **Figure 38**.

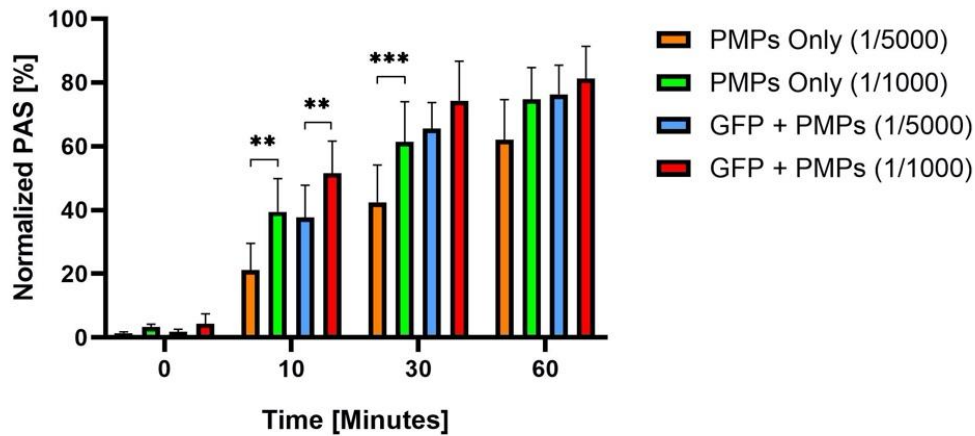


**Figure 38: Static experiments comparison between PMP / PLT equal to 1 / 1000 and 1 / 5000 (N=7, n=14). Data, shown as mean ± SD. \*\* p<0.01, \*\*\* p<0.001**

A significant difference was found between concentration ratios 1 / 5000 and 1 / 1000 PMP / PLT at 10 minutes with a p-value less than 0.01 (\*\*, mean ± SD: 21.15 ± 6.40; 39.40 ± 7.40) and at 30 minutes with p-value less than 0.001 (\*\*\*, mean ± SD: 42.4 ± 6.11; 61.35 ± 8.81). When PMPs were added to GFP, a significant difference between the two concentrations was only found at 10 minutes (\*\*, mean ± SD: 37.70 ± 10.12; 51.5 ± 10.13).

## 5.2.2 PMP effects on platelet activation compared with ADP

As PMPs were determined to be pro-coagulant, their impact on platelet activation was measured in comparison to and in tandem with a biochemical agonist, ADP.

### 1 / 1000 PMP / PLT concentration ratio



The influence of PMPs in concertation ratio equal to 1 / 1000 PMP / PLT and ADP [10 and 20  $\mu$ M] on platelet activation was investigated. The mean values of PAS assay outputs are summarized in **Table 7** and **Figure 39**.

<b>Normalized PAS mean values [%] - (1 / 1000 PMP / PLT)</b>						
<b>TIME [Min]</b>	<b>GFP only</b>	<b>GFP + PMPs</b>	<b>GFP + ADP</b>		<b>GFP + PMPs + ADP</b>	
			<b>10<math>\mu</math>M</b>	<b>20<math>\mu</math>M</b>	<b>10<math>\mu</math>M</b>	<b>20<math>\mu</math>M</b>
<b>0</b>	0.53 $\pm$ 0.1	1.77 $\pm$ 0.3	0.52 $\pm$ 0.1	0.83 $\pm$ 0.5	2.17 $\pm$ 1.2	2.47 $\pm$ 0.4
<b>10</b>	2.20 $\pm$ 1	27.52 $\pm$ 2.2	3.55 $\pm$ 1.5	3.80 $\pm$ 0.6	29.24 $\pm$ 3.4	30 $\pm$ 1.9
<b>30</b>	25.32 $\pm$ 7.2	57.94 $\pm$ 3	33.79 $\pm$ 3.1	34.15 $\pm$ 2.7	57.52 $\pm$ 5.2	65.88 $\pm$ 9.3
<b>60</b>	61.54 $\pm$ 7.6	68.70 $\pm$ 5.3	60.55 $\pm$ 8.9	68.55 $\pm$ 1.3	73.85 $\pm$ 3.5	72.60 $\pm$ 7

**Table 7: Normalized PAS values with respect to sonicated GFP of the static experiments with concentration ratio equal to 1 / 1000 PMP / PLT (N=5, n=10)**

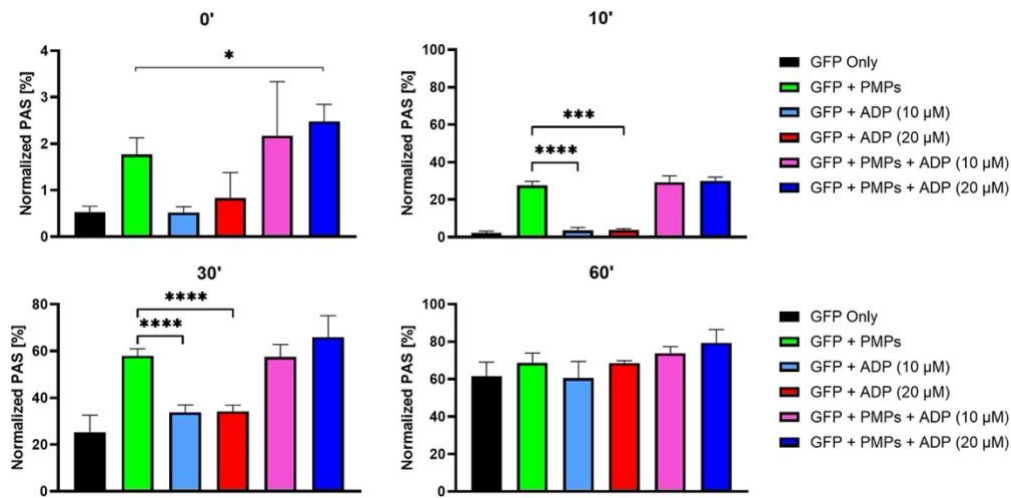


**Figure 39: Comparison of thrombin production between PMP (1 / 1000 PMP / PLT) and ADP [10 and 20 μM] (N=5, n=10). Data, shown as mean ± SD. \* p < 0.05, \*\*\* p < 0.001, \*\*\*\* p < 0.0001**

GFP + PMPs were compared with GFP + ADP and GFP + PMPs + ADP.

According to the statistical analysis, at 0 minutes data showed a significant difference between GFP + PMPs and GFP + PMPs + ADP [20 μM] less than 0.05 (\*).

After 10 minutes of incubation, GFP + PMPs with respect to GFP + ADP [20 μM] showed a significant difference with p-value less than 0.001 (\*\*\*). GFP + PMPs with respect to ADP [10 μM] showed a significant difference with p-value less than 0.0001 (\*\*\*\*).

After 30 minutes of incubation, it was shown that GFP + PMPs with respect GFP + ADP [20 μM] and ADP [10 μM] showed a significant difference with p-value less than 0.0001 (\*\*\*\*).

At 60 minutes of incubation, no significant difference was found.

Significant differences were observed only between GFP + ADP and GFP + PMPs while no significant differences were found between GFP + PMPs and GFP + ADP + PMPs over all the incubation periods. Therefore, the thrombin production generated by PMPs is considerably higher with respect the one promoted by ADP.

*1 / 5000 PMP / PLT concentration ratio*

The influence of PMPs in concertation ratio equal to 1 / 5000 PMP / PLT and ADP [10 and 20  $\mu$ M] on platelet activation was investigated. The mean values of PAS assay outputs are summarized in **Table 8, Figure 40**.

Normalized PAS mean values [%] - 1 / 5000 (PMP / PLT)						
TIME [Min]	GFP Only	GFP + PMPs	GFP + ADP		GFP + PMPs + ADP	
			10 $\mu$ M	20 $\mu$ M	1 / 5000- 10 $\mu$ M	1 / 5000- 20 $\mu$ M
0	0.53 $\pm$ 0.1	0.94 $\pm$ 0.2	0.52 $\pm$ 0.1	0.83 $\pm$ 0.5	1.23 $\pm$ 0.2	1.34 $\pm$ 0.2
10	2.20 $\pm$ 1	15.5 $\pm$ 1.78	3.55 $\pm$ 1.5	3.80 $\pm$ 0.6	16.80 $\pm$ 6.7	20.36 $\pm$ 2.8
30	25.32 $\pm$ 7.2	47.45 $\pm$ 3.1	33.79 $\pm$ 3.1	34.15 $\pm$ 2.7	47.54 $\pm$ 0.7	55.17 $\pm$ 1.8
60	61.54 $\pm$ 7.6	69 $\pm$ 0.2	60.55 $\pm$ 8.9	68.55 $\pm$ 1.3	70.90 $\pm$ 3.5	79.34 $\pm$ 3.5

**Table 8: Normalized PAS values with respect to sonicated GFP of static experiments with concentration ratio equal to 1 / 5000 PMP / PLT (N=5, n=10)**

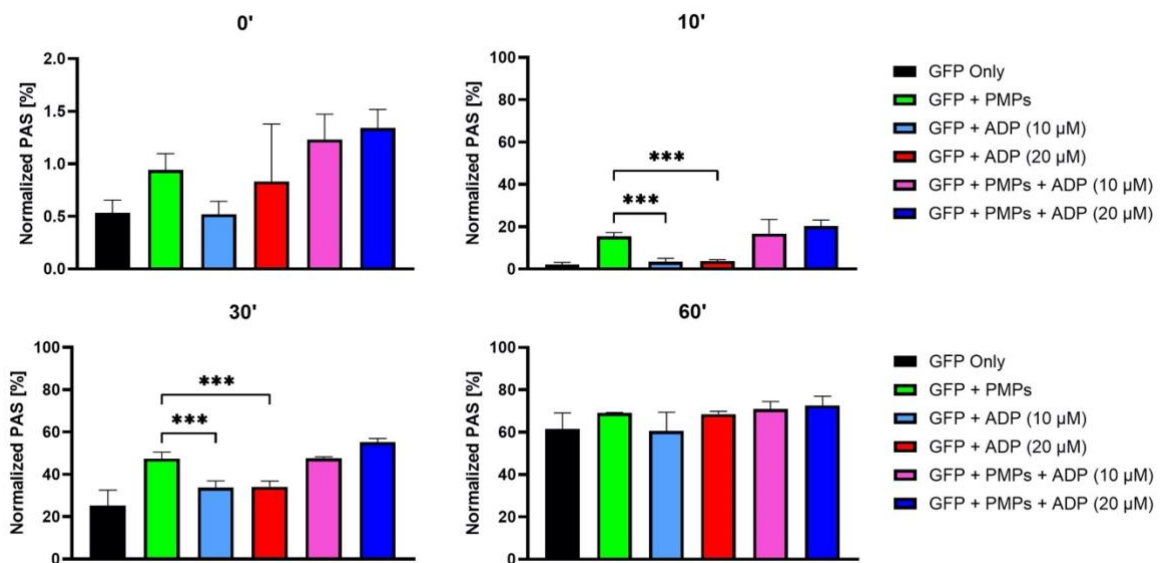


**Figure 40: Comparison of thrombin production between PMP (1 / 5000 PMP / PLT) and ADP [10 and 20 μM] (N=5, n=10). Data, shown as mean ± SD. \* p< 0.05, \*\*\* p<0.001**

A statistical analysis was provided to establish whether the data are reliable.

According to the statistical analysis, at 0 minutes data did not show statistical differences between GFP + PMPs and GFP + ADP and between GFP + PMPs and GFP + PMPs + ADP.

After 10 minutes of incubation, it was seen that GFP + PMPs and GFP+ADP [20 μM] and ADP [10 μM] showed a significant difference with p-value less than 0.001 (\*\*\*).

After 30 minutes of incubation, it was seen that the GFP + PMPs and GFP + ADP [20 μM] and ADP [10 μM] showed a significant difference with p-value less than 0.001 (\*\*\*). At 60 minutes of incubation, no significant difference was found.

Significant differences were observed only between GFP + ADP and GFP + PMPs while no significant differences were found between GFP + PMPs and GFP + ADP + PMPs over all the incubation periods. Therefore, the thrombin production generated by PMPs is considerably higher with respect one promoted by ADP.

### *Dynamics of thrombin production over time*

The thrombin production trends over time was shown by **Figure 41**.

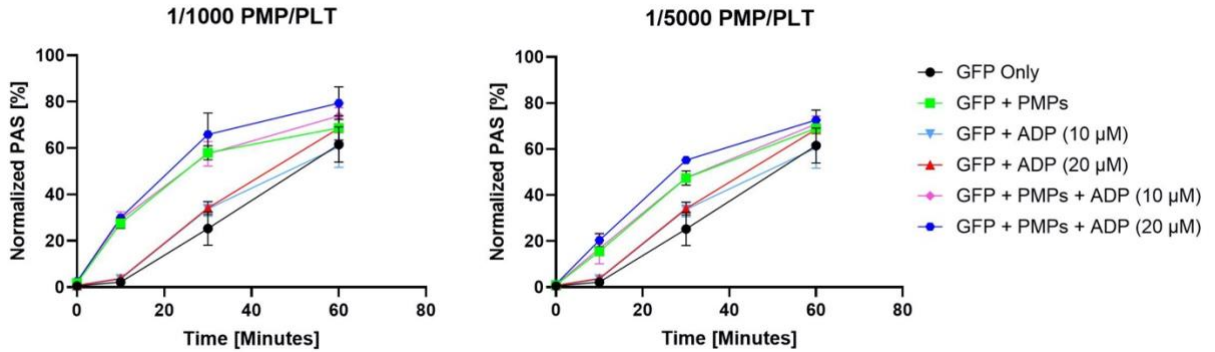


**Figure 41: Thrombin production plotted as a function of the time (N=5, n=10). Data are shown as mean  $\pm$  SD.**

GFP + ADP [10 and 20  $\mu$ M] showed a trend similar to the GFP-only although, with slightly higher values. GFP + PMPs and GFP + PMPs + ADP showed similar behaviors and close values between each other, for both the concentrations of PMPs used. Thus, the ADP action is almost negligible. This suggests that PMPs are not only activator, but also that their action is predominant with respect to a physiological agonist, as ADP.

### 5.3 Dynamic experiments

#### *Pro-thrombotic behavior of PMPs under shear-stress conditions*

The sample GFP + PMPs was subjected to two different shear stresses in order to simulate physiological and pathological dynamic conditions.

The present experiments were focused on the effect of mechanical loading on platelet activation in combination with PMP presence. GFP + PMPs were exposed to 30 dyne/cm<sup>2</sup> and 70 dyne/cm<sup>2</sup>, in two different experiments, of laminar shear in the hemodynamic shearing device for 2 minutes.

#### *1 / 1000 PMP / PLT concentration ratio*

**Table 9** shows the mean normalized PAS at different incubation periods of GFP + PMPs non-stimulated and of GFP + PMPs stimulated at 30 dyne/cm<sup>2</sup>. **Table 10** shows the mean normalized PAS at different incubation periods of GFP + PMPs non-stimulated and of GFP + PMPs stimulated at 70 dyne/cm<sup>2</sup>. In **Figure 42** are compared data of GFP + PMPs stimulated and non-stimulated by different shears.

<b>Normalized PAS mean values [%]- 1 / 1000 PMP / PLT</b>			
<b>TIME [min]</b>	<b>GFP-only</b>	<b>GFP+PMP Non-stimulated</b>	<b>GFP+PMP Stimulated 30 dyne/cm<sup>2</sup></b>
<b>0</b>	0.60±0.1	6.79±1.7	1.59±0.6
<b>10</b>	1.38±0.5	35.42±4.1	34.80±2.5
<b>30</b>	23.45±4.2	72.52±7	74.84±3.5
<b>60</b>	65.40±6.8	85.34±2.7	84.38±2.2

**Table 9: Normalized PAS values with respect to sonicated GFP of samples processed at 30 dyne/cm<sup>2</sup>. PMP / PLT concentration ratio equal to 1 / 1000 (N=4, n=8)**

Normalized PAS mean values [%]-1 / 1000 PMP / PLT			
TIME [min]	GFP-only	GFP + PMPs Non-stimulated	GFP + PMPs Stimulated 70 dyne/cm <sub>2</sub>
0	0.42±0.1	1.36±0.9	1.79±0.8
10	1.77±0.6	36±2.3	34.31±3.9
30	24.77±5.2	73.62±3	72.27±8.9
60	66.51±5	84.30±6.1	79.58±6.3

**Table 10: Normalized PAS values with respect to sonicated GFP of samples processed at 70 dyne/cm<sup>2</sup>. PMP / PLT concentration ratio equal to 1 / 1000 (N=4, n=8)**

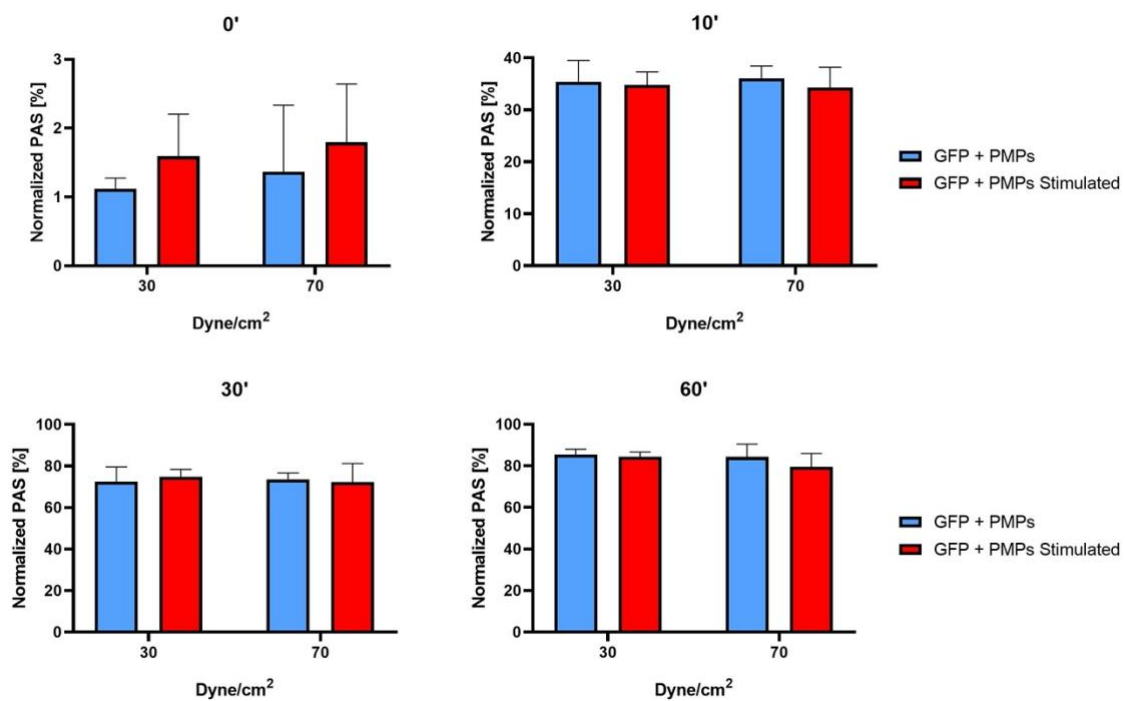


**Figure 42: GFP + PMPs samples, plotted as a function of shear applied (N=4, n=8).**

**Data, shown as mean ± SD.**

In all the comparisons between stimulated and non-stimulated GFP + PMPs, no significant differences were observed. Accordingly, the effect generated by these shears on platelets activation was negligible with respect the PMPs activity. Indeed, this indicates that the mechanical stimulation did not contribute to a further thrombin production.

*1 / 5000 PMP / PLT concentration ratio*

**Table 11** shows the normalized PAS mean at different incubation periods of GFP + PMPs non-stimulated and of GFP + PMPs after 30 dyne/cm<sup>2</sup> stimulation. **Table 12** shows the normalized PAS mean at different incubation periods of GFP + PMPs non-stimulated and of GFP + PMPs after 70 dyne/cm<sup>2</sup>. In **Figure 43** are shown data of GFP + PMPs stimulated and non-stimulated by different shears.

<b>Normalized PAS mean values [%]- 1 / 5000 PMP / PLT</b>			
<b>TIME [min]</b>	<b>GFP-only</b>	<b>GFP+PMP Non-stimulated</b>	<b>GFP+PMP Stimulated 30 dyne/cm<sup>2</sup></b>
<b>0</b>	0.60±0.1	1.59±0.6	0.60±0.1
<b>10</b>	1.38±0.5	13.22±1.5	12.12±1.1
<b>30</b>	23.45±4.1	48.82±8.2	50.16±5.3
<b>60</b>	65.40±6.7	68.32±9.8	68.17±5.8

**Table 11: Normalized PAS values with respect to sonicated GFP of samples processed at 30 dyne/cm<sup>2</sup>. PMP / PLT concentration ratio equal to 1 / 5000 (N=4, n=8)**



Normalized PAS mean values [%]			
TIME [min]	GFP-only	GFP+PMP Non-stimulated	GFP+PMP Stimulated 70 dyne/cm <sup>2</sup>
0	0.42±0.1	0.60±0.1	0.77±0.1
10	1.77±0.6	14.27±1.2	13.87±3
30	24.77±5.2	52.86±7.9	50.45±4.3
60	66.51±5	75±4.6	70±4.3

**Table 12: Normalized PAS values with respect to sonicated GFP of samples processed at 70 dyne/cm<sup>2</sup>. PMP / PLT concentration ratio equal to 1 / 5000 (N=4, n=8)**

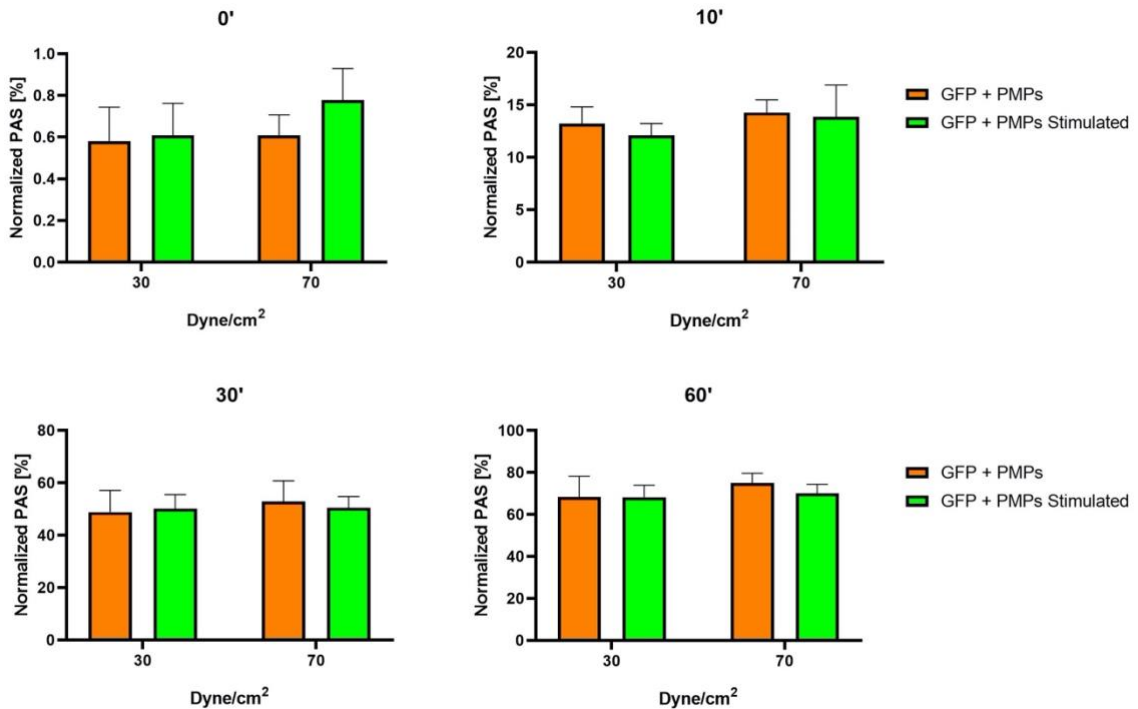


**Figure 43: GFP + PMPs samples plotted as a function of shear applied (N=4, n=8).**

Data, shown as mean ± SD. \* p<0.05

In all the comparisons no significant differences were observed. Accordingly, the effect generated by these shears on platelets activation was negligible with respect the PMPs activity. Indeed, this indicates that the mechanical stimulation did not contribute to a further thrombin production.

*Comparison between effect of 30 and 70 Dyne/cm<sup>2</sup>*

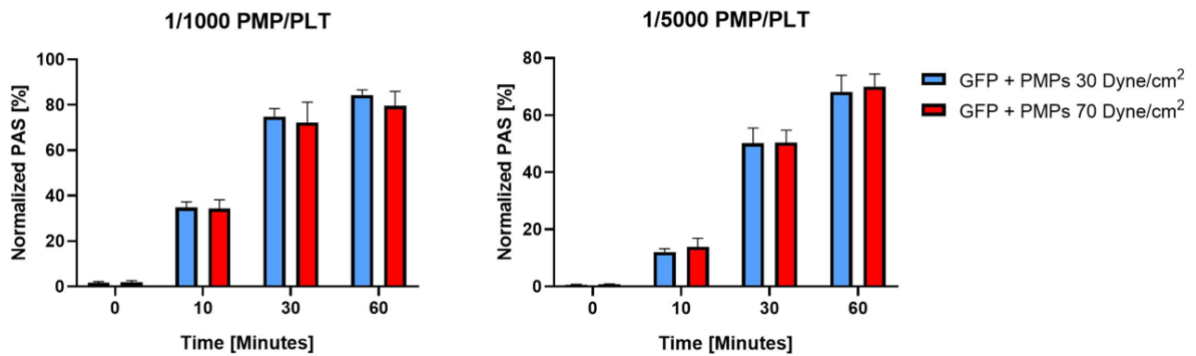


**Figure 44:** GFP + PMPs samples plotted as a function of time (N=4, n=8). Data, shown as mean ± SD

The samples were not affected differently by 30 and 70 dyne/cm<sup>2</sup>. **Figure 44** shows that there were no significant differences between GFP + PMPs exposed to 30 dyne/cm<sup>2</sup> and GFP + PMPs exposed to 70 dyne/cm<sup>2</sup> for both the concentrations of PMPs used.

### *Dynamics of thrombin production over time*

**Figure 45** shows the production of thrombin over different incubation periods for all the samples here analyzed.

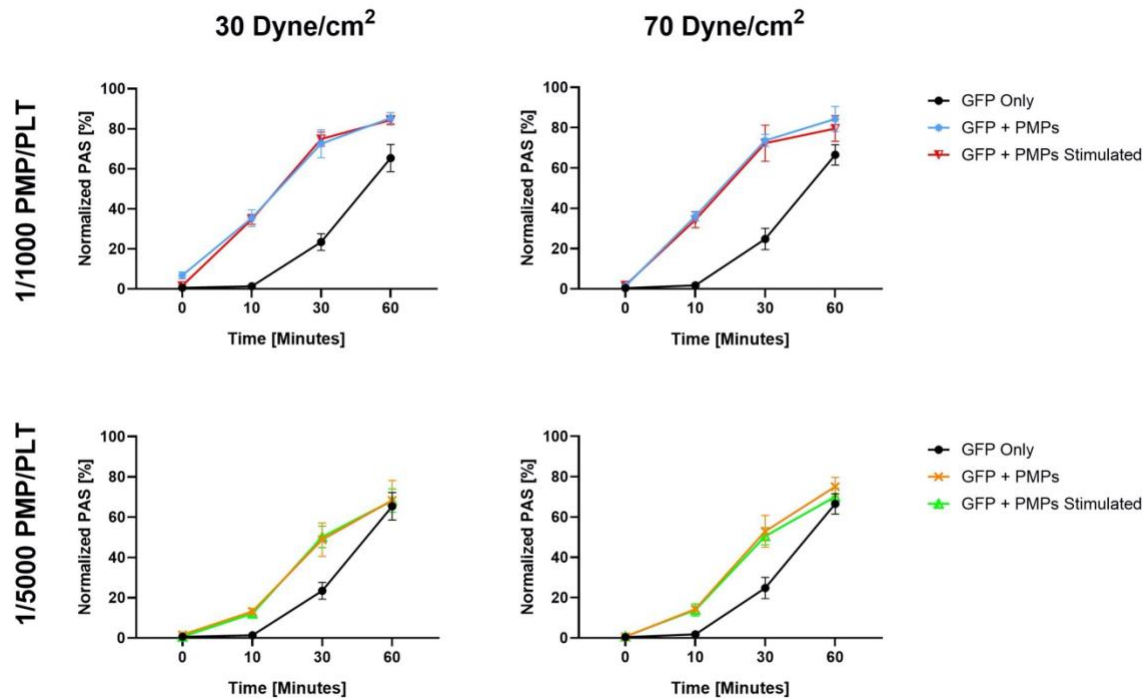


**Figure 45:** Thrombin production plotted as a function of time (N=4, n=8). Data are shown as mean  $\pm$  SD.

The thrombin production rate increased significantly between 0 and 30 minutes for GFP + PMPs stimulated and non-stimulated. The shear did not affect the thrombin production rate. Indeed, the curves, stimulated vs non-stimulated, showed the same trend. At 60 minutes, the rate of thrombin produced by all samples tended to saturate. However, the presence of PMPs in the samples promoted a faster achievement of maximum thrombin production.

## 6. Discussion

This work was aimed at investigating the procoagulant effect of PMPs under static and dynamic conditions. Moreover, PMPs effects were compared with respect to another physiological coagulation agonist (ADP). The work involved also a preliminary phase aimed to the characterization and optimization of PMP production, isolation and storage.

### *PMP production, isolation and storage*

Exposure to cold-temperatures, sonication and calcium ionophore were investigated for PMP production. All three methods effectively formed microparticles, however the effect of temperature was highly variable. According to Jy et al., freezing and thawing cycle alters PMPs properties [151]. Sonication and calcium ionophore led to an increase in the number of PMPs of 5 and 10 times respectively compared to the quiescent sample. The same results were obtained by Baj-Krzyworzeka et al. [152].

Although calcium ionophore was the most efficient method of producing PMPs, its presence in solution with platelets would activate them making impossible to distinguish the effective contribution of other agonists. Thus, sonication was the method chosen for further experiments.

Refrigeration was studied to store PMPs. In agreement with the results obtained, PMPs can be stored at 4°C up to 10 days without undergoing variations in number. The same conclusion was found by Gamonet et al. who demonstrate that, once stored at 4°C, the PMP amount is stable for 7 days [153].

The two investigated techniques compared to achieve PMP isolation were microcentrifugation and microfiltration. The microcentrifugation protocol used here combines methods found in literature [107], [154]. Our results showed that two sequential centrifugation steps (1310 and 2940 g) effectively isolated PMPs without volume loss. Moreover, microcentrifugation allowed to isolate small volumes (100 – 1000 µl) which could not be processed by microfiltration.

### *PMP Thrombogenicity under static conditions*

PMPs, in solution with platelets, were able to generate much higher thrombin quantities than those generated by platelets alone. Thrombin production by PMPs was found to be depend on both PMP concentration and incubation period. Moreover, it was found that low concentration ratios (1 / 1000 - 1 / 5000 PMP / PLT) and periods (up to 60 minutes) were necessary to avoid saturating the assay.

Literature supports our findings that PMPs are procoagulant [129] [130] [131]. According to Kireev et al., PMPs membranes have 50- to 100-fold higher specific procoagulant activity than activated platelets [130].

PMP ability to support thrombin generation was hence demonstrated *in vitro*, suggesting that it would have significant effects *in-vivo* [132]. Since thrombin is a physiological coagulation agonist, its production by PMPs could lead to the activation and consequent aggregation of platelets. In a physiological environment, in fact, pro-coagulant activity would not be the only PMP contribution to platelet aggregation. As reported in literature [134][135][136], PMPs not only amplify the procoagulant activity of platelets due to the membrane lipid composition but they also affect clot formation, *in vivo* condition.

The reason of different amount of thrombin produced by PMPs-only and GFP + PMPs could be address to the additive effects of platelets (GFP). According to Jesty et al. a sample containing inactivated platelets (GFP-only) generates an increasing rate of thrombin in time [140]. Nevertheless, it was noticed that by using a high physiological concentration of PMPs the procoagulant action was to be attributed more to the presence of PMPs.

Another interesting result was the fact that thrombin production was PMP concentration-dependent. The same result was achieved by Kireev et al. [130]. Indeed, they noticed that the maximal thrombin production rapidly increased with the increase of the concentration of PMPs added.

### *PMP thrombogenicity compared with ADP*

When the action of ADP was compared with the PMPs one, it was concluded that the latter produced thrombin in greater quantities. Indeed, solution of GFP + PMPs + ADP showed almost the same thrombin production than the sample GFP + PMPs.

Therefore, the thrombogenic activity of PMPs was shown to be significantly superior with respect to the action promoted by ADP on platelets activation. According to P.J Sims et al. who studied and compared several different agonists, ADP is considered a weak agonist of the coagulation [155]. This led us to suppose that PMPs are strong activators able to surmount the ADP pro-coagulant action, under these conditions.

#### *PMP thrombogenicity tested under shear-stress conditions*

Constant shear levels were applied to simulate dynamic conditions. 30 dyne/cm<sup>2</sup> simulates a shear stress present in physiological environment (1-50 dyne/cm<sup>2</sup>, venous and arteriosus range) while 70 dyne/cm<sup>2</sup> simulates a shear stress beyond physiological range [156]. Platelets and PMPs in solution were exposed to a constant shear stress and then compared to a non-stimulated samples. Platelets with an addition of PMPs, in presence and absence of shear, did not show significant differences over time for both shear levels applied. The mechanical shear was found not to contribute to an increment of thrombin production.

According to Leytin et al., physiologic shear stresses (30 dyne/cm<sup>2</sup>) did not affect the platelet responses [137].

In the non- physiologic case (70 dyne/cm<sup>2</sup>), it was observed that an increase in shear stress level did not correspond in a thrombin increment.

Therefore, it was assumed that the effect induced by the applied shear was too low to be distinguishable from the effect induced by PMPs already present. Indeed, Sheriff et al., documented that the shear threshold for which platelet activation occurs is around 70 dyne/cm<sup>2</sup> and that the number of activated platelets is shear magnitude-dependent [138].

Thus, the PMPs created by the effect of high-shear on platelets did not make a significant contribution with respect to PMPs added to platelets before exposure.

In conclusion, from the first experiments we determined that PMPs effectively are pro-coagulant. Successively, it was demonstrated that the PMPs have a higher procoagulant activity than ADP-activated platelets. Finally, in dynamic conditions, it was established that the platelet activation, in presence of additive concentration of PMPs, is not affected by the shear constant stimulation up to 70 dyne/cm<sup>2</sup>.

## 7. Conclusion

The goal of this thesis was to investigate the thrombogenic effect of platelet-derived microparticles. This work has been performed by a joint collaboration between Politecnico di Milano and University of Arizona.

The clinical importance of microparticles resulting from vesiculation of platelets is increasingly recognized. Yet fundamental questions about their formation and role in human diseases and hemostasis are just beginning to be understood at the cellular and molecular level. Moreover, PMP manipulation techniques are still not well established and validated.

Our study showed that:

- (1) PMPs act as a pro-coagulant factor
- (2) The thrombogenic potential related to PMPs is higher than that of ADP
- (3) The presence of high PMP concentration makes the shear stress effect negligible

The main limitation of the work is that our in-vitro approach, by using GFP, does not replicate completely the physiological conditions. Indeed, it is harder to infer whether PMPs are also procoagulant in vivo, because influences of blood flow (shear stress), adhesive reactions, or soluble factors including coagulation factors, anti-coagulation factors, and cofactors would ultimately determine the activity of these vesicles. Moreover, the PAS assay did not allow to test higher concentration (non-physiological) of PMPs because of the quick saturation reached.

Among future experiments we planned to include a comparison between the pro-coagulant activity of the PMPs compared to that of the shear. Specifically, the pro-coagulant action of the platelets subjected to mechanical shear is compared with the action of the platelets influenced

by the presence of PMPs only. In addition, since in pathologies such as severe stenoses, stresses approach 350 to 1400 dyne/cm<sup>2</sup> and in presence of exogenous devices such as MCS systems they reach peaks of 1000 and 2000 dyne/cm<sup>2</sup>, we planned to simulate such stimuli to re-create similar pathological conditions. These two set of experiments, briefly shown, were temporary postpone due to the inevitable situation generated by COVID-19.



## 8. References

- [1] Michelson A D, "Platelets", ELSEVIER, pp. 403-411, 2007
- [2] Yuana Y, Bertina R M, Osanto S, "Pre-analytical and analytical issues in the analysis of blood microparticles" , *Thrombosis and Haemostasis*, vol. 150, no.3, pp. 396-408, 2010
- [3] Baj-Krzyworzeka M, Majka M, Pratico D, Ratajczak J, Vilaire G, Kijowski J, Reza R, Janowska-Wieczorek A, Ratajczak M Z, "Platelet-derived microparticles stimulate proliferation, survival, adhesion, and chemotaxis of hematopoietic cells", *Experimental Hematology*, vol. 30, no. 5, pp. 450-459, 2002
- [4] Girdhar G, Xenos M, Alemu Y, Chiu W C, Lynch B E, Jesty J, Bluestein D, "Device thrombogenicity emulation: A novel method for optimizing mechanical circulatory support device thromboresistance," *PLoS One*, vol. 7, no. 3, pp. 1–10, 2012
- [5] Perrotta P L, Parsons J, Rinder H M, Snyder E L, "Platelet Transfusion Medicine" In *Platelets*, Elsevier, pp. 1275-1303, 2013
- [6] Italiano J E, Mairuhu A, Flaumenhaft R, "Clinical Relevance of Microparticles from Platelets and Megakaryocytes", *Current opinion in hematology*, vol. 17, no. 6, pp. 578-84, 2010
- [7] Basu D, Kulkarni R, "Overview of blood components and their preparation", *Indian J. Anaesth.*, vol. 58, no. 5, pp. 529–537, 2014
- [8] Institute for Quality and Efficiency in Health Care (IQWiG), "What does blood do?," *Inf. Heal. Online*, 2015.
- [9] Dean L, "Blood Groups and Red Cell Antigens", pp. 1–6, 2005
- [10] Lienhard D et al., "Does centrifugation matter? Centrifugal force and spinning time alter the plasma metabolome", *Metabolomics*, vol. 12, no. 10, p. 159, 2016

- [11] World Health Organization, "Use of Anticoagulant in Diagnostic Laboratory Investigations", 2002
- [12] Pretorius E, "The adaptability of red blood cells", *Cardiovascular Diabetology*, vol. 12, no. 1, pp. 1-7, 2013.
- [13] Diez-Silva M, Dao M, Han J, Lim C T, Suresh S, "Shape and Biochemical Characteristics of Human Red Blood Cells in Health and Disease", *MRS Bull.*, vol. 35, no. 5, pp. 382–388, 2010
- [14] Palis J, "Primitive and definitive erythropoiesis in mammals", *Frontiers in Physiology*, vol. 5, pp. 1–9, 2014
- [15] Osler W, "On certain problems in the physiology of the blood corpuscles", *The Medical News*, vol.48, pp.421–25, 1886.
- [16] Ghoshal K, Bhattacharyya M, "Overview of Platelet Physiology: Its Hemostatic and Nonhemostatic Role in Disease Pathogenesis", *The Scientific World Journal*, pp. 1–16, 2014
- [17] Hartwig J H, "The platelet: Form and Function", *Seminars in Hematology*, vol. 43, no. supplement 1, pp. 94–100, 2006
- [18] Dalla Valle F, "Studio dell'aggregazione piastrinica con aggregometro ad elettrodi multipli (multiplate®) e della disfunzione endoteliale con tecnica eco color doppler in soggetti trombofilici."
- [19] Hickerson D H M and Bode A P, "Flow cytometry of platelets for clinical analysis," *Hematol. Oncol. Clin. North Am.*, vol. 16, no. 2, pp. 421–454, 2002.
- [20] Moreau T et al., "Large scale production of platelet forming megakaryocytes from human pluripotent stem cells by a chemically defined forward programming approach", *Nature Communications*, vol. 7, pp. 1-16, 2016

- [21] Wen Q, Goldenson B, Crispino J D, “Normal and Malignant Megakaryopoiesis”; *Expert Reviews in Molecular Medicine*, vol. 13, pp. 1-18, 2011
- [22] Nakeff A, Maat B, “Separation of Megakaryocytes From Mouse Bone Marrow by velocity Sedimentation”, *Blood*, vol. 43, no. 4, pp. 591–595, 1974
- [23] Patel S R, Hartwig J H, Italiano E, “The biogenesis of platelets from megakaryocyte proplatelets”, *The Journal of Clinical Investigation*, vol. 115, no. 12, pp. 3348–3354, 2005
- [24] Gear A R, Camerini D, “Platelet chemokines and chemokine receptors: Linking hemostasis, inflammation, and host defense”, *Microcirculation*, vol. 10, no. 3–4, pp. 335–350, 2003
- [25] Holinstat M, “Normal platelet function”, *Cancer Metastasis Reviews*, vol. 36, no. 2, pp. 195–198, 2017.
- [26] Lam F W, Vijayan K V, Rumbaut R E, “Platelets and their interactions with other immune cells”, *Comprehensive Physiology*, vol. 5, no. 3, pp. 1265–1280, 2015
- [27] Kemperman H, De Lange D W, Kesecioglu J, Roest M, Schrijver I T, “Soluble P- selectin as a Biomarker for Infection and Survival in Patients With a Systemic Inflammatory Response Syndrome on the Intensive Care Unit”, *Biomarker Insights*, vol. 12, pp. 1–6, 2017
- [28] Manka D et al., “Critical role of platelet P-selectin in the response to arterial injury in apolipoprotein-E-deficient mice”, *Arteriosclerosis, Thrombosis and Vascular Biology*, vol. 24, no. 6, pp. 1124–1129, 2004
- [29] Wagner D D, Frenette P S, “The vessel wall and its interactions”, *Blood*, vol. 111, no. 11, pp. 5271–5281, 2008
- [30] Zarbock A, Polanowska-Grabowska R K, Ley K, “Platelet-neutrophil-interactions: Linking hemostasis and inflammation”, *Blood Reviews*, vol. 21, no. 2, pp. 99–111, 2007

- [31] Moore K L et al., “Identification of a specific glycoprotein ligand for P-selectin (CD62) on myeloid cells”, *Journal of Cell Biology*, vol. 118, no. 2, pp. 445–456, 1992
- [32] Hartwig H et al., “Platelet-derived PF4 reduces neutrophil apoptosis following arterial occlusion”, *Thrombosis Haemostasis*, vol. 111, no. 3, pp. 562–564, 2013
- [33] Bakogiannis C, Sachse M, Stamatelopoulos K, Stellos K, “Platelet-derived chemokines in inflammation and atherosclerosis”, *Cytokine*, pp. 1043–4666, 2017
- [34] Thachil J, “Platelets and infections in the resource-limited countries with a focus on malaria and viral haemorrhagic fevers”, *British Journal of Haematology*, vol. 177, no. 6, pp. 960– 970, 2017
- [35] Putri I H, Tunjungputri R N, De Groot P G, Van Der Ven A J, De Mast Q, “Thrombocytopenia and Platelet Dysfunction in Acute Tropical Infectious Diseases”, *Seminars in Thrombosis and Hemostasis*, vol. 44, no. 7, pp. 683–690, 2018
- [36] Haemmerle M, Stone R L, Menter D G, Afshar-kharghan V, Sood A K, “The Platelet Lifeline to Cancer : Challenges and Opportunities”, *Cancer Cell*, vol. 33, no. 6, pp. 965–983, 2018
- [37] Bailey S E, Ukoumunne O C, Shephard E, “How useful is thrombocytosis in predicting an underlying cancer in primary care? A systematic review”, *Family Practice*, vol. 34, no. 1, pp. 4–10, 2017
- [38] Huong P T, Nguyen L T, Nguyen X, Lee S K, “The Role of Platelets in the Tumor-Microenvironment and the Drug Resistance of Cancer Cells”, *Cancers*, vol. 11, no. 2, p. 240, 2019
- [39] Palta S, Saroa R, Palta A, “Overview of the coagulation system”, *Indian J. Anaesth.*, vol. 58, no. 5, pp. 515–523, 2014

- [40] Dahms S O, Demir F, Huesgen P F, Thom K, Brandstetter H, “Sirtilins - the new old members of the vitamin K-dependent coagulation factor family”, *Journal of Thrombosis and Haemostasis*, vol. 17, no. 3, pp. 470–481, 2019
- [41] Green D, “Coagulation cascade”, *Hemodialysis International*, vol. 10, no. 2, pp. 10–12, 2006
- [42] Macfarlane R G, “An Enzyme Cascade in the Blood Clotting Mechanism, and its Function as a Biochemical Amplifier”, *Nature*, vol. 202, pp. 498–499, 1964
- [43] Davie E W, Rattnoff O D, “Waterfall Sequence for Intrinsic Blood Clotting”, *Science*, vol. 145, no. 3638, pp. 1310–1312, 1964
- [44] Hepner M, Karlaftis V, “Antithrombin”, in *Haemostasis*, vol. 992, pp. 355–364, 2013
- [45] Previtali E, Bucciarelli P, Passamonti S M, Martinelli I, “Risk factors for venous and arterial thrombosis”, *Blood Transfusion*, vol. 9, no. 2, pp. 120–138, 2011
- [46] Găman A M, Ȃman G D, “Deficiency Of Antithrombin III ( AT III ) - Case Report and Review of the Literature”, *Current Health Science Journal*, vol. 40, no. 2, pp. 141–143, 2014
- [47] Stavenuiter F, Bouwens E, Mosnier L O, “Down-regulation of the clotting cascade by the protein C pathway”, *Hematology Education*, vol. 7, no. 1, pp. 365–374, 2013
- [48] Gale A J, “Current Understanding of Hemostasis”, *Toxicologic Pathology*, vol. 39, no. 1, pp. 273–280, 2011
- [49] Periyah M H, Halim A S, A Saad, “Mechanism action of platelets and crucial blood coagulation pathways in Hemostasis”, *International Journal of Hematology-Oncology and Stem Cell Research*, vol. 11, no. 4, pp. 319–327, 2017
- [50] Broos K, Feys H B, De Meyer S F, Vanhoorelbeke K, Deckmyn H, “Platelets at work in primary hemostasis”, *Blood Reviews*, vol. 25, no. 4, pp. 155–167, 2011

- [51] Tomaiuolo M, Brass L F, Stalker T J, “Regulation of platelet activation and coagulation and its role in vascular injury and arterial thrombosis”, *Interventional Cardiology Clinics*, vol. 6, no. 1, pp. 1–12, 2017
- [52] Hou Y, Carrim N, Wang Y, Gallant R C, Marshall A, “Platelets in hemostasis and thrombosis: Novel mechanisms of fibrinogen-independent platelet aggregation and fibronectin-mediated protein wave of hemostasis”, *Journal of Biomedical Research*, vol. 29, no. 6, pp. 437–444, 2015
- [53] Margraf A, Nussbaum C, Sperandio M, “Ontogeny of platelet function”, *Blood Advances*, vol. 3, no. 4, pp. 692–703, 2019
- [54] Marazzato G, Vincoli V T, “Ottimizzazione di un Protocollo Sperimentale volto all’Analisi del Potenziale Trombogenico di Dispositivi per il Trattamento del Sangue Indice”, 2014.
- [55] Taylor J O, Meyer R S, Deutsch S, Manning K B, “Development of a computational model for macroscopic predictions of device-induced thrombosis”, *Biomechanics and Modelling in Mechanobiology*, vol. 15, no. 6, pp. 1713–1731, 2016
- [56] Barmore W, Bracken B, “Biochemistry, Clotting Factors”, 2018
- [57] Hickerson D, Bode A P, “Flow cytometry of platelets for clinical analysis”, *Hematology Oncology. Clinics of North America*, vol. 16, no. 2, pp. 421–454, 2002
- [58] Girolami A, Ferrari S, Cosi E, Santarossa C, Randi M L, “Vitamin K-Dependent Coagulation Factors That May be Responsible for Both Bleeding and Thrombosis (FII, FVII, and FIX)”, *Clinical and Applied Thrombosis/Hemostasis*, vol. 24, no. 9 suppl, p. 42S–47S, 2018
- [59] Antoniak S, “The coagulation system in host defense”, *Research and Practice in Thrombosis and Haemostasis*, vol. 2, no. 3, pp. 549–557, 2018
- [60] Smith S A, Travers R J, Morrissey J H, “How it all starts: initiation of the clotting cascade”, *Critical Reviews in Biochemistry and Molecular Biology*, vol. 50, no. 4, pp. 326–336, 2015

- [61] Wu Y, “Contact pathway of coagulation and inflammation”, *Thrombosis Journal*, vol. 13, no. 17, 2015
- [62] Chinnaraj M, Planer W, Pozzi N, “Structure of Coagulation Factor II: Molecular Mechanism of Thrombin Generation and Development of Next-Generation Anticoagulants”, *Frontiers in Medicine*, vol. 5, no. 281, 2018
- [63] Weisel J W, Litvinov R I, “Fibrin Formation, Structure and Properties”, vol. 82, pp. 405-456, 2017
- [64] Kattula S, Byrnes J R, Wolberg A S, “Fibrinogen and fibrin in hemostasis and thrombosis”, *Arteriosclerosis, Thrombosis and Vascular Biology*, vol. 37, no. 3, pp. 13–21, 2017
- [65] Chargaff E, West R, “The biological significance of the thromboplastic protein of blood”, *Journal of Biological Chemistry*, vol. 166, pp. 189–197, 1946
- [66] O’Brian J R, “The platelet-like-activity of serum”, *British Journal of Haematology*, vol. 1, pp. 223–228, 1995
- [67] Wolf P, “The nature and significance of platelet products in human plasma”, *British Journal of Haematology*, vol. 13, pp. 269–288, 1967
- [68] Heijnen H F, Schiel A E, Fijnheer R et al., “Activated platelets release two types of membrane vesicles: Microvesicles by surface shedding and exosomes derived from exocytosis of multivesicular bodies and alpha-granules.” *Blood*, vol. 94, pp. 3791–3799, 1999
- [69] Miyazaki Y, Nomura S, Miyake T et al., “High shear stress can initiate both platelet aggregation and shedding of procoagulant containing microparticles” *Blood*, vol. 88, pp.3456–3464, 1996
- [70] Holme P A, Orvim U, Hamers M J et al., “Shear- induced platelet activation and platelet microparticle formation at blood flow conditions as in arteries with a severe stenosis”, *Arteriosclerosis, Thrombosis and Vascular Biology*, vol. 17, pp. 646–653, 1997

[71] Gemmell C H, Ramirez S M, Yeo E L et al., “Platelet activation in whole blood by artificial surfaces: Identification of platelet-derived microparticles and activated platelet binding to leukocytes as material-induced activation events”, *The Journal of Laboratory and Clinical Medicine*, vol. 125, pp. 276–287, 1995

[72] Sims P J, Faioni E M, Wiedmer T et al., “Complement proteins C5b-9 cause release of membrane vesicles from the platelet surface that are enriched in the membrane receptor for coagulation factor Va and express prothrombinase activity”, *Journal of Biological Chemistry*, vol. 263, pp. 18205–18212, 1988

[73] Bode A P, Knupp C L, “Effect of cold storage on platelet glycoprotein Ib and vesiculation”, *Transfusion*, vol. 34, pp. 690-696, 1994

[74] Burnier L, Fontana P, Kwak B R, Scherrer A, “Cell-derived microparticles in haemostasis and vascular medicine”, *Thrombosis and Haemostasis*, vol. 101, No. 3, pp. 439-451, 2009

[75] Bevers E M, Comfurius P, Zwaal R F, “Changes in membrane phospholipid distribution during platelet activation”, *Biochimica Biophysica Acta*, vol. 736, pp. 57-66, 1983

[76] Heijnen H F, Schiel A F, Fijnheer R et al., “Activated platelets release two types of membrane vesicles: Microvesicles by surface shedding and exosomes derived from exocytosis of multivesicular bodies and alpha-granules”, *Blood*, vol. 94, pp. 3791-3799, 1999

[77] Sims P J, Wiedmer T, Esmon C T et al., “Assembly of the platelet prothrombinase complex is linked to vesiculation of the platelet plasma membrane. Studies in Scott syndrome: An isolated defect in platelet procoagulant activity” *Journal Biological Chemistry*, vol. 264, pp. 17049-17057, 1989

[78] Larsson A, Nilsson B, Eriksson M, “Thrombocytopenia and platelet microvesicle formation caused by *Legionella pneumophila* infection”, *Thrombosis Research*, vol. 96, pp. 391-397, 1999



- [79] Nomura S, Shouzu A, Nishikawa M et al., “Significance of platelet-derived microparticles in uremia” *Nephron*, vol. 63, pp. 485, 1993
- [80] Tans G, Rosing J, Thomassen M C et al., “Comparison of anticoagulant and procoagulant activities of stimulated platelets and platelet-derived microparticles”, *Blood*, vol. 77, pp. 2641-2648, 1991
- [81] Merten M, Pakala R, Thiagarajan P et al., “Platelet microparticles promote platelet interaction with subendothelial matrix in a glycoprotein IIb/IIIa-dependent mechanism”, *Circulation*, vol. 99, pp. 2577-2582, 1999
- [82] Forlow S B, McEver R P, Nollert M U, “Leukocyte–leukocyte interactions mediated by platelet micro-particles under flow”, *Blood*, vol. 95, pp. 1317-1323, 2000
- [83] Toti F, Satta N, Fressinaud E et al., “Scott syndrome, characterized by impaired transmembrane migration of procoagulant phosphatidylserine and hemorrhagic complications, is an inherited disorder”, *Blood*, vol. 87, pp. 1409-1415, 1996
- [84] Dachary–Prigent J, Pasquet J M, Fressinaud E et al., “Aminophospholipid exposure, microvesiculation and abnormal protein tyrosine phosphorylation in the platelets of a patient with Scott syndrome: A study using physiologic agonists and local anaesthetics”, *British Journal of Haematology*, vol. 99, pp. 959-967, 1997
- [85] Bettache N, Gaffet P, Allegre N et al., “Impaired redistribution of aminophospholipids with distinctive cellshape change during Ca<sup>2+</sup>-induced activation of platelets from a patient with Scott syndrome”, *British Journal of Haematology*, vol. 91, pp. 873-878, 1998
- [86] Shcherbina A, Rosen F S, Remold–O’Donnell E, “Pathological events in platelets of Wiskott–Aldrich syndrome patients”, *British Journal of Haematology*, vol. 106, pp. 875-883, 1999

- [87] Jy W, Horstman L L, Arce M et al., "Clinical significance of platelet microparticles in autoimmune thrombocytopenias" *Journal of Laboratory Clinical Medicine*, vol. 119, pp. 334-345, 1992
- [88] Visentin G P, Moghaddam M, Collins J L et al., "Antibodies associated with heparin-induced thrombocytopenia (HIT) report conformational changes in platelet factor 4 (PF4) induced by linear polyanionic compounds", *Blood*, vol. 90, no. 1, pp. 460a, 1997
- [89] Warkentin T E, C P Hayward, Boshkov L K et al., "Sera from patients with heparin-induced thrombocytopenia generate platelet-derived microparticles with procoagulant activity: An explanation for the thrombotic complications of heparin-induced thrombocytopenia", *Blood*, vol. 84, pp. 3691-3699, 1994
- [90] Morel O, Jesel L, Chauvin M et al., "Eptifibatide- induced thrombocytopenia and circulating procoagulant platelet-derived microparticles in a patient with acute coronary syndrome", *Journal of Thrombosis and Haemostasis*, vol. 1, pp. 2685-2687, 2003
- [91] Wiedmer T, Hall S E, Ortel T L et al., "Complement-induced vesiculation and exposure of membrane prothrombinase sites in platelets of paroxysmal nocturnal hemoglobinuria", *Blood*, vol. 82, pp. 1192-1196, 1993
- [92] Biró E, Sturk–Maquelin K N, Vogel G M et al., "Human cell-derived microparticles promote thrombus formation in vivo in a tissue factor-dependent manner", *Journal of Thrombosis and Haemostasis*, vol. 1, pp.2561-2568, 2003
- [93] McGill M, Fugman D A, Vittorio N et al., "Platelet membrane vesicles reduced microvascular bleeding times in thrombocytopenic rabbits" *Journal of Laboratory Clinical Medicine*, vol. 109, pp. 127-133, 1987
- [94] Chandler W L, "Microparticle counts in platelet-rich and platelet-free plasma, effect of centrifugation and sample-processing protocols", *Blood Coagulation and Fibrinolysis*, vol. 24, no. 2, pp. 125-132, 2013

- [95] Poncelet P, Robert S, Bailly N, “Tips and tricks for flow cytometry-based analysis and counting of microparticles”, *Transfusion and Apheresis Science* , vol. 53, no. 2, pp. 110-126, 2015
- [96] Robert S, Poncelet P, Lacroix R et al., “Standardization of platelet-derived micro-particle counting using calibrated beads and a Cytomics FC500 routine flow cyto-meter: a first step towards multicenter studies?”, *Journal of Thrombosis and Haemostasis*, vol. 7, pp. 190-197, 2009
- [97] Shet A S, Aras O, Gupta K et al., “Sickle blood contains tissue factor-positive micro-particles derived from endothelial cells and monocytes”, *Blood*, vol. 102, pp. 2678-2683, 2003
- [98] Nieuwland R, Van Der Pol E, Gardiner C, Sturk A, “Platelet-Derived Microparticles”, *Platelets*, pp. 453-467, 2013
- [99] Sala V, “Ultrafast scanning electron microscopy charge dynamics at semiconductor and insulator surfaces”, 2018
- [100] Jones C G, “Scanning electron microscopy: preparation and imaging for SEM”, *Forensic microscopy for skeletal tissue*, vol. 915, pp. 1-20, 2012
- [101] Yuana Y, Oosterkamp T H, Bahatyrova S, Ashcroft B, Garcia R P, Bertina R M et al., “Atomic force microscopy: a novel approach to the detection of nanosized blood microparticles”, *Journal of Thrombosis and Haemostasis*, vol. 8, no. 2, pp. 311-314 , 2010
- [102] Engvall E et al., “Enzyme-linked immunosorbent assay, Elisa”, *The Journal of Immunology*, vol. 109, no. 1, pp 129-130, 1972
- [103] Aupeix K, Hugel B, Martin T, Bischoff P, Lill H, Pasquali J L et al., “The significance of shed membrane particles during programmed cell death in vitro, and in vivo, in HIV-1 infection”, *Journal of Clinical Investigation*, vol.99, no. 7, pp. 1546-1554, 1997

- [104] Nomura S, Shouzu A, Taomoto K, Togane Y, Goto S, Ozaki Y et al., “Assessment of an ELISA kit for platelet-derived microparticles by joint research at many institutes in Japan”, *Journal of Atherosclerosis and Thrombosis*, vol. 16, no. 6, pp. 878-887, 2009
- [105] Miyamoto S, Marcinkiewicz C, Edmunds L H, Niewiarowski S, “Measurement of platelet microparticles during cardiopulmonary bypass by means of captured ELISA for GPIIb/IIIa”, *Thrombosis and Haemostasis*, vol. 80, no. 2, pp. 225-230, 1998
- [106] Konoshenko M Y, “Isolation of Extracellular Vesicles: General Methodologies and Latest Trends”, *BioMed Research International*, pp. 1-27, 2018
- [107] Menck K et al., “Isolation and characterization of Microvesicles from peripheral blood”, *Jove (Journal of visualized experiments)*, vol. 119, pp. 550-557, 2017
- [108] Mrvar-Brečko A, Šuštar V, Janša V, Štukelj R, Janša R, Mujagić E, Kruljc P, Iglič A, Hägerstrand H, Kralj-Iglič V, “Isolated microvesicles from peripheral blood and body fluids as observed by scanning electron microscope”, *Blood Cells, Molecules, and Diseases*, vol. 44, no.4, pp. 307-312, 2010
- [109] Burnouf T, Goubran H A, Chou M, Devos D, Radosevic M, “Platelet microparticles: Detection and assessment of their paradoxical functional roles in disease and regenerative medicine”, *Blood Reviews*, vol. 28, no. 4, pp. 155-166, 2014
- [110] Xu R, Greening D W, Zhu H J, Takahashi N, Simpson R J, “Extracellular vesicle isolation and characterization: toward clinical application”, *The Journal of Clinical Investigation*, vol. 126, pp. 1152-1162, 2016
- [111] Campoy I, Lanau L, Altadill T et al., “Exosome-like vesicles in uterine aspirates: A comparison of ultracentrifugation-based isolation protocols”, *Journal of Translational Medicine*, vol. 14, no. 1, pp. 1-12, 2016

- [112] Nordin J Z, Lee Y, Vader P et al., “Ultrafiltration with size- exclusion liquid chromatography for high yield isolation of extracellular vesicles preserving intact biophysical and functional properties”, *Nanomedicine: Nanotechnology, Biology and Medicine*, vol. 11, no. 4, pp. 879-883, 2015
- [113] Witwer K W, Buza E I, Bemis L T et al., “Standardization of sample collection, isolation and analysis methods in extra- cellular vesicle research”, *Journal of Extracellular Vesicles*, vol. 2, no. 1, pp. 1-25, 2013
- [114] Crescitelli R, Lasser C, Szabo T G et al., “Distinct RNA profiles in subpopulations of extracellular vesicles: apoptotic bodies, microvesicles and exosomes,” *Journal of Extracellular Vesicles*, vol. 2, no.1, pp.1-9, 2013
- [115] Merchant M L, Powell D W, Wilkey D W et al., “Microfiltration isolation of human urinary exosomes for characterization by MS”, *Proteomics -Clinical Applications*, vol. 4, no. 1, pp. 84-96, 2010
- [117] Miguet L, Sanglier S, Schaeffer C et al., “Microparticles: a new tool for plasma membrane sub-cellular proteomic”, *Subcellular Biochemistry*, vol. 43, pp. 21-34, 2007
- [118] Josic D, Clifton J G, “Mammalian plasma membrane proteomics”, *Proteomics*, vol. 7, pp. 3010–3029, 2007
- [119] Wu C C, MacCoss M J, Howell K E et al., “A method for the comprehensive proteomic analysis of membrane proteins”, *Nature Biotechnology*, vol. 21, pp. 532-538, 2003
- [120] Smalley D M, Ley K, “Plasma-derived microparticles for biomarker discovery”, *Clinical Laboratory*, vol. 54, pp. 67-79, 2008
- [121] Smalley D M, Root K E, Cho H et al., “Proteomic discovery of 21 proteins express- ed in human plasma-derived but not platelet-derived microparticles”, *Thrombosis and Haemostasis*, vol. 97, pp.67-80, 2007

- [122] Garcia B A, Smalley D M, Cho H et al., “The platelet microparticle proteome”, *Journal of Proteome Research*, vol. 4, pp.1516-1521, 2005
- [123] Hoffman R A, Johnson T S, Britt W B, “Flow cytometric electronic direct current volume and radiofrequency impedance measurements of single cells and particles”, *Cytometry: Journal of Quantitative Cell Science*, vol. 1, no. 6 pp. 377–384, 1981
- [124] Zwicker J I, Liebman H A, Neuberg D et al., “Tumor-derived tissue factor-bearing microparticles are associated with venous thromboembolic events in malignancy”, *Clinical Cancer Research*, vol. 15, no. 22, pp. 6830-6840, 2009
- [125] Kaszuba M, McKnight D, Connah M T et al., “Measuring sub nanometer sizes using dynamic light scattering”, *Journal of Nanoparticle Research*, vol. 10, pp. 823-829, 2008
- [126] Lawrie A S, Albanyan A, Cardigan R A et al., “Microparticle sizing by dynamic light scattering in fresh-frozen plasma”, *Vox Sanguinis*, vol. 96, no. 3, pp. 206-212, 2009
- [127] Harrison P, Dragovic R, Albanyan A et al., “Application of dynamic light scattering to the measurement of microparticles”, *Journal of Thrombosis and Haemostasis*, vol. 7, no. supplement 2, 2009
- [128] Filipe V, Hawe A, Jiskoot W, “Critical evaluation of Nanoparticle Tracking Analysis (NTA) by NanoSight for the measurement of nanoparticles and protein aggregates”, *Pharmaceutical Research*, vol. 27, pp. 796–810, 2010
- [129] Berckmans R J, Nieuwland R, Böing A N et al., “Cell- derived microparticles circulate in healthy humans and support low grade thrombin generation”, *Thrombosis and Haemostasis*, vol. 85, pp. 639-646, 2001
- [130] Kireev D A, Popenko N Y, Pichugin A V, Pantelev M A, Krymskaya O V et al., “Platelet microparticle membranes have 50- to 100-fold higher specific procoagulant activity than activated platelets”, *Thrombosis and Haemostasis*, vol. 97, no.3, pp. 424-435, 2007

- [131] Nieuwland R et al., “Cell-Derived Microparticles Generated in Patients During Cardiopulmonary Bypass Are Highly Procoagulant”, *Circulation*, vol. 96, no. 10, pp. 3534-3541, 1997
- [132] Wang Z T, Wang Z, Hu Y W, “Possible roles of platelet-derived microparticles in atherosclerosis”, *Atherosclerosis*, vol. 248, pp 10-16, 2016
- [133] Christersson C, Thulin Å, Siegbahn A, “Microparticles during long-term follow-up after acute myocardial infarction. Association to atherosclerotic burden and risk of cardiovascular events”, *Thromb Haemost.*; Vol. 117, No.8, pp: 1571-1581, 2017
- [134] Suades R, Padro T, Vilahur G, Badimon L. Circulating and platelet-derived microparticles in human blood enhance thrombosis on atherosclerotic plaques. *Thrombosis and Haemostasis*, vol. 108, pp. 1208-19, 2012
- [135] Suades R, Padró T, Vilahur G, Martin-Yuste V, Sabaté M, Sans-Roselló J, Badimon L, “Growing thrombi release increased levels of CD235a+ microparticles and decreased levels of activated platelet-derived microparticles. Validation in ST-elevation myocardial infarction patients.”, *Journal of Thrombosis and Haemostasis*, vol. 13, n. 10, pp. 1776-1786, 2015
- [136] Ramacciotti E, Hawley A, Farris D, Ballard N, Wroblewski S, Myers D, Henke P, Wakefield T, “Leukocyte- and platelet-derived microparticles correlate with thrombus weight and tissue factor activity in an experimental mouse model of venous thrombosis”, *Thrombosis and Haemostasis*, vol. 101, n. 4, pp.748-754, 2009
- [137] Leytin V, Allen D J, Mykhaylov S, Mis L, Lyubimov E V, Garvey B, Freedman J, “Pathologic high shear stress induces apoptosis events in human platelets”, *Biochemical and Biophysical Research Communications*, vol. 320, no. 2, pp. 303-310, 2004

[138] Sheriff J, Tran P L, Hutchinson M, DeCook T, Slepian M, Bluestein D, Jetsy J, “Repetitive Hypershear Activates and Sensitizes Platelets in a Dose-Dependent Manner”, *Artificial Organs*, vol. 40, no. 6, pp. 586-595, 2016

[139] Consolo F, Valerio L, Brizzola S, Rota P, Marazzato G, Vincoli V, Reggiani S, Redaelli A, Fiore G, “On the Use of the Platelet Activity State Assay for the In Vitro Quantification of Platelet Activation in Blood Recirculating Devices for Extracorporeal Circulation”, *Artificial Organs*, vol. 40, no.10, pp 971-80, 2016

[140] Jesty J, Bluestein D, “Acetylated prothrombin as a substrate in the measurement of the procoagulant activity of platelets: elimination of the feedback activation of platelets by thrombin”, *Analytical Biochemistry*, vol. 272, pp. 64-70, 1999

[141] Hidaka H, Asano T, “Platelet cyclic 3':5'-nucleotide phosphodiesterase released by thrombin and calcium ionophore”, *Journal of Biological Chemistry*, vol. 251, pp. 7508-7516, 1976

[142] Matijevic N et al., “Decline in platelet microparticles contributes to reduced hemostatic potential of stored plasma”, *Thrombosis Research*, vol. 128, n. 1, pp. 35-41, 2011

[143] Bode A P, Knupp C L, “Effect of cold storage on platelet glycoprotein Ib and vesiculation”, *Transfusion*, vol. 34, no.8, pp. 690-696, 1994

[144] Keuren J F, Magdeleyns E J, Govers-Riemslog J W, Lindhout T, Curvers J, “Effects of storage-induced platelet microparticles on the initiation and propagation phase of blood coagulation”, *British Journal of Haematology*, vol. 134, pp. 307-313, 2006

[145] Rubin O, Crettaz D, Canellini G, Tissot J D, Lion N, “Microparticles in stored red blood cells: an approach using flow cytometry and proteomic tools”, *Vox Sanguinis*, vol. 95, no. 4, pp. 288-297, 2008



- [146] Soares J S, Sheriff J, Bluestein D, “A novel mathematical model of activation and sensitization of platelets subjected to dynamic stress histories”, *Biomechanics and Modeling in Mechanobiology*, vol. 12, no.6, pp. 1127-1141, 2013
- [147] Bludszuweit C, “Model for a General Mechanical Blood Damage Prediction. *Artificial Organs*”, vol. 19, no. 7, pp. 583-589, 1995
- [148] Einav S, Dewey C F, Hartenbaum H, “Cone-and-plate apparatus: a compact system for studying well-characterized turbulent flow fields”, *Experiments in Fluids*, vol. 16, pp. 196-202, 1994
- [149] Girdhar G, Bluestein D, “Biological effects of dynamic shear stress in cardiovascular pathologies and devices”, *Expert Review of Medical Devices*, vol. 5, no. 2, pp. 167-181, 2008
- [150] Xenos M, Girdhar G, Alemu Y, Jesty J, Slepian M, Einav S, Bluestein D, “Device Thrombogenicity Emulator (DTE) - Design optimization methodology for cardiovascular devices: A study in two bileaflet MHV designs”, *Journal of Biomechanics*, vol. 43, no. 12, pp. 2400-2409, 2010
- [151] Jy W, Horstman L, Jimenez J, Ahn Y, Biro E, Nieuwland R, Sturk A, Dignat-George F, Sabatier F, Camoin-Jau L et al., “Measuring circulating cell-derived microparticles.”, *Journal of Thrombosis and Haemostasis*, vol. 2, pp. 1842-1851, 2004
- [152] Baj-Krzyworzeka M, Majka M, Pratico D, Janina Ratajczak<sup>a</sup>, Vilaire G, Kijowski J, Reca R, Wieczorek A J, Ratajczak M Z, “Platelet-derived microparticles stimulate proliferation, survival, adhesion, and chemotaxis of hematopoietic cells”, *Experimental Hematology* Vol. 30 pp: 450–459, 2002
- [153] Gamonet C, Mourey G, Aupet S, Biichle S, Petitjean R, Vidal C et al., “How to quantify microparticles in RBCs? A validated flow cytometry method allows the detection of an increase in microparticles during storage”, *Transfusion*, vol. 57, pp. 504-516, 2017

[154] Aatonen M et al., “Isolation of Platelet-Derived Extracellular Vesicles”, *Method in Molecular Biology*, vol. 1545, pp. 177-188, 2017

[155] Sims J P, Wiedmer T S, Esmon C T, Weissll H J, Shattil S J, “Assembly of the Platelet Prothrombinase Complex is Linked to Vesiculation of the Platelet Plasma Membrane”, *Journal of Biological Chemistry*, vol. 264, no. 29, pp. 17049-17057, 1989

[156] Girdhar G et al., “Dynamic Shear Stress Induced Platelet Activation in Blood Recirculation Devices: Implications for Thrombogenicity Minimization”, *American Society of Mechanical Engineers*, pp. 231–232, 2009